

**INVESTIGATING THE EFFECTS OF
ELECTROMAGNETIC FIELDS DUE TO HIGH VOLTAGE
TRANSMISSION LINES ON DETONATOR FIRING
CIRCUITS**

W.F.M.Fernando

(108884B)



University of Moratuwa, Sri Lanka.
Electronic Theses & Dissertations
www.lib.mrt.ac.lk

Degree of Master of Science

Department of Electrical Engineering

University of Moratuwa

Sri Lanka

May 2015

**INVESTIGATING THE EFFECTS OF
ELECTROMAGNETIC FIELDS DUE TO HIGH
VOLTAGE TRANSMISSION LINES ON DETONATOR
FIRING CIRCUITS**

W.F.M. Fernando

(108884B)



University of Moratuwa, Sri Lanka.
Electronic Theses & Dissertations
www.lib.mrt.ac.lk

Thesis submitted in partial fulfillment of the requirements for the degree
Master of Science

Department of Electrical Engineering

University of Moratuwa

Sri Lanka

May 2015

Declaration

“I declare that this is my own work and this thesis does not incorporate without acknowledgement any material previously submitted for a Degree or Diploma in any other University or institute of higher learning and to the best of my knowledge and belief it does not contain any material previously published or written by another person except where the acknowledgement is made in the text.

Also, I hereby grant to University of Moratuwa the non-exclusive right to reproduce and distribute my thesis/dissertation, in whole or in part in print, electronic or other medium. I retain the right to use this content in whole or part in future works (such as articles or books).”



University of Moratuwa, Sri Lanka.

Electronic Theses & Dissertations

www.lib.mrt.ac.lk

Signature of the candidate

Date:

(W.F.M.Fernando)

The above candidate has carried out research for the Masters under our supervision.

Signature of the Supervisor

Date:

(Eng. W.D.A.S. Wijayapala)

Signature of the Supervisor

Date:

(Dr. Asanka S. Rodrigo)

Abstract

High voltage A.C. transmission is the common mode adopted in transmitting bulk electrical power from one station to the other all over the world. Associated with these overhead transmission lines are the electric and magnetic fields emanating from these which could have a coupling influence on devices in its proximity. Detonator is one such electro explosive device (EED) that is susceptible to electromagnetic coupling when placed in proximity to the transmission lines which in turn could cause inadvertent misfires.

This report focuses on the computational modeling of electric and magnetic fields around overhead high voltage transmission lines at various voltage levels and line configurations starting from fundamental electromagnetic principles and the verification of those models by field measurements. MATLAB software was used in modeling the field profiles and the model is capable of accommodating any configuration with any number combination of conductors. The overhead transmission line parameters used in this report are from the present line configurations in practice in Sri Lanka. The measured values of electric and magnetic fields are compared with the modeled values for the verification of models. The possibility of shielding these extra low frequency electromagnetic fields are also discussed briefly.

Electrical detonator is one type of Electro Explosive Devices (EEDs) that is used to initiate blast sequences. the susceptibility of these devices to the electric and magnetic fields emanating from nearby high voltage transmission lines are comprehensively examined under scenarios of nominal rated loads, infrequent high loads, emergency short-time loads, faults, lightning and switching surges. Investigating the impacts of field couplings and possible unintentional misfires under different scenarios, safe distance levels for operation of detonators in the proximity of transmission lines are proposed for different voltages and line configurations.

Acknowledgement

First and foremost I wish to express my appreciation and sincere thanks to the Department of Electrical Engineering of University of Moratuwa for providing me the opportunity of following the Master's Degree Program in Electrical Installations. I also sincerely thank the Senior Lecturers Eng. W.D.A.S. Wijayapala and Dr. Asanka S. Rodrigo of Electrical Department of University of Moratuwa who encouraged, guided and supported me as research supervisors to attain the goals of the project despite their heavy work schedules and responsibilities. Their advice and insight were immeasurably vital and significant. I also express my sincere thanks to Eng. D. Sajjana de Silva, Deputy Director(Mines), Geological Survey and Mines Bureau for his invaluable contributions and support as a supervisor of this research.

I would extend my sincere gratitude to Transmission Planning branch, Transmission Design branch, DD1 Distribution Planning branch and my dear colleagues of Transmission Projects branch of the Ceylon Electricity Board. My special thanks go to Mining Engineer, Mr. G.M.M. Rangana and his staff of W.A. Perera & Co. for the assistance provided in the field testing activities.



University of Moratuwa, Sri Lanka.
Electronic Theses & Dissertations
www.lib.mrt.ac.lk

While I regret for my inability to specifically mention each and every individual, I am grateful to all the Lecturers and the staff of the Department of Electrical Engineering of University of Moratuwa and my colleagues who were helpful in numerous ways to make my endeavor a success.

Last, but not least, I thank my beloved family members for their appreciation, support and understanding in achieving this aspiration.

Table of Contents

Declaration	i
Abstract	ii
Acknowledgement	iii
List of Figures	vii
List of Tables	x
List of Abbreviations	xi
List of Symbols	xii
Annexes	xiii

Chapters

1. Introduction	1
1.1 General	1
1.2 Research Initiating Statement	2
1.3 The Objectives	2
1.4 The Methodology	3
1.5 Results and Disseminations	4
2. Electro Explosive Devices and Detonator Firing Circuits	5
2.1 Electrical Detonator	5
2.2 Blasting Explosives	7
2.3 Blasting Geometry	8
2.4 Detonator Circuit Arrangements	10
2.5 Literature Survey on different Modeling methods	11
2.6 Specification of a Detonator	14
3. Modeling the Electromagnetic Field	15
3.1 Modeling the Electric Field	15
3.1.1 Assumptions	15

3.1.2	Electric field and Electric Potential	16
3.1.3	Addition of Potential Line charges	18
3.1.4	Modeling the line charges	19
3.1.5	Representation of Line Voltage in phasor form	22
3.1.6	Electrical field at a point in space	23
3.1.7	Magnitude of E	25
3.1.8	Calculation of Potential	25
3.1.9	Flow Chart for Modeling & Simulation of Electric Field around Transmission Line	26
3.1.10	Transmission Line Data	27
3.1.11	Average conductor height above ground	29
3.1.12	Simulations using MATLAB	31
3.2	Modeling the Magnetic Field	35
3.2.1	Assumptions	35
3.2.2	Modeling for 'n' number of conductors	36
3.2.3	Considering the effects of earth's return currents	37
3.2.4	Resultant effect of magnetic field intensity	37
3.2.5	Representation of Line Currents in Phasor form	38
3.2.6	Flow Chart for Modeling & Simulation of Magnetic Field around Transmission	39
3.2.7	Simulation of magnetic field profiles using MATLAB	40
4.	Measuring the field values physically under the transmission lines and shielding of the fields	43
4.1	Measuring the electric field under the transmission lines	43
4.1.1	Instruments used for measuring	44
4.1.2	Recording the measurements	44
4.1.3	Plotting the profiles of measured electric field values vs modeled values	46
4.1.4	Comparison of the measured values and the modeled values and verification of model	47
4.2	Measuring the magnetic field under the transmission lines	48
4.2.1	Instruments and recording of measurements	48

4.2.2	Plotting the profiles of measured magnetic field values and the modeled values and verification of model	50
4.3	Shielding the electromagnetic field under transmission lines	52
4.3.1	Shielding the electric field	52
4.3.1.1	Shielding by a vertical grid of grounded wires	52
4.3.1.2	Designing a vertical grid of grounded wires	53
4.3.1.3	Shielding by a horizontal grid of grounded wires	56
4.3.2	Shielding the magnetic field	57
5.	Susceptibility of detonators to the electric fields & magnetic fields	59
5.1	Electric Field couplings	59
5.1.1	Testing of detonators placed inside electric fields	59
5.1.2	Testing of detonators placed inside electric fields	57
5.2	Magnetic field couplings	63
5.2.1	Relationship between induced emf (E) and magnetic flux (B)	63
5.2.1.1	The time taken by detonator for firing	65
5.2.2	Minimum flux density requirement for firing	65
5.2.3	Inducements of current in the detonator circuits caused by surges occurring in the transmission lines	68
5.2.4	Inducements caused by transmission line faults	69
5.2.5	Inducements caused by travelling lightning waves in transmission lines	71
5.2.6	Inducements caused by switching surges in transmission lines	72
5.3	Safe Distances	74
5.4	Discussion on Results	75
6.	Conclusions & Recommendations	77
6.1	Conclusions	77
6.2	Recommendations	78
	References	79



LIST OF FIGURES

	Page	
Figure 2.1	Electrical Detonator with lead wires	6
Figure 2.2	Schematic cross-section of an electrical detonator	6
Figure 2.3	Blasting geometry	8
Figure 2.4	Charged Bore Hole	9
Figure 2.5	Series connected detonator circuits	10
Figure 2.6	Forward and reverse parallel detonator circuits	10
Figure 2.7	Forward and reverse parallel closed loop detonator circuits	10
Figure 2.8	Discretization of the System	13
Figure 3.1	Field of a line charge (for an infinitely long conductor)	15
Figure 3.2	Incremental potential difference	17
Figure 3.3	Cylindrical Gaussian Surface	18
Figure 3.4	Group of line charges	18
Figure 3.5	Multi-conductor line for calculation of Maxwell's potential coefficients	19
Figure 3.6	Electric field at a point in space due to charge q and its mirror image	23
Figure 3.7	Flow diagram for electric field modeling and simulation	26
Figure 3.8	Transmission line parameters	27
Figure 3.9	The average height above ground calculation for 220kV lines	31
Figure 3.10	Electric field variation with height above ground	32
Figure 3.11	3D scheme of electric field variation for 132kV D/C configuration	32
Figure 3.12	Electric field variation for 220kV double circuit line 1m above ground	33
Figure 3.13	Electric field variation for 132kV double circuit line 1m above ground	33
Figure 3.14	Electric field variation for 33kV double circuit, triangular and horizontal configurations, 1m above ground	34

Figure 3.15	Space potential variation for 220kV and 132kV double circuit lines 1m above ground	34
Figure 3.16	An infinitely long conductor carrying current I	35
Figure 3.17	Coordinate system for magnetic field calculations	36
Figure 3.18	Flow diagram for magnetic field modeling and simulation	39
Figure 3.19	Magnetic field variations with respect to height and distance	40
Figure 3.20	3D scheme of magnetic field variations for 220kV D/C configuration	40
Figure 3.21	Magnetic field variation for 220kV double circuit line 1m above ground	41
Figure 3.22	Magnetic field variation for 132kV double circuit line 1m above ground	41
Figure 3.23	Magnetic field variations for 33kV for triangular, vertical double circuit and horizontal configurations 1m above ground	42
Figure 4.1	Location selected for taking measurements in 220kV line	43
Figure 4.2	Taking measurements under the transmission lines keeping the e-field meter as distant as possible, 1m above ground	44
Figure 4.3	Electric field profiles comparing the modeled and measured values for 220kV double circuit configuration	46
Figure 4.4	Electric field profiles comparing the modeled and measured values for 132kV double circuit configuration	46
Figure 4.5	Electric field profiles comparing the modeled and measured values for 33kV double circuit configuration	47
Figure 4.6	Taking magnetic field measurements under the transmission lines 1m above ground	48
Figure 4.7	Magnetic field profiles comparing the modeled and measured values for 220kV double circuit configuration	50
Figure 4.8	Magnetic field profiles comparing the modeled and measured values for 132kV double circuit configuration	51
Figure 4.9	Magnetic field profiles comparing the modeled and measured values for 33kV double circuit configuration	51

Figure 4.10	Geometry of a vertical grid	53
Figure 4.11	The Kaduwela Outer Circular highway construction site	54
Figure 4.12	Shielding efficiency of vertical grids of Wires	55
Figure 4.13	Vertical grid shield of equally spaced wires	56
Figure 4.14	Edge factor for horizontal grid of shield wires	57
Figure 5.1	Investigating the behavior of detonator placed in an electric field in open air	60
Figure 5.2	Investigating the induced currents in a conductor placed in an electric field	61
Figure 5.3	Acceptable electrical field strength for a commercially available electrical detonator	62
Figure 5.4	Changing flux-linkage and Lenz's law	63
Figure 5.5	Induced emf in the wire loop	63
Figure 5.6	Battery loop	64
Figure 5.7	1 m ² detonator circuit loop	65
Figure 5.8	Flux density variations 0.5m above ground for different loadings for 220kV double circuit twin conductor configuration	66
Figure 5.9	Flux density variations 0.5m above ground for different loadings for 132kV double circuit twin conductor configuration	67
Figure 5.10	Flux density variations 0.5m above ground for different loadings for 33kV double circuit Lynx conductor configuration	67
Figure 5.11	A typical current surge that occurs in a transmission line	68
Figure 5.12	A phase to earth fault that occurred in Kotmale- Biyagama 220kV transmission line	69
Figure 5.13	Flux density variations 0.5m above ground due to a line fault of 20kA for 220kV double circuit twin conductor configuration	71
Figure 5.14	Flux density variations 0.5m above ground due to lightning surge for 220kV double circuit twin conductor configuration	72
Figure 5.15	Flux density variations 0.5m above ground due to switching surge for 220kV double circuit twin conductor configuration	73

LIST OF TABLES

	Page	
Table 2.1	Ingredients of blasting explosives	8
Table 2.2	Drilling Parameters	9
Table 2.3	Charging Parameters	9
Table 3.1	220kV double circuit transmission line data	27
Table 3.2	132kV double circuit transmission line data	28
Table 3.3	33kV Double circuit transmission line data	28
Table 3.4	33kV horizontal configuration line data	29
Table 3.5	33kV triangular configuration line data	29
Table 3.6	Typical input data for electric and magnetic field calculations	30
Table 3.2	Calculation of average ground clearance	31
Table 4.1	Electric field measurements for Kotugoda – Veyangoda 220kV line	45
Table 4.2	Magnetic field measurements for Kotugoda – Veyangoda 220kV line	49
Table 5.1	The currents corresponding to different loading conditions, faults, lightning and switching conditions	74
Table 5.2	The safe distances corresponding to different loading conditions, faults, lightning and switching conditions	74
Table 5.3	Recommended Distaces for Commercial AM Transmitters	76
Table 5.4	Recommended safe distances from FM, VHF/UHF Transmitters	76
Table 6.1	Statement of safe distances for the operation of detonators	77

LIST OF ABBREVIATIONS

Abbreviation	Description
CEB	Ceylon Electricity Board
GSMB	Geological Survey and Mines Bureau
MATLAB	Matrix Laboratory software
EE	Electrical Engineer
IEEE	Institute of Electrical & Electronic Engineers
GSS	Grid Sub Station
DC	Direct Current
AC	Alternative Current
STC	Standard Test Conditions
RMS	Root Mean Square
EED	Electro-Explosive Device
ICNIRP	International Commission on Non Ionizing Radiation Protection
IRPA	International Radiation Protection Association
WHO	World Health Organization



University of Moratuwa, Sri Lanka.
Electronic Theses & Dissertations
www.lib.moratuwa.lk

LIST OF SYMBOLS

Symbol	Description
E	Electric Field, V/m
V	Voltage, Volts
I	Current in Amperes
T	Tesla
μT	Micro Tesla
mG	Milli-Gauss
B	Magnetic Flux Density in T
H	Magnetic Field Intensity
Wb	Webers
Kg	Kilo-grams
C	Coulomb
Q, q	Charge in Coulomb
D	Bundle Diameter in m
d	conductor diameter in m
r	Sub conductor radius
N, n	Number of sub conductors
S	Sub conductor spacing
V_p	Potential at point P
μ_0	Permeability of free space
ϵ_0	Permittivity of free space



University of Moratuwa, Sri Lanka.
 Electronic Theses & Dissertations
 Charge in Coulomb.lk

ANNEXES

- Annex 1** Request Letter issued by GSMB requesting a study on susceptibility of detonators to electromagnetic fields emanating from transmission lines
- Annex 2** Specification of a short Delay Detonator used in Sri Lanka.
- Annex 3** MATLAB code written for electric field around 220kV double circuit twin zebra configuration
- Annex 4** MATLAB code written for magnetic field around 220kV double circuit twin zebra configuration.
- Annex 5** Electric field measuring data for Kotugoda – Katunayake 132kV Line
- Annex 6** Electric field measuring data for Bolawatta – Nattandiya 33kV Line
- Annex 7** Magnetic field measuring data for Kotugoda – Katunayake 132kV Line
- Annex 8** Magnetic field measuring data for Bolawatta – Nattandiya 33kV Line



Introduction

1.1 General and Background

Over the last few decades, electricity has become a vital commodity in our day today life and it is increasingly proving to be an integral part of our modern life. The increase in power demand has increased the need for transmitting huge amount of power over long distances. Large transmission line configurations with high voltage and current levels generate large values of low frequency electromagnetic field stresses which in turn have significant interference on electrical and electronic equipment, accessories, circuits and other conducting bodies mainly operating in frequency range below UHF. This research mainly focuses on the fields emanating from high voltage transmission lines and their electromagnetic coupling effects on Electro Explosive Devices (EEDs) and their firing circuits.

The Sri Lankan commercial electric power system operates at a frequency of 50 Hz, or cycles per second, meaning that the field increases and decreases its intensity 50 times per second. The interactions of the fields emanated from transmission lines also oscillate at the same frequency. The electromagnetic field levels in the proximity of a high voltage transmission line depends on a number of variables, including but not limited to the voltages, currents, overall geometry of the structures holding the conductors, the type of conductors, phase spacing, sag and earth wires used. Hence, in the modeling and calculation process, each voltage level of the transmission lines has been considered separately and calculated independently for the specific structure geometry and conductor type used.

The strength of an EMF increases significantly with decreasing distance from the source. The strength of an electric field is proportional to the voltage of the source. Thus, the electric fields beneath high voltage transmission lines far exceed those below the lower voltage distribution lines at the same distance. The magnetic field strength, by contrast, is proportional to the current in the lines, so that a relatively low voltage line with a high current load may produce a magnetic field that is as high as those produced by some higher voltage transmission lines.

With the rapid development impetus in progress in the country, the need for enhancing the infrastructure to cater to that requirement is indispensable and a prerequisite. The development of road network, electricity, water and sanitation, housing and transportation are essentials in this respect. The construction of these facilities, sometimes, involves blasting of ground rocks in order to level and pave the right of way. Further, processed rock and rock metal are imperative

raw materials that contribute towards the construction industry. This essential raw material is produced through the explosive blasting industry which is a prime industry in our modern society. It plays some part-direct or indirect- in practically everything we build, make, use and enjoy. Without explosives and blasting industry, available where and when they are needed, public works and private enterprises would be badly hampered. Therefore, facilitating proper handling, use, transportation and storage of explosive materials in blasting industry while providing safeguards for life and property are in the interest of the whole community.

The interference and coupling of electromagnetic fields emanating from transmission line becomes an issue when the explosive blasting activities are performed in the vicinity of these. Since, the electrical detonator (one kind of electro explosive devices) and associated circuits are used as the means of initiating explosions, these electromagnetic fields could cause inductive coupling with the circuitry. The main research issue in concern is that whether there a possibility that these coupling would induce significant voltages and threshold level currents that could initiate premature or unintentional explosions and if so what are the safe distances for operation from transmission lines.

1.2 Research Initiating Statement.



University of Moratuwa, Sri Lanka.
Electronic Theses & Dissertations
www.lib.mrt.ac.lk

The Geological Survey and Mines Bureau (GSMB) has made an official request to investigate the possibility of unintentional / premature firing of electrical detonators due to induced electricity (or extraneous electricity) from high voltage transmission lines in sites and mines where explosive blasting are carried out. This endangers human lives and property. Therefore, it is essential avoiding such unanticipated situations through careful study and provide guidelines of safe distances ensuring safe operations in explosive blastings. Hence, a study is to be carried out for investigating the electromagnetic fields emanating from different voltage levels and circuit configurations of high voltage transmission lines present in Sri Lanka and determine safe distances for operation. The request letter tendered by GSMB is attached as **Annex 1**.

1.3 Objectives

- To investigate the electromagnetic fields around high voltage transmissions lines of 220kV, 132kV and 33kV and thereby, analyze the sensitivity over detonator firing circuits and make recommendations for safe feasible operations.
- To prepare a statement of safe distances of operation for these firing circuits in order to avoid inappropriate triggering.

1.4 Methodology

i. Study of detonators, circuit arrangements and explosives

Visit detonator blasting sites and study specification of detonators, different circuit configurations, types of detonators and explosive materials used in Sri Lanka and different conditions under which explosions are carried out.

ii. Literature survey

Do a literature survey on the Electro Explosive Devices(EEDs), the theories behind joule heating of bridge wire due to electromagnetic radiation [1],[3],[5] susceptibility of EEDs to electric and magnetic fields [3],[4],[19] modelling approaches of fields around transmission lines [2],[6],[11],[13],[14] and shielding of electric and magnetic fields [6],[17].

iii. Modeling the electromagnetic field

Modeling the electric and magnetic fields under transmission lines for different voltage and circuit configurations starting from basic principles of electromagnetic theory.

iv. Simulation using software

Simulate the model using standard software to determine the field profiles and their magnitudes around the transmission lines and investigate the field variation profiles with distance.

v. Taking physical measurements

Measure the electric and magnetic fields physically under the transmission lines using standard measuring meters with real time voltage and current values.

vi. Comparison of the model and measured values

Compare the simulated values with the measured values in the field and finding actual reasons for deviations.

vii. Investigate the induced currents due to electric fields

Study the induced currents in conductors and detonators in the presence of electric fields.



viii. Investigate the induced currents due to magnetic field variations

Investigate the impact and inducements on the detonator circuits due to magnetic fields emanated by rated nominal loads, infrequent high loadings, emergency short term loads, line faults, switching currents and travelling lightning waves.

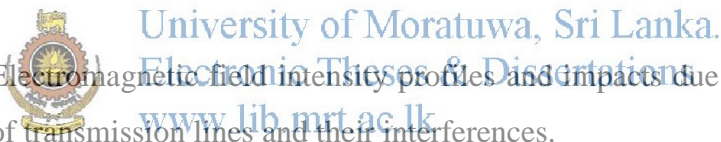
ix. Safe Distances for operation

Prepare a statement of safe distance levels for operations of detonator blasting circuits for different voltages and transmission line configurations taking the results obtained from vi and vii into account.

x. Shielding arrangement

Study and design a suitable shielding arrangement to mitigate the electric field and to investigate the possibility of shielding the magnetic fields or else to find alternative solutions.

1.5 Results & Dissemination

- 
- Electromagnetic field intensity profiles and impacts due to different configurations of transmission lines and their interferences.
 - Statement of safe distance levels for operation of Electro Explosive Devices (EEDs) for firing explosives for different overhead transmission line configurations and voltages.

Electro Explosive Devices and Detonator Firing Circuits

2.1 Electrical Detonator

Electrical detonator is one type of Electro Explosive Devices (EEDs) that is used to initiate blast sequences. Electrical detonators are compact devices that are designed to safely initiate and control the performance of larger explosive charges. They contain relatively sensitive high explosives which can be initiated by electrical or shock energy from an external source. All electrical detonators contain components that can be initiated by sufficient impact of electrical energy. These characteristics make them the most dangerous explosive products in industrial application and they must be stored, transported, handled and used according to set procedures and regulations.

The commercially available electric detonator in Sri Lanka is called a match-type blasting cap. In this type, the bridgewire is usually surrounded by a proprietary pyrotechnic mix or coating which is in turn surrounded by a primary explosive which is in contact with the main charge [3]. The principle of operation of this type of electric detonator used in Sri Lanka is that, when a high enough electric current is passed through its lead wires, a bridge wire is heated in the fuse head to the ignition temperature providing the initial activation energy, which then ignites the ignition charge (similar to a match) which in turn initiates the explosive in bottom of the detonator after a time determined by the length and content of the delay element. The type of detonators used in Sri Lanka is match-type detonators with bridge wire and in this type, ignition charge is closely bonded with the bridge wire. The match-type EEDs have been found to be susceptible to such low levels of energy (4-6 mJ) and the safe operation of these EEDs is vital when in use near sources that emits electromagnetic radiation [8] such as high voltage transmission lines. The normal operation current profiles, both constant current and pulsed excitation, are well known, as is the ignition temperature. However, as safety and reliability are of great concern, both in the operation and storage of EEDs, the susceptibility of these devices to transient or spurious fields is also of interest.

Under normal explosive operations, electrical energy is introduced into the detonator from the exploder (hand-driven magneto or charged capacitor) via a primary circuit wire (shot-firing cable) and detonator leads.

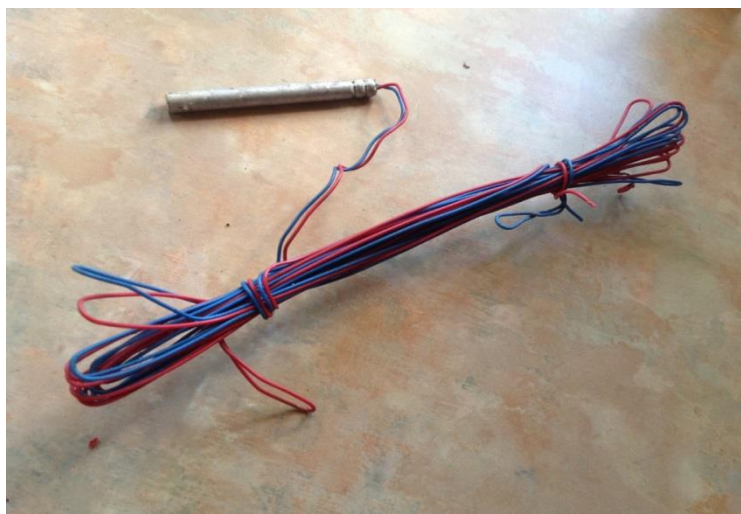


Figure 2.1 : Electrical Detonator with lead wires

The only type of detonators used in Sri Lanka are called ‘short-delay’ detonators because the delay times vary in increments of 25ms and the longest delays found are 500ms and 1 second. The timing of the pyrotechnic delay element is accurate to within 8ms.

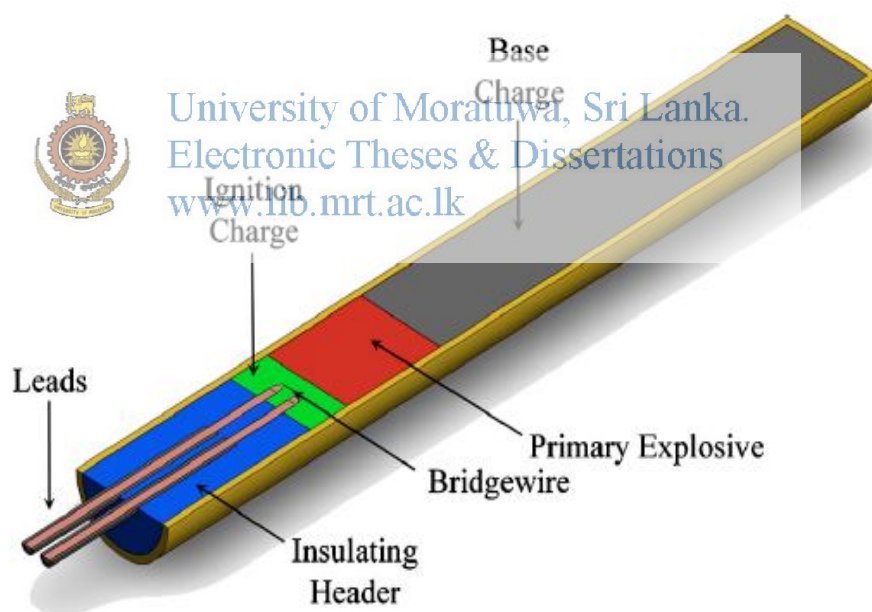


Figure 2.2: Schematic cross-section of an electrical detonator

Since electric detonators are designed to fire when electrical energy is supplied to them, any extraneous source of electric current represents a potential source for initiation. Sources such as lightning, high voltage power lines, radio transmitters, and static electricity must be avoided. There are also occurrences where the energy from lightning has traveled several miles along transmission lines, pipes or cables into an underground mine and can represent an unsuspected source for initiation of electric detonators.

When using electric detonators, the continuity and resistance of the individual detonator as well as the entire circuit needs to be tested with a blasting galvanometer. A blasting galvanometer is used to check the individual detonators prior to making the primer and again prior to stemming the borehole. Care should be taken when stemming a borehole to prevent any possible damage to the detonator leg wires. Once the circuit is completely wired, it should be checked again. When the blast line is connected to the circuit, the resistance needs to be checked prior to connecting the blasting unit.

Electronic detonator systems are new technology advancements for the initiation of blasts in mining operations. Several advantages for electronic detonators are precise timing, reduced vibrations, a reduced sensitivity to stray electrical currents and radio frequencies, and a great reduction in misfires through more precise circuit testing.

Electronic detonators have been designed to eliminate the pyrotechnic fuse train that is a component of electric detonators, thus improving timing accuracy and safety. For the electronic detonators, typically an integrated circuit and a capacitor system internal to each detonator separate the leg wires from the base charge. The circuitry consists of a microchip, PLC logic and delay circuits. Depending on the design features of the electronic detonator, the safety and timing accuracy can be greatly improved. The electronic detonator is obviously a more complex design compared to an electric detonator. A specially designed blast controller unique to each manufactured system transmits a selectable digital signal to each wired electronic detonator. The signal is identified by each electronic detonator and the detonation firing sequence is accurately assigned. The manufacturer's control unit used in accordance with the unit's specified operating procedures will show any incomplete circuits during hookup prior to initiation of the explosive round. The wired round won't fire until all detonators in the circuit are properly accounted for with respect to the current blasting plan layout.

2.2 Blasting Explosives

Blasting explosives are agents that:

- Comprises ingredients that by themselves are non-explosive.
- Can only be detonated by a high explosive charge placed within it. The explosive charge comprises of a detonator inserted inside gelignite (water-gel) capsules. All blasting agents contain the following essential components:

Oxidizer	A chemical that provides oxygen for the reaction. Typical oxidizers are ammonium nitrate and calcium nitrate.
Fuel	A chemical that reacts with oxygen to produce heat. Common fuel used is diesel fuel oil.
Sensitizer	Provides the heat source ('hot spot') to drive the chemical reaction of oxidizer and fuel. Sensitizers are entrapped air bubbles or pockets within the explosive.

Table 2.1 : Ingredients of blasting explosives

The most common explosive used in Sri Lanka is Ammonium Nitrate Fuel Oil (ANFO) consists of small granules of ammonium nitrate (AN) coated with a special grade of fuel oil (FO).

2.3 Blasting Geometry

The explosive blasting using electrical detonators have to be carefully planned so as to achieve the desired results. Number of bore holes, their diameter and depth, spacing between the bore holes will be decided by the size of the burden and the final rock metal sizes to be achieved as a result of the blasting. Therefore, the blasting geometry has to be carefully planned by experienced and skilled persons in the industry.

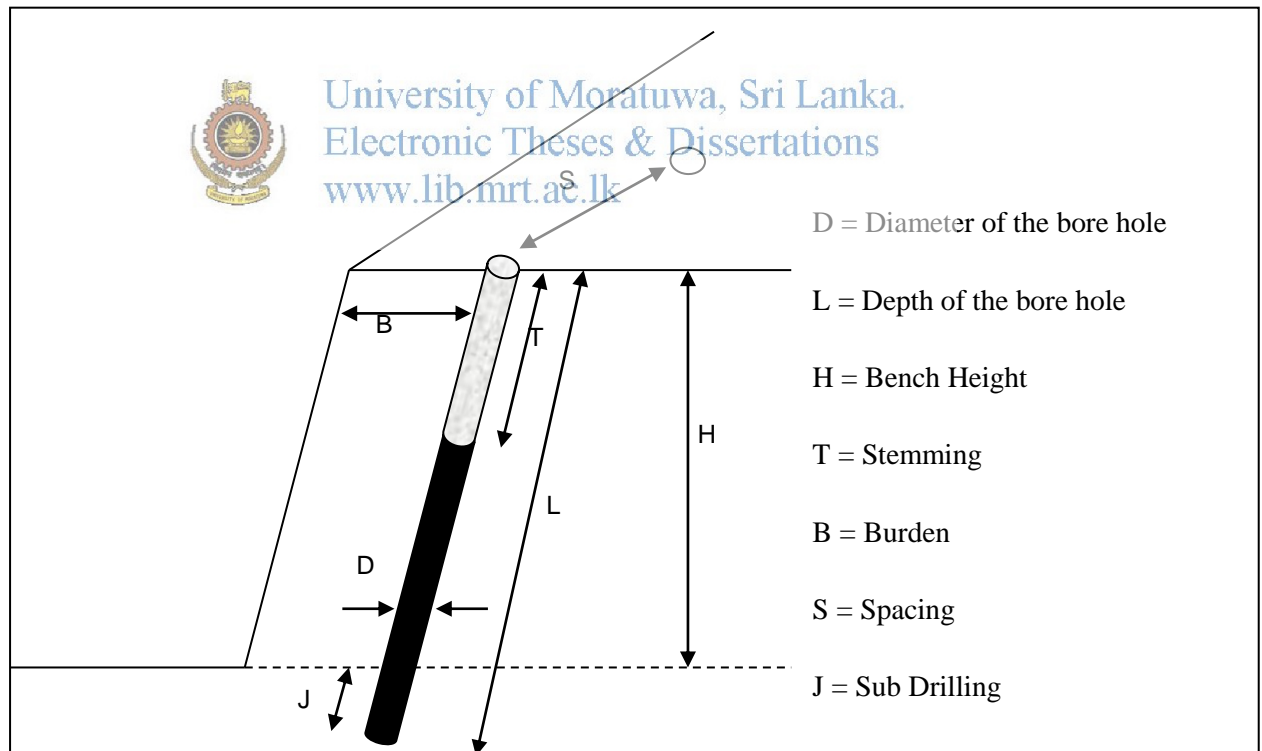


Figure 2.3: Blasting geometry

A typical example of three explosive blasting done at the Arangala blasting site by W.A. Perera & Company is given below. The drilling of bore hole details and the corresponding explosive charging are also given.

DRILLING PARAMETERS	Blast Number 01	Blast Number 02	Blast Number 03
Diameter of a bore hole	64mm	64mm	64mm
Depth of a bore hole	03m (10ft)	03m (10ft)	6m (20ft)
Burden	1.45m (4.8ft)	1.45m (4.8ft)	1.83m (6ft)
Spacing	1.52m (5.0ft)	1.52m (5.0ft)	2.2m (7ft)
No. of bore holes	10	15	03

Table 2.2 Drilling Parameters

Charging Parameters		Blast Number 01	Blast Number 02	Blast Number 03
Charge per hole	Detonators	01 Nos.	01 Nos.	01No
	Gelignite	130g	130g	390g
	NH ₄ NO ₃	1700g	1700g	6000g
Charge per blast	Detonators	10 Nos.	15 Nos.	03Nos.
	Gelignite	1.3Kg	1.95Kg	1.17Kg
	NH ₄ NO ₃	17Kg	25.5Kg	18Kg



University of Moratuwa, Sri Lanka.
Electronic Theses & Dissertations
www.lib.mrt.ac.lk

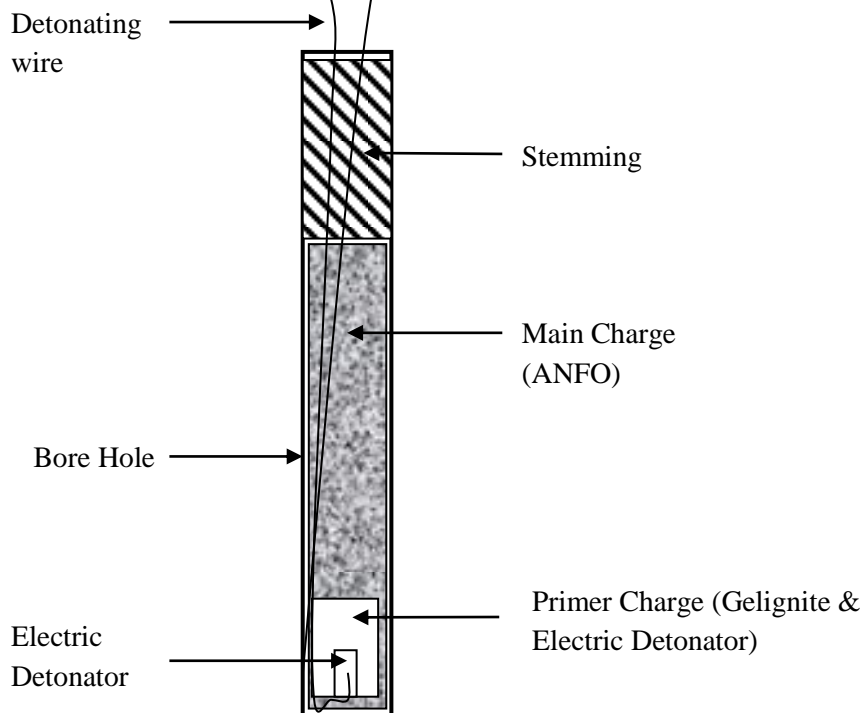


Figure 2.4: Charged Bore Hole

2.4 Detonator Circuit Arrangements

The simplest and most convenient way to connect electric detonators is in series. If one or more detonator connections are faulty then the entire circuit will not fire, eliminating the possibility of having explosive in the broken rock after firing. Connection in series allows the entire circuit to be tested for continuity and resistance from a safe place. In a parallel circuit, in which each detonator is connected across two common wires, each detonator or set of detonators is independent of the others. The circuit resistance is lower but even if one of the connections is faulty the remainder will fire, resulting in unexploded charges in the muck pile. In general, detonator circuits are connected in a combination of series and parallel loops.

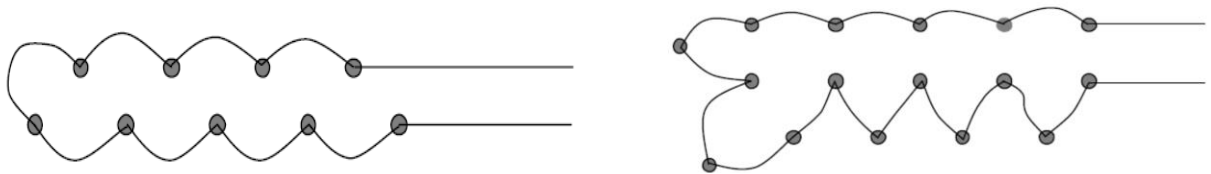


Figure 2.5: Series connected detonator circuits



Figure 2.6: Forward and reverse parallel detonator circuits

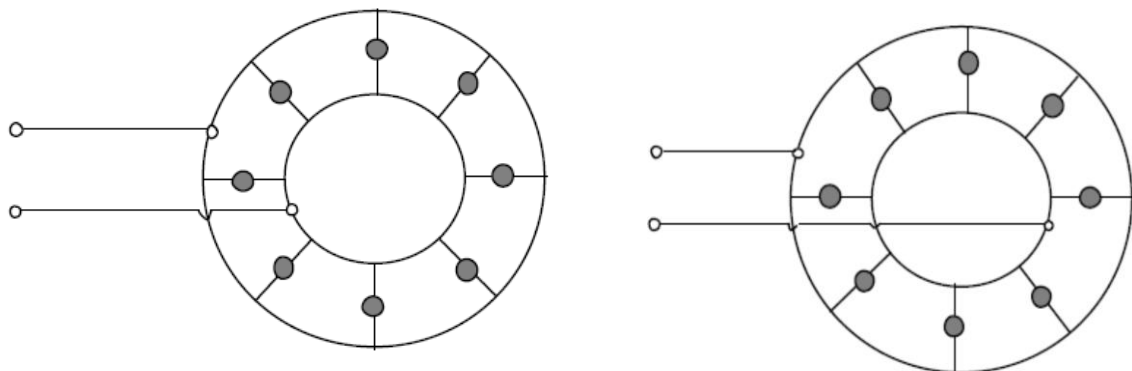


Figure 2.7: Forward and reverse parallel closed loop detonator circuits

Since electrical detonators are designed to fire when electrical energy is supplied to them, any extraneous source of electrical current represents a potential source and a threat for initiation. Sources such as lightning, high voltage transmission power lines, radio transmitters and static electricity carries severe threats in unintentional and unanticipated firing and should be avoided.

There are also occurrences where the energy from lightning travels several miles as travelling waves along the power transmission lines and this too can represent an unsuspected source for initiation of electric detonators. Direct and indirect lightning strokes could initiate the entire detonator circuit of a part of the circuit to fire. If there is any sign of thunder storms approaching or any probability of occurrence lightning, all electric detonation activities should be suspended.

2.5 Literature Survey on different modeling methods

There were three algorithms I analyzed in the modeling of electromagnetic fields around transmission lines. The features of the three algorithms I found in the literature survey are as follows.

2.5.1. Particle Swarm Optimization (PSO)

In this algorithm, the intelligence of the swarm is used to find the optimal arrangement of conductors that would produce minimum magnetic field near high voltage overhead power transmission lines. The PSO is a robust stochastic nonlinear evolutionary computation technique based on the movement and intelligence of swarms. PSO depends on the social interaction between independent agents, here called particles, during their search for the optimum solution using the concept of fitness. The fitness defines how well the position vector of each particle satisfies the requirements of the optimization problem[11].



University of Moratuwa, Sri Lanka
Electronic Theses & Dissertations
www.lib.mrt.ac.lk

It is noted that most buildings represent good conductors at 50/60 Hz frequency, and thus can shield the electric field. On the contrary, these buildings are almost transparent to magnetic fields. Based on that, only the magnetic field is minimized here, i.e., the magnetic field value is the fitness function. In fact, when we included both the magnetic and electric fields in the fitness function, we obtained essentially similar results to that when only the magnetic field is considered.

The x and y components of the velocity and the position represented by the x, y coordinates, for each particle m, are updated by the following equations[7].

$$V_{mn,x}^t = W V_{mn,x}^{t-1} + c_1 U_{n1}^t (P_{mn,x}^t - X_{mn}^{t-1}) + c_2 U_{n2}^t (g_{n,x}^t - X_{mn}^{t-1})$$

$$X_{mn,y}^t = X_{mn}^{t-1} + \Delta t (V_{mn,x}^t)$$

$$V_{mn,y}^t = W V_{mn,y}^{t-1} + c_1 U_{n1}^t (P_{mn,y}^t - y_{mn}^{t-1}) + c_2 U_{n2}^t (g_{n,y}^t - y_{mn}^{t-1})$$

$$y_{mn,y}^t = y_{mn}^{t-1} + \Delta t (V_{mn,y}^t)$$

where superscripts t and $t-1$ are time indices of the current and the previous iterations, U_{n1} and U_{n2} are two different uniformly distributed random numbers in the interval $\{0,1\}$, w is the “inertial weight” in the range $\{0,1\}$, and p_{mm} , g_n are the personal and global best positions (the subscripts x , y refer to the x and y components), respectively. The parameters c_1 and c_2 are scaling factors of local and global bests; a value of 2 is a good choice for both parameters [7]. The subscript m is the particle number in the swarm while n indicates the parameter to be optimized, and the time-step Δt is usually chosen to be one.

2.5.1.1 Solution Algorithm

The following algorithm minimizes the magnetic field under overhead transmission lines.

- I. Specify the constraints of the problem: minimum spacing between conductors, and limits of the region in which the particles will search for suitable arrangement of conductors (see Fig. 1).
- II. Distribute the particles (different arrangements of conductors) in the selected region, specify a time step for particle movement (here unity), initialize the population with a random velocity (v) vector (here zero initial velocity), and initialize the stop criterion with a value much smaller than $4.0 \mu\text{T}$. Specify the maximum number of iterations that should not be exceeded.
- III. Evaluate the fitness function (here the magnetic field value) for each particle.
- IV. If the magnetic field value $<$ the personal best value, then replace the personal best value by the new magnetic field value.
- V. If the magnetic field value $<$ the global best value, then replace the global best value by the new magnetic field value.
- VI. If the fitness is \leq the stop criterion or maximum number of iterations is reached, then stop; a solution is found. Otherwise, update position and velocity of particles according to (1) ($c_1=c_2=2$ and $w=0.7$), and go to step 3.

2.5.2 Finite Element Method

In this method, a two-dimensional finite element model is built lateral to the transmission line. The potential distribution over each element is approximated by a polynomial. Instead of solving the field equations directly, the principle of minimum potential energy is used to obtain the potential distribution over the whole model.

The ratio of the largest size to the smallest size in a finite element model of a transmission line is about 10,000. The circular boundary of the model has a radius of about 100 m, while the radius of the conductors is a few centimeters. Therefore, special attention must be paid to obtain a regular mesh with well-formed elements. This ensures an accurate solution of the field problem. Figure 1.3 shows part of the finite element model around a set of the phase conductors [12].

A mathematical model of electric fields (\mathbf{E}) radiating around a transmission line is usually expressed in the wave equation (Helmholtz's equation) as derived from Faraday's law[1].

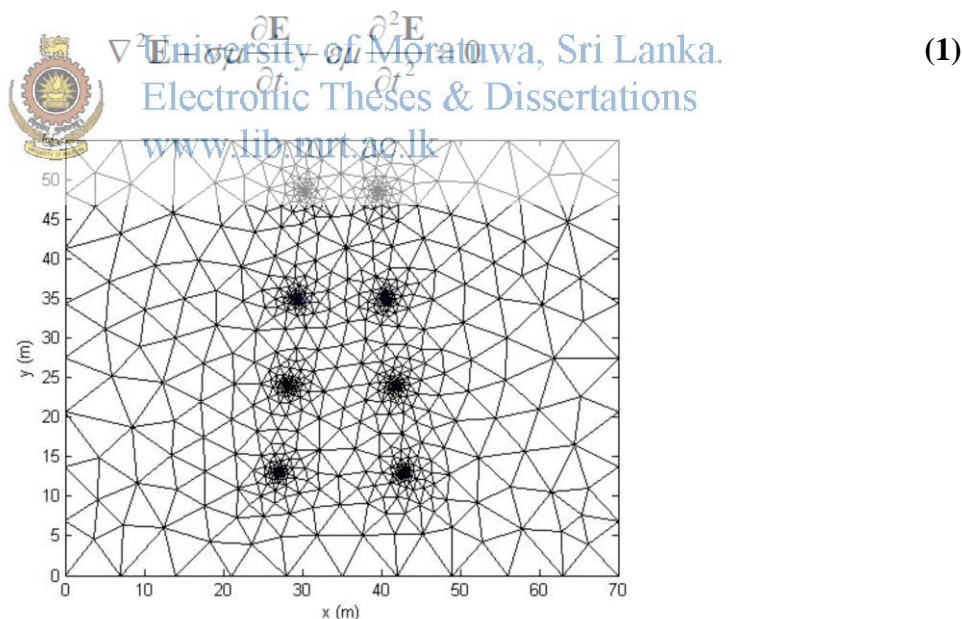


Figure 2.8 Discretization of the System[12]

A mathematical model of magnetic fields (\mathbf{B}) for transmission lines is performed in form of the magnetic field intensity (\mathbf{H}), which related to the equation, $\mathbf{B} = \mu\mathbf{H}$. This model can be characterized by using the wave equation (Helmholtz's equation) derived from the Ampere's law[1].

$$\nabla^2 \mathbf{H} - \sigma\mu \frac{\partial \mathbf{H}}{\partial t} - \epsilon\mu \frac{\partial^2 \mathbf{H}}{\partial t^2} = 0 \quad (2)$$

Due to the similarity between (1) and (2), formulation of the FEM used for the magnetic field problems is mathematically the same. One can point out this similarity by replacing the electric field (\mathbf{E}) with the magnetic field intensity (\mathbf{H}). This paper has considered the system governing by using the time harmonic mode and representing the electric field in complex form, $\mathbf{E} = Ee^{j\omega t}$, therefore,

$$\frac{\partial \mathbf{E}}{\partial t} = j\omega E \quad \text{and} \quad \frac{\partial^2 \mathbf{E}}{\partial t^2} = -\omega^2 E$$

employing the complex form of the electric fields and assuming that the system is excited with a single frequency source, Equation (1) can be transformed to an alternative form as follows.

$$\nabla^2 E - j\omega\sigma\mu E + \omega^2\epsilon\mu E = 0$$

The overhead transmission lines are essentially unbounded. Applying Dirichlet constraints at an outer circular boundary surface at a finite distance from the transmission lines, the potential distribution will not correspond to the real distribution and will be somewhat compressed. The earth is supposed to have an infinite conductivity, yielding the electric field lines to be perpendicular to surface. It has to be mentioned that the unbounded system may be avoided using a special technique dealing with the open boundary problems [12]. The accuracy of the finite element solution depends not only on the element distribution, but also on the order of the finite element approach.

2.5.3. Analytical Method

This is the method that is used in modeling the electric and magnetic fields around the transmission lines in this research paper. The models are derived from fundamental principles of electromagnetism and possess high accuracy when compared with the field measuring values also. The electric field is modeled assuming the line conductors to be equivalent charges and the magnetic field is represented in the vectorial form in the analysis.

2.6 Specification of a typical detonator

The specification for Supreme short delay detonators used in Sri Lanka is given as **Annex 2**.

MODELING THE ELECTROMAGNETIC FIELD AROUND TRANSMISSION LINE

3.1 Electric Field Modeling

3.1.1 Assumptions;

1. The conductors are infinitely long and straight.
2. The earth is a perfect conductor.
3. The permittivity of air is independent of weather and equal to the permittivity of free space.
4. Shielding effects from structures at ground potential are ignored.

From Coulomb's Law, for charges of Q_1 & Q_2 , it is empirically derived that,

$$F = \frac{Q_1 \cdot Q_2}{4\pi\epsilon_0 R^2} \quad \text{in Newtons}$$

Electric field intensity E is the vector force on a unit positive charge

$$E = \frac{F}{Q}$$

$$E = \frac{Q}{4\pi\epsilon_0 R^2} \hat{a}_R \quad \text{or} \quad E_r = \frac{Q}{4\pi\epsilon_0 r^2}$$


University of Moratuwa, Sri Lanka.
Electronic Theses & Dissertations
www.lib.mrt.ac.lk

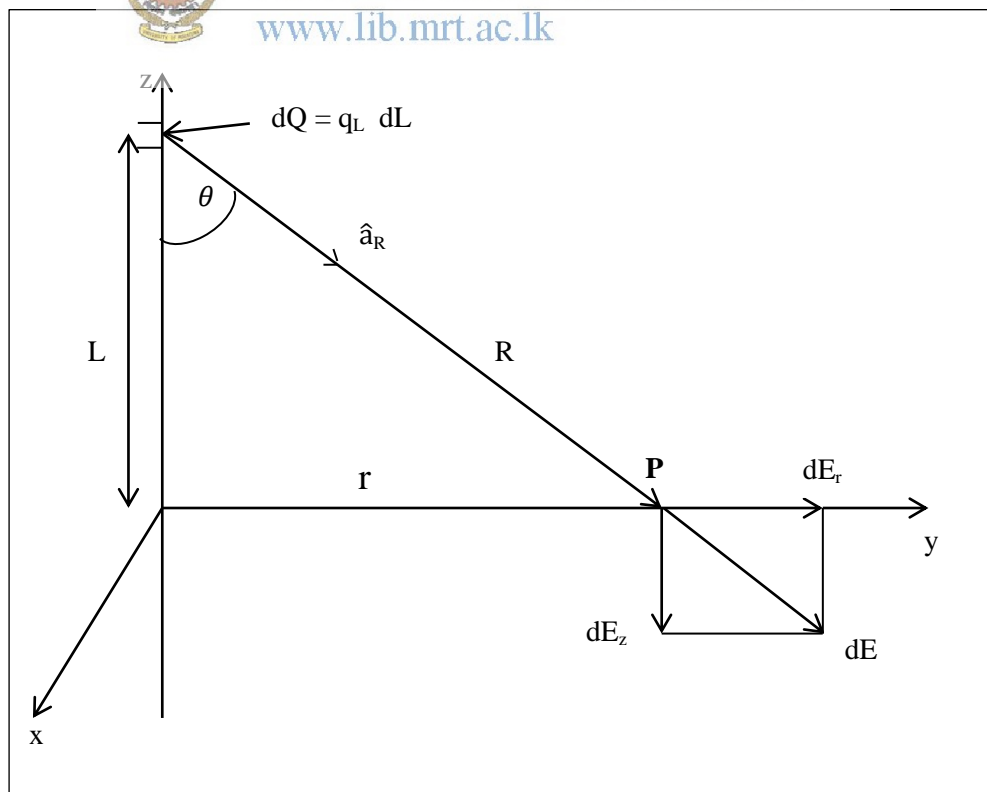


Figure 3.1 Field of a line charge (for an infinitely long conductor)

In a cylindrical coordinate system, as shown in the figure 3.1, the electrical field intensity, E at any and every point resulting from a uniform line charge density q_L could be determined as follows. Incremental field at P due to incremental charge

$$dQ = q_L dL \quad \text{we have}$$

$$dE = \frac{q_L dL}{4\pi\epsilon_0 R^2} \quad \text{or}$$

$$dE_r = \frac{q_L dL \sin \theta}{4\pi\epsilon_0 R^2} = \frac{q_L dL}{4\pi\epsilon_0 R^2} \cdot \frac{y}{R} = \frac{q_L dL r}{4\pi\epsilon_0 R^3}$$

Replacing $R^2 = L^2 + r^2$ and summing the contributors from every element of charge

$$E_r = \int_{-\infty}^{\infty} \frac{q_L r dL}{4\pi\epsilon_0 (L^2 + r^2)^{3/2}}$$

$$= \frac{q_L}{2\pi\epsilon_0} r \left[\frac{1}{r^2} \frac{L}{\sqrt{L^2 + r^2}} \right]_{-\infty}^{\infty}$$



University of Moratuwa, Sri Lanka.
Electronic Theses & Dissertations
www.lib.mrt.ac.lk

$$E_r = \frac{q_L}{2\pi\epsilon_0 r}$$

(3.1)

3.1.2 Electric field and electric potential

By definition of Potential difference, over a small length of δl if the potential drop is δv ,

$$\text{then } \delta v = - E \cdot \delta l$$

$$E = - \frac{\partial v}{\partial l}$$

Components in x, y, z direction

$$E_x = - \frac{\partial v}{\partial x}, \quad E_y = - \frac{\partial v}{\partial y} \quad \& \quad E_z = - \frac{\partial v}{\partial z}$$

At any point $\mathbf{E} = i_x E_x + i_y E_y + i_z E_z$

$$= -\left\{ i_x \left[\frac{\partial v}{\partial x} \right] + i_y \left[\frac{\partial v}{\partial y} \right] + i_z \left[\frac{\partial v}{\partial z} \right] \right\}$$

$$\mathbf{E} = -\text{grad } V = -\nabla V$$

(3.2)

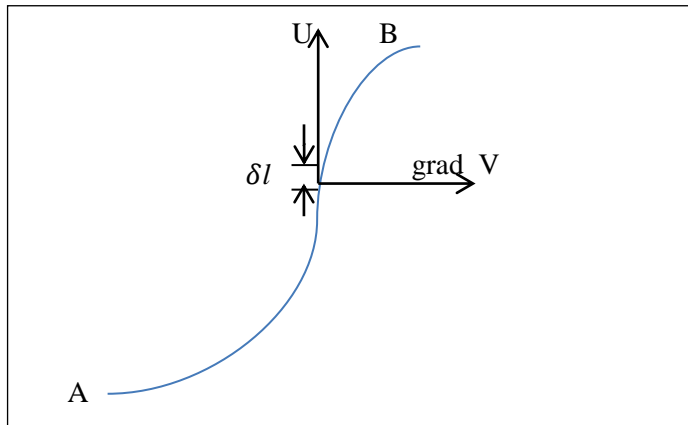


Figure 3.2 Incremental potential difference
 University of Moratuwa, Sri Lanka.
 Electronic Theses & Dissertations
www.lib.mrt.ac.lk

Potential Difference

$$V_B - V_A = \int_A^B \left(\frac{\partial v}{\partial l} \right) \cdot dl$$

$$\left[\frac{\partial v}{\partial l} \right] dl = dV = (\text{grad } V) \cdot dl$$

$$V_A - V_B = \int_A^B (\text{grad } V) \cdot dl$$

Z components cancels off . Hence,

$$\vec{E}(x, y) = -\nabla \cdot V(x, y)$$

(3.3)

For any infinitely long straight line charge

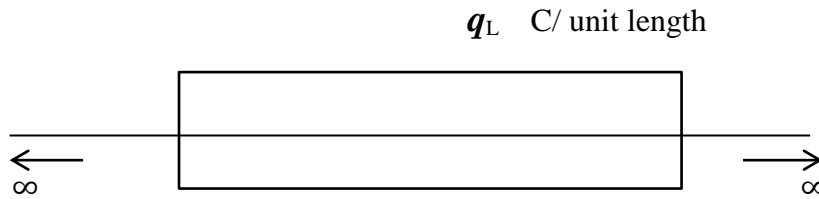


Figure 3.3 Cylindrical Gaussian Surface

For a suitable Gaussian Surface of concentric cylinder of radius r ,

$$\mathbf{E} = \frac{q_L}{2\pi\epsilon_0 r} \hat{\mathbf{r}}$$

For evaluation of the potential (work done in bringing a unit charge from infinity)



3.1.3 Addition of Potential Line charges ;

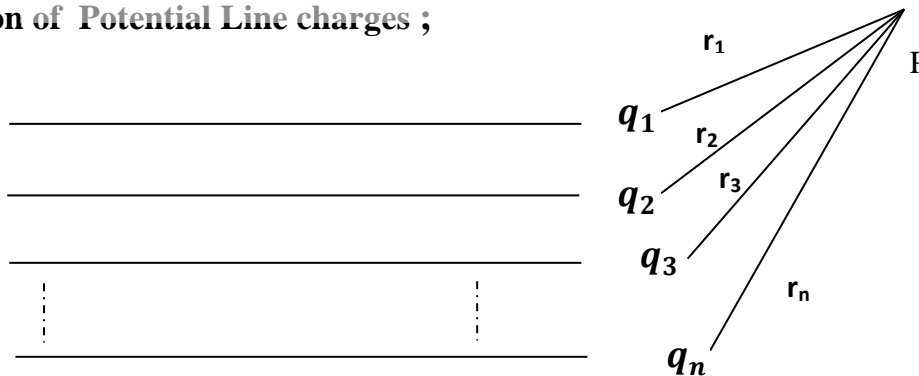


Figure 3.4 Group of line charges

For a group of line conductors, by using the principle of superposition,

$$V_p = \left[\frac{1}{2\pi\epsilon_0} \right] (q_1 \ln(r_1) + q_2 \ln(r_2) + \dots + q_n \ln(r_n))$$

Considering the special case of when there are two line charges and they are equal and opposite,

$$V_p = \left[\frac{q}{2\pi\epsilon_0} \right] \{ \ln(r_1) - \ln(r_2) \} \tag{3.4}$$

3.1.4 Modeling the line charges

$$d_{eq} = D \sqrt[n]{\frac{n \cdot d}{D}}$$

$$D = \frac{S}{\sin \pi/n}, \quad r_{eq} = (N \cdot r \cdot R^{N-1})^{1/N}$$

D – Bundle Diameter

d – sub conductor diameter

r – sub conductor radius

N, n – no. of sub conductor

S – sub conductor spacing

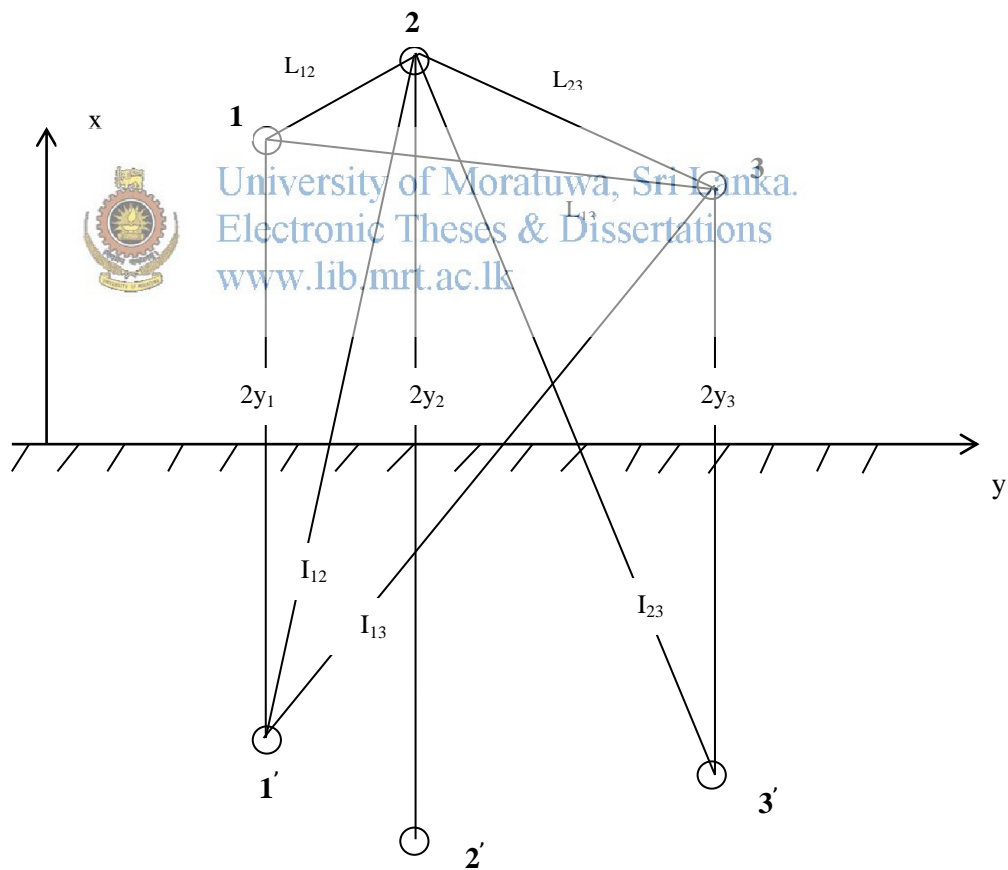


Figure 3.5 Multi-conductor line for calculation of Maxwell's potential coefficients

Starting from Gauss's Law and from equation 3.3, it can be derived that the potential of conductor 1 due to its own charge and its image charge with respect to ground,

$$V_{1,1} = \left(\frac{q_1}{2\pi\epsilon_0} \right) \ln \left(\frac{2y_1}{d/2} \right)$$

$$\begin{aligned}
&= \left(\frac{q_1}{2\pi\epsilon_0} \right) \ln \frac{\text{Distance of cond. from negative charge}}{\text{distance of cond. from positive charge}} \\
&= \left(\frac{q_1}{2\pi\epsilon_0} \right) \cdot P_{11}
\end{aligned}$$

$$P_{11} = \ln \left(\frac{2y_1}{d/2} \right) - \text{Maxwell's self-potential coefficient}$$

Similarly,

$$\begin{aligned}
V_{1,2} &= \left(\frac{q_2}{2\pi\epsilon_0} \right) \ln \frac{\text{Distance of cond. from } -q_2}{\text{distance of cond. from } +q_2} = \left(\frac{q_2}{2\pi\epsilon_0} \right) \ln \left(I_{12}/L_{12} \right) \\
&= \left(\frac{q_2}{2\pi\epsilon_0} \right) \cdot P_{12}
\end{aligned}$$

For a system of n conductors (or phases) above ground, the potentials of conductors will be,

$$\begin{aligned}
V_1 &= \frac{Q_1}{2\pi\epsilon} \ln \left(\frac{2Y_1}{r} \right) + \frac{Q_2}{2\pi\epsilon} \ln \left(\frac{I_{12}}{L_{12}} \right) + \dots + \frac{Q_n}{2\pi\epsilon} \ln \left(\frac{I_{1n}}{L_{1n}} \right) \\
V_n &= \frac{Q_1}{2\pi\epsilon} \ln \left(\frac{I_{1n}}{L_{1n}} \right) + \frac{Q_2}{2\pi\epsilon} \ln \left(\frac{I_{2n}}{L_{2n}} \right) + \dots + \frac{Q_n}{2\pi\epsilon} \ln \left(\frac{2Y_{1n}}{r} \right)
\end{aligned}$$



University of Moratuwa, Sri Lanka.
Electronic Theses & Dissertations
www.lib.mrt.ac.lk

In Matrix form $[V]_n = [P]_{nn} [Q]_n$

$[V]_n = [V_1, V_2, \dots, V_n]_n$ - Potentials with respect to ground

$[Q]_n = [Q_1, Q_2, \dots, Q_n]_t$ - Conductor charges

$[P]_{nn}$ - Maxwell's Potential Matrix

$$P_{ii} = \frac{1}{2\pi\epsilon} \ln \left(\frac{4y_i}{d_i} \right) \quad \text{for } i = j$$

Considering x,y co-ordinate system,

$$I_{ij} = \left[(x_i - x_j)^2 + (Y_i + Y_j)^2 \right]^{\frac{1}{2}} \quad \text{and} \quad L_{ij} = \left[(x_i - x_j)^2 + (Y_i - Y_j)^2 \right]^{\frac{1}{2}}$$

$$P_{ij} = \frac{1}{2\pi\epsilon} \ln \left[\frac{(x_i - x_j)^2 + (Y_i + Y_j)^2}{(x_i - x_j)^2 + (Y_i - Y_j)^2} \right]^{\frac{1}{2}} \quad \text{for } i \neq j$$

And,

$$[Q] = [P]^{-1} [V]$$

← Array of phase – earth voltage (kV)
← Inverse of Maxwell Potential Matrix $\left(\frac{m}{F}\right)$

Line Charge

The capacitance matrix of the n-conductor system is;

$$[C]_{nn} = 2\pi\epsilon \cdot [P]_{nn}^{-1} = 2\pi\epsilon [M]_{nn}$$

$$[P] = \begin{bmatrix} P_{11} & P_{21} & P_{31} & \dots & P_{i1} & \dots & P_{n-11} & P_{n1} \\ P_{12} & P_{22} & P_{32} & & & & & \\ P_{13} & P_{23} & P_{33} & & & & & \\ & P_{24} & & & & & & \\ & & & & & & & \\ P_{1j} & \dots & \dots & \dots & P_{ij} & \dots & \dots & \\ & & & & & & & \\ P_{1n-1} & & & & & & & \\ P_{1n} & \dots & \dots & \dots & \dots & \dots & \dots & P_{nn} \end{bmatrix}_{n \times n}$$

Once the Potential Matrix is known, the inverse of the matrix, $[P]^{-1}$ could be determined.

Since, $[P]^{-1}$ is known,

$[Q] = [P]^{-1} [V]$ could be determined .

3.1.5 Representation of line voltage in phasor form

$$V_i = (V_{ph-ph\ rms}) \angle \text{phase angle } \phi_i$$

$$V_i = \frac{V_{pp\ rms}}{\sqrt{3}} \cos(\phi_i) + j \frac{V_{pp\ rms}}{\sqrt{3}} \sin(\phi_i)$$

\swarrow
 $\sqrt{-1}$

$$[V]_n = (V_i)_{n \times 1} \quad \text{kV}$$

$$[V] = \begin{bmatrix} V_{a_1} \\ V_{b_1} \\ V_{c_1} \\ \vdots \\ V_{e_n} \end{bmatrix} \qquad [Q] = \begin{bmatrix} Q_{a_1} \\ Q_{b_1} \\ Q_{c_1} \\ \vdots \\ Q_{e_n} \end{bmatrix}$$



University of Moratuwa, Sri Lanka.
Electronic Theses & Dissertations

www.lib.mrt.ac.lk

Considering the real and imaginary components,

$$[Q]_n = (q_i)_{n \times 1} = (q_i(\text{re}) + j q_i(\text{im}))_{n \times 1}$$

$$= [Q_{\text{re}}] + j [Q_{\text{im}}]$$

$$[Q_{\text{re}}] = [P]^{-1} [V_{\text{re}}] \quad \text{and} \quad [Q_{\text{im}}] = [P]^{-1} [V_{\text{im}}]$$

3.1.6 Electrical field at a point in space

For a line charge of Conductor i with its mirror image,

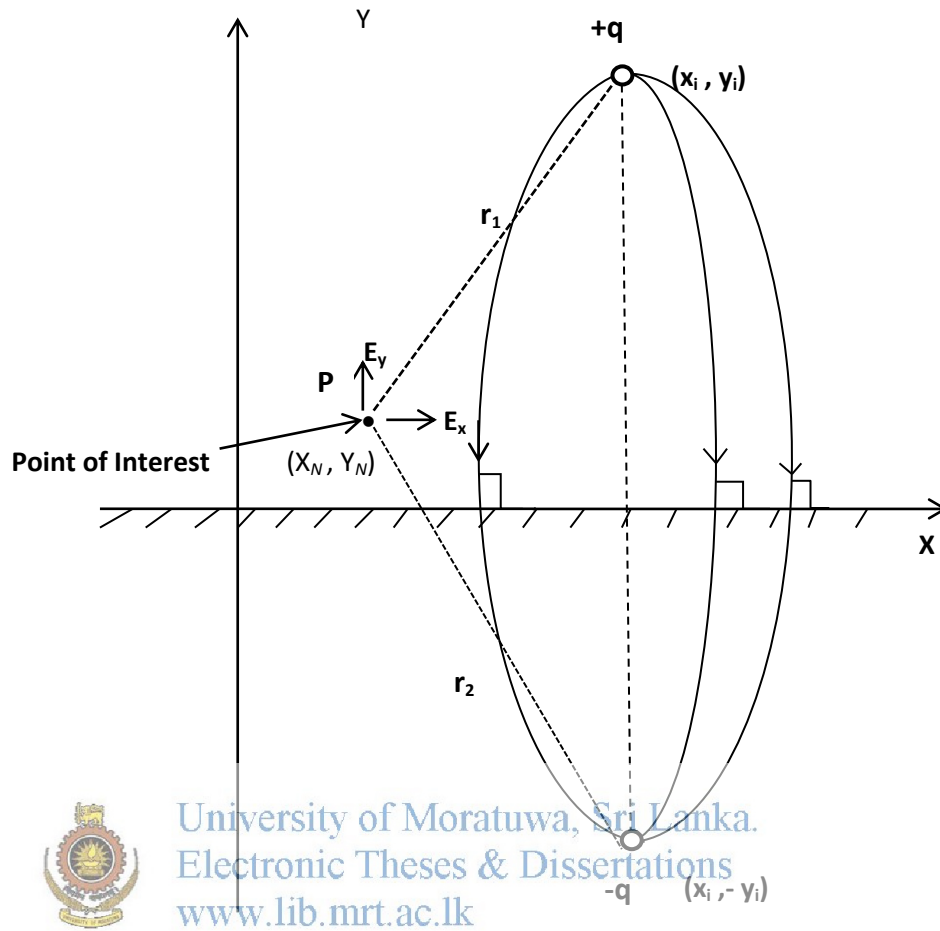


Figure 3.6 Electric field at a point in space due to charge q and its mirror image

$$V_P = \left\{ \frac{q}{2\pi\epsilon} \ln \frac{r_1}{Y_i} - \frac{q}{2\pi\epsilon} \ln \frac{r_2}{Y_i} \right\} = V_{N,i}$$

$$r_1 = \sqrt{(X_i - X_N)^2 + (Y_i - Y_N)^2} \quad , \quad r_2 = \sqrt{(X_i - X_N)^2 + (Y_i + Y_N)^2}$$

$$V_{N,i} = \frac{q}{2\pi\epsilon_0} \left\{ \ln \left(\frac{\sqrt{(X_i - X_N)^2 + (Y_i - Y_N)^2}}{Y_i} \right) - \ln \left(\frac{\sqrt{(X_i - X_N)^2 + (Y_i + Y_N)^2}}{Y_i} \right) \right\}$$

For the total charge in the i^{th} conductor q_i

$$q_i = q_{r,i} + j q_{im,i}$$

$$V_{N,i} = \frac{(q_{r,i} + j q_{im,i})}{2\pi\epsilon} \left\{ \ln \left(\frac{\sqrt{(X_i - X_N)^2 + (Y_i - Y_N)^2}}{Y_i} \right) - \ln \left(\frac{\sqrt{(X_i - X_N)^2 + (Y_i + Y_N)^2}}{Y_i} \right) \right\} \quad (3.4)$$

The space potential is due to all conductors 1, 2, 3 n

$$V_N = V_{N,1} + V_{N,2} + V_{N,3} + \dots + V_{N,n} = \sum_{i=1}^n V_{N,i} \quad (3.5)$$

$$= V_{rN} + j V_{imN}$$

$$|V_N| = (V_{rN}^2 + V_{imN}^2)^{1/2}$$

From equation 3.2, we have

$$\vec{E}(x, y) = -\nabla V(x, y)$$

Therefore,

$$E_{x,i} = \frac{(q_{r,i} + j q_{im,i})}{2\pi\epsilon_0} \left\{ \frac{(X_N - X_i)}{(X_i - X_N)^2 + (Y_i - Y_N)^2} - \frac{(X_N - X_i)}{(X_i - X_N)^2 + (Y_i + Y_N)^2} \right\}$$

$$E_{y,i} = \frac{(q_{r,i} + j q_{im,i})}{2\pi\epsilon_0} \left\{ \frac{(Y_N - Y_i)}{(X_i - X_N)^2 + (Y_i - Y_N)^2} - \frac{(Y_N - Y_i)}{(X_i - X_N)^2 + (Y_i + Y_N)^2} \right\}$$



University of Moratuwa, Sri Lanka
Electronic Theses & Dissertations
www.lib.mrt.ac.lk

Horizontal components and vertical components of E_x , E_y are calculated for all the conductors, 1, 2, 3 n

$$\vec{E}_x = E_{x,1} + E_{x,2} + \dots + E_{x,n} = \sum_{i=1}^n E_{x,i}$$

$$\vec{E}_y = E_{y,1} + E_{y,2} + \dots + E_{y,n} = \sum_{i=1}^n E_{y,i}$$

$$\vec{E}_x = \vec{E}_{x,re} + j \vec{E}_{x,im} \quad \vec{E}_y = \vec{E}_{y,re} + j \vec{E}_{y,im}$$

$$\vec{E}_{re} = E_{x,re} \cdot \hat{u}_x + E_{y,re} \cdot \hat{u}_y \quad \hat{u}_x, \hat{u}_y \text{—Unit vectors in the directions of } x \text{ \& } y$$

$$\vec{E}_{im} = E_{x,im} \cdot \hat{u}_x + E_{y,im} \cdot \hat{u}_y$$

3.1.7 Magnitude of E

$$E = \sqrt{|E_{re}^2| + |E_{im}^2|}$$

$$= \sqrt{E_{x,re}^2 + E_{x,im}^2 + E_{y,re}^2 + E_{y,im}^2}$$

$$\text{Phase } \angle : \theta_r = \tan^{-1} \left(\frac{E_{im}}{E_{re}} \right)$$

3.1.8 Calculation of potential

From equations 3.5 & 3.4.

$$V_{N,i} = \frac{(q_{r,i} + j q_{im,i})}{2\pi\epsilon} \left\{ \ln \left(\frac{\sqrt{(X_i - X_N)^2 + (Y_i - Y_N)^2}}{Y_i} \right) \right\}$$

$$- \frac{(q_{r,i} + j q_{im,i})}{2\pi\epsilon} \left\{ \ln \left(\frac{\sqrt{(X_i - X_N)^2 + (Y_i + Y_N)^2}}{Y_i} \right) \right\}$$

$$V_N = \sum_{i=1}^n V_{N,i}$$

$$V_N = V_{N,re} + j V_{N,im}$$

Magnitude of Potential is given by

$$V_N = \sqrt{\left(\sum_{i=1}^n V_{i,re} \right)^2 + \left(\sum_{i=1}^n V_{i,im} \right)^2}$$

3.1.9 Flow chart for modeling & simulation of electric field around transmission line

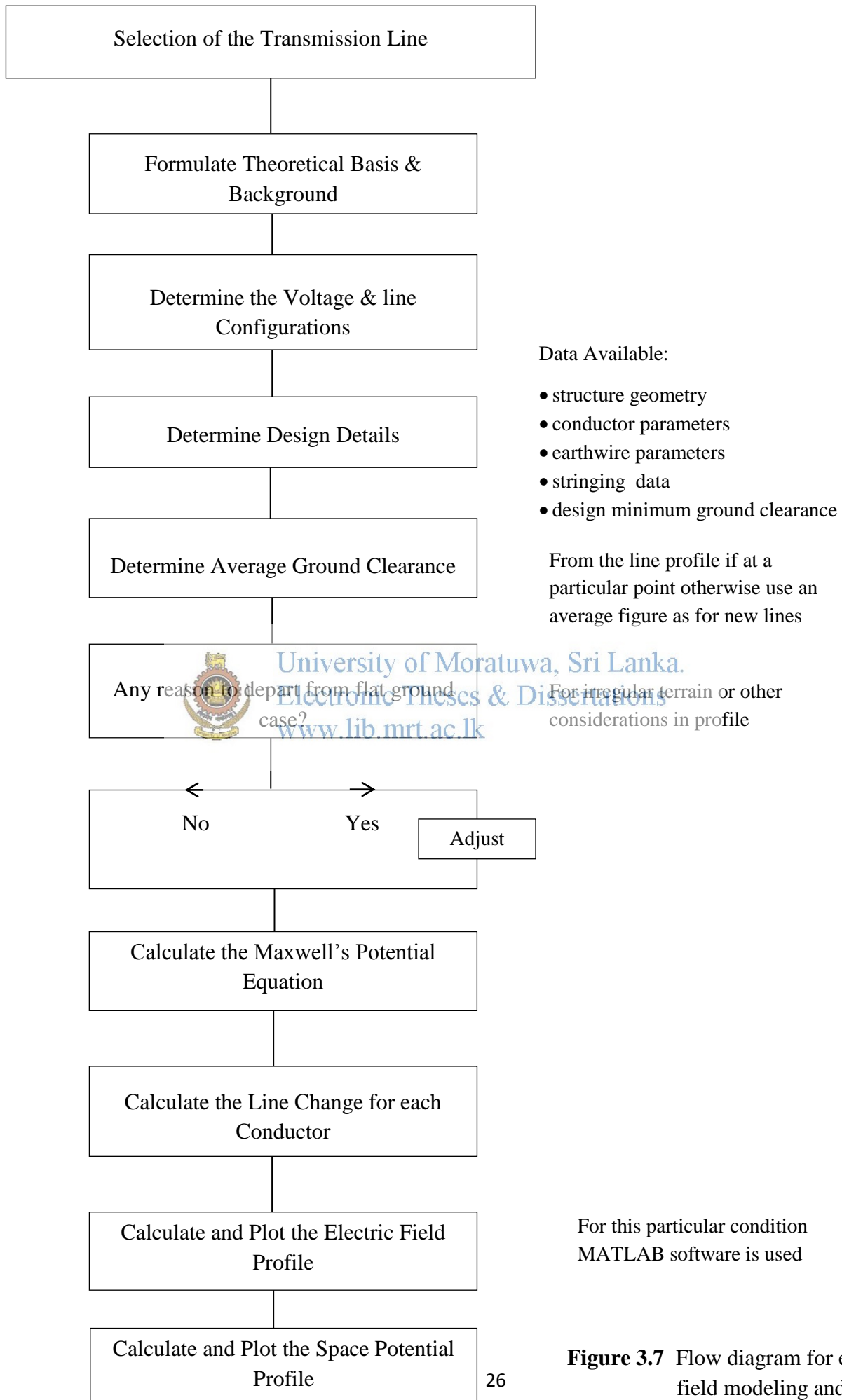


Figure 3.7 Flow diagram for electric field modeling and simulation

3.1.10 Transmission line data

Transmission line data, like the minimum clearance from ground, height of conductors at the tower level, the length of the basic span, distance of conductors from the tower center, number of conductors, conductor spacing in the bundle and the conductor diameter were considered in developing the model. Data for Three tower types, TDL, TDL+6 and TDL+12 used in Sri Lanka are given in Table 3.1 and 3.2 for 132kV and 220kV lines.

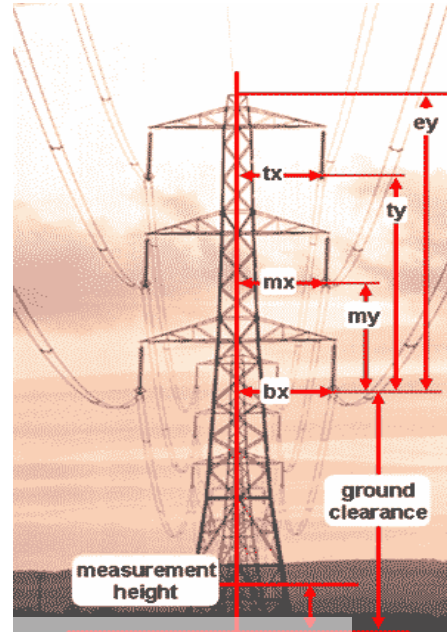


Figure 3.8 Transmission line parameters

conductor	dimension direction	code on diagram	Voltage	tower type			units
				TDL	TDL+6	TDL+12	
earth wire	horizontal from tower centre	Double EW	220kV	6720	6720	6720	mm
	vertical above bottom phase	ey		19925	19925	19925	mm
top phase	horizontal from tower centre	tx		6720	6720	6720	mm
	vertical above bottom phase	ty		11375	11375	11375	mm
middle phase	horizontal from tower centre	mx		6900	6900	6900	mm
	vertical above bottom phase	my		5800	5800	5800	mm
bottom phase	horizontal from tower centre	bx		7800	7800	7800	mm
	Ground to Bottom Phase	-		17710	23710	29710	mm
	Minimum Ground Clearance			7010	13010	19010	mm
conductor bundle	Number of conductors			2	2	2	
	Spacing			200	200	200	mm
	Diameter			28.62 (ACSR, Zebra)			mm

Table 3.1 220kV double circuit transmission line data

Dimensions		Code on diagram	Voltage	tower type			units
Conductor	Direction			TDL	TDL+6	TDL+12	
Earth wire	horizontal from tower centre	Double EW	132kV	3660	3660	3660	mm
	vertical above bottom phase	ey		14290	14290	14290	mm
Top phase	horizontal from tower centre	tx		3660	3660	3660	mm
	vertical above bottom phase	ty		8530	8530	8530	mm
Middle phase	horizontal from tower centre	mx		3705	3705	3705	mm
	vertical above bottom phase	my		4230	4230	4230	mm
Bottom phase	horizontal from tower centre	bx		4010	4010	4010	mm
	Ground to Bottom Phase	-		15235	21235	27235	mm
	Minimum Ground Clearance			6700	12700	18700	mm
Conductor in bundle	number of conductors			2	2	2	
	Spacing			200	200	200	mm
	Diameter			28.62 (ACSR, Zebra)			mm

Table 3.2 132kV double circuit transmission line data

33kV Vertical Double Circuit Dimensions		Max.	Min.	units
Conductor	Direction			
Top phase	horizontal from tower centre	3.0	2.5	m
	vertical to bottom	3.0	2.4	m
middle phase	horizontal from tower centre	3	2.5	m
	vertical to bottom	1.5	1.2	m
Bottom phase	horizontal from tower centre	3.2	2.7	m
	vertical to ground	13	6.5	m
conductor	number of conductors	1	1	
	diameter	12.3/19.6		mm
	vertical to ground	13	6.5	m

Table 3.3 33kV Double circuit transmission line data

Dimensions for Horizontal Formation		Max.	Min.	Units
Conductor	Direction			
Right phase	horizontal from tower centre	0.95	0.95	m
	vertical to ground	13	5	m
middle phase	horizontal from tower centre	0	0	m
	vertical to ground	13	5	m
Left phase	horizontal from tower centre	0.95	0.95	m
	vertical to ground	13	5	m
conductor	number of conductors	1	1	
	diameter	12.3		mm

Table 3.4 33kV horizontal configuration line data

Triangular Formation Dimensions		Max.	Min.	Units
Conductor	Direction			
Top phase	horizontal from tower centre	0	0	m
	vertical to lower phase	2.0	2.0	m
Lower left phase	horizontal from tower centre	1.6	1.6	m
	vertical to ground	13	6.5	m
Lower right phase	horizontal from tower centre	1.6	1.6	m
	vertical to ground	13	6.5	m
conductor	number of conductors	1	1	
	diameter	12.3		mm

Table 3.5 33kV triangular configuration line data

3.1.11 Average conductor height above ground

The input for field calculation requires an “average conductor height” - which is determined by ground clearance (at certain load conditions) and sag (at the same set of conditions). It is assumed that the ground is flat unless there is sufficient information available to make an assessment for the case being considered.

It can be shown (using parabolic equations) that the average conductor sag is 2/3 of overall sag when measured from the points of attachment. Alternatively, the average conductor height is equal to ground clearance at the low point of the parabola, plus 1/3 sag. Conductor electrical loading (calculated or assumed) causes a conductor temperature rise above ambient but the temperature will normally remain below that corresponding to maximum design load (minimum (design) ground clearance is based on this maximum load).

Typical Inputs for Field Calculations		
Input	Existing Line	Typical Values for 220kV D/C lines
(a) Reference height for field calculations:	Known	1m
(b) Overhead Earthwire data:		
- No. of wires	Known	2
- X and Y coordinates of each wire	Known	6.72m, 31.56m
- size (diameter) of wires	Known	18.2mm
(c) Phase Conductor data:		
- No. of phase conductors	Known	4
- X, Y coordinates-bundle/conductor	Known	Considered for Each phase separately
- size (diameter) of wires	Known	28.62mm
- sub-conductor spacing	Known	200mm
(e) Voltage details for Conductors:		
- phase to phase voltage	Known	220kV
- phase angle	Known	0, 120, 240
(e) Current details for Conductors:		
- current and direction in each wire	Known	Considered for Each phase separately
- phase angle for each current	Known	0, 120, 240
(f) Earths conductivity	Known / Assumed	0.001 – 0.002 S/m

Table 3.6 Typical input data for electric and magnetic field calculations

3.1.11.1 Average height above ground = (minimum ground clearance at max design temperature) + (additional height due to assumed operating temperature below max design temperature) + (1/3 sag at that assumed operating temperature).

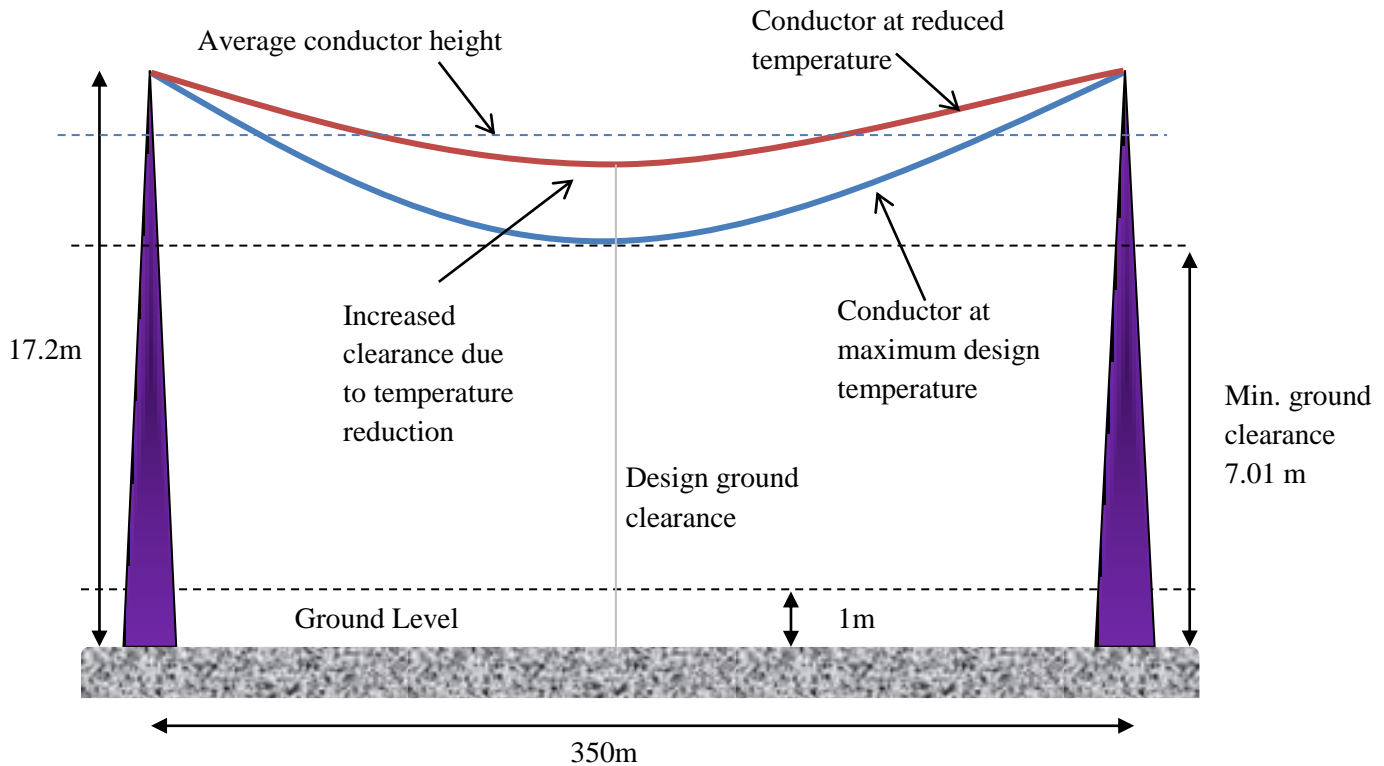


Figure 3.9 The average height above ground calculation for 220kV lines



University of Moratuwa, Sri Lanka.
Electronic Theses & Dissertations
www.lib.mrt.ac.lk

Voltage (kV)	Basic Span (m)	Ground Clearance (m)	Buffer (m)	Sag @ EDS (Average Daily Stress)(m)	Sag @ Maximum Temperature (75oC)(m)	Average Ground Clearance (m)
220	350	7	0.3	8.637	10.316	11.558
132	300	6.7	0.3	6.214	7.793	10.350
33	300	5.5	0.3	5.255	6.812	8.808

Table 3.7 Calculation of average ground clearance

3.1.12 Simulations using MATLAB

Once all the data was available, MATLAB programming was used for determining the electric field profiles. MATLAB is a programming language that is widely used as a tool for numerical computation and visualization. It was originally designed for solving linear algebra type problems using matrices. Its name is derived from MATrix LABoratory. For array based input data, MATLAB is a handy tool for rigorous and complicated calculations.

The MATLAB code written for 220kV double circuit twin zebra configuration is attached as **Annex 3**. Some of the profiles drawn are given below. The model develop can accommodate

any number of conductors in any configuration and takes the effect of earth conductors also into consideration in calculations.

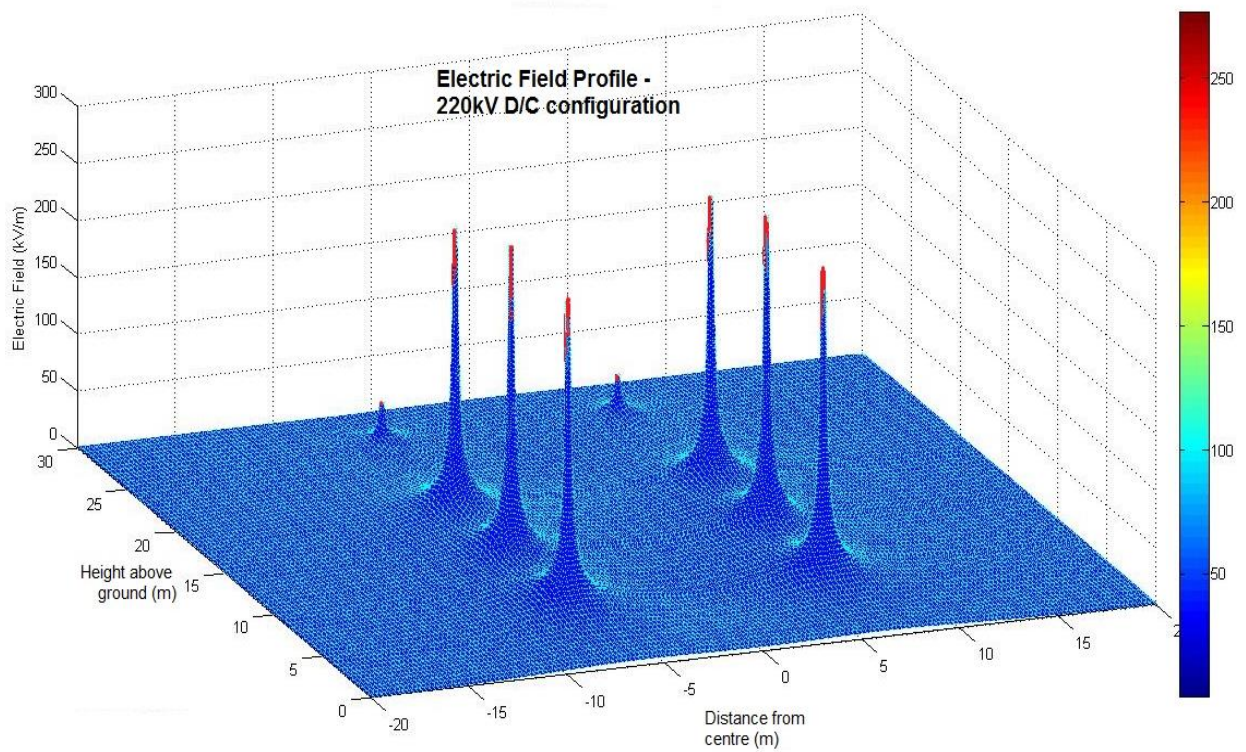


Figure 3.10 Electric field variation with height above ground
 University of Moratuwa, Sri Lanka.
 Electronic Theses & Dissertations
www.lib.mrt.ac.lk
 Electric Field Profile variation 0 - 5m above ground

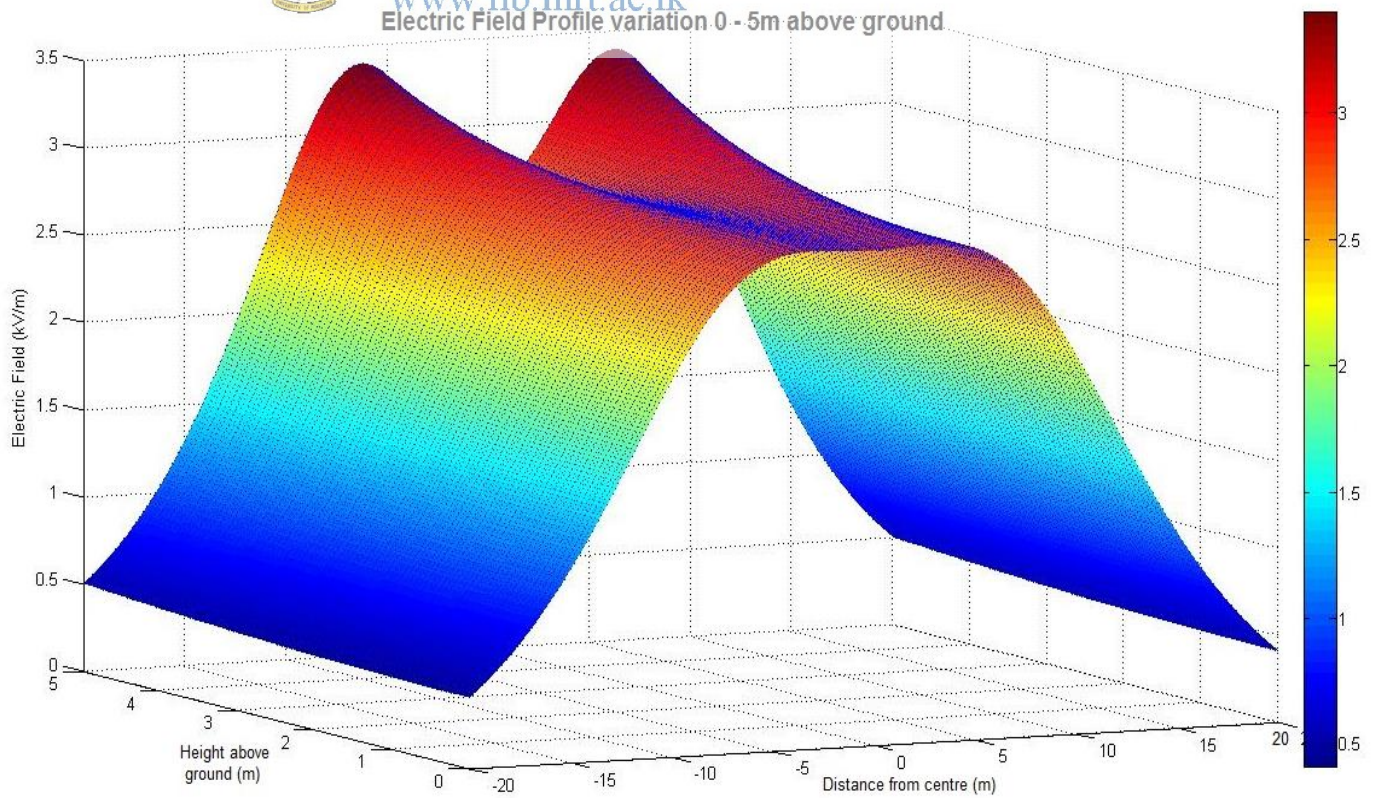


Figure 3.11 3D scheme of electric field variation for 132kV D/C configuration

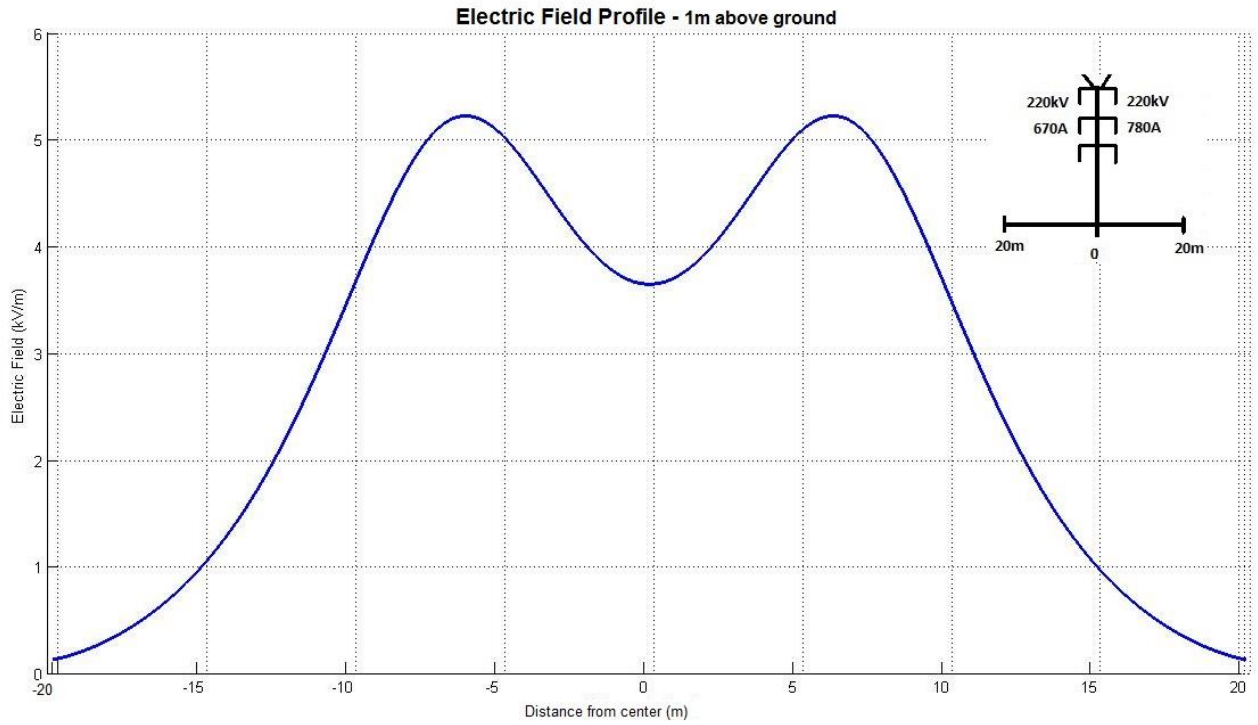


Figure 3.12 Electric field variation for 220kV double circuit line 1m above ground

Similarly, electric field profiles can be drawn with the line data for 132kV and 33kV.

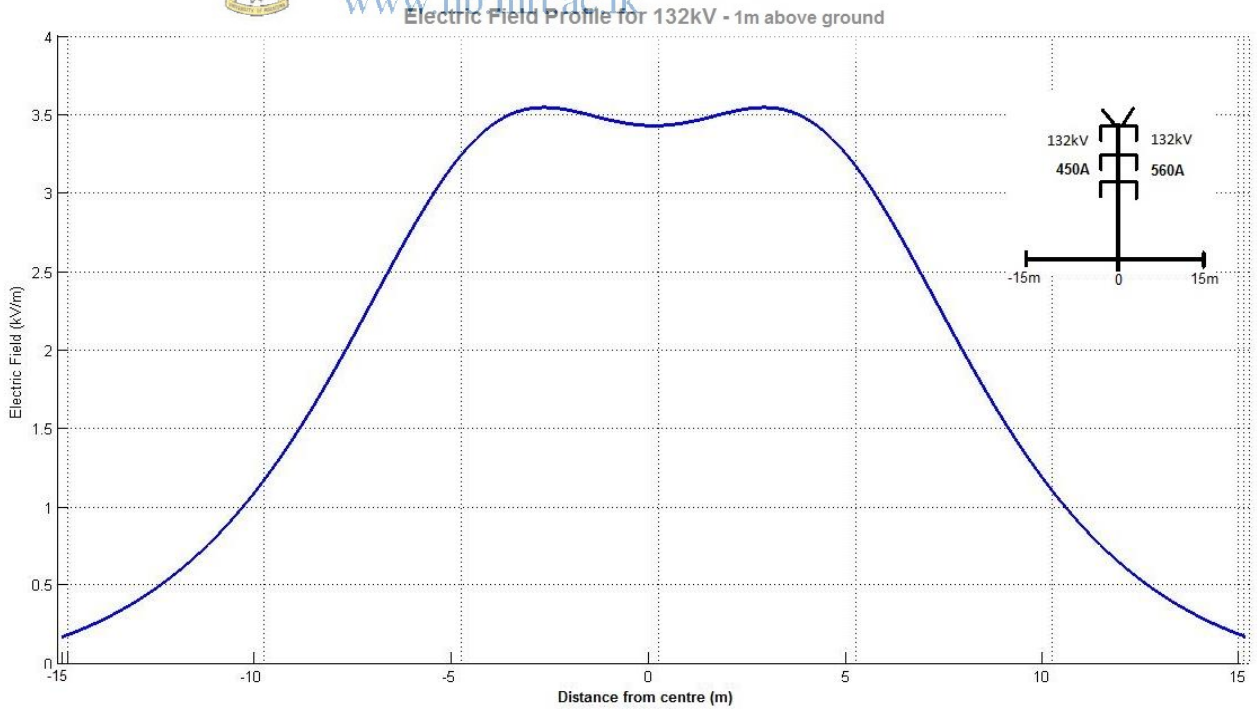


Figure 3.13 Electric field variation for 132kV double circuit line 1m above ground

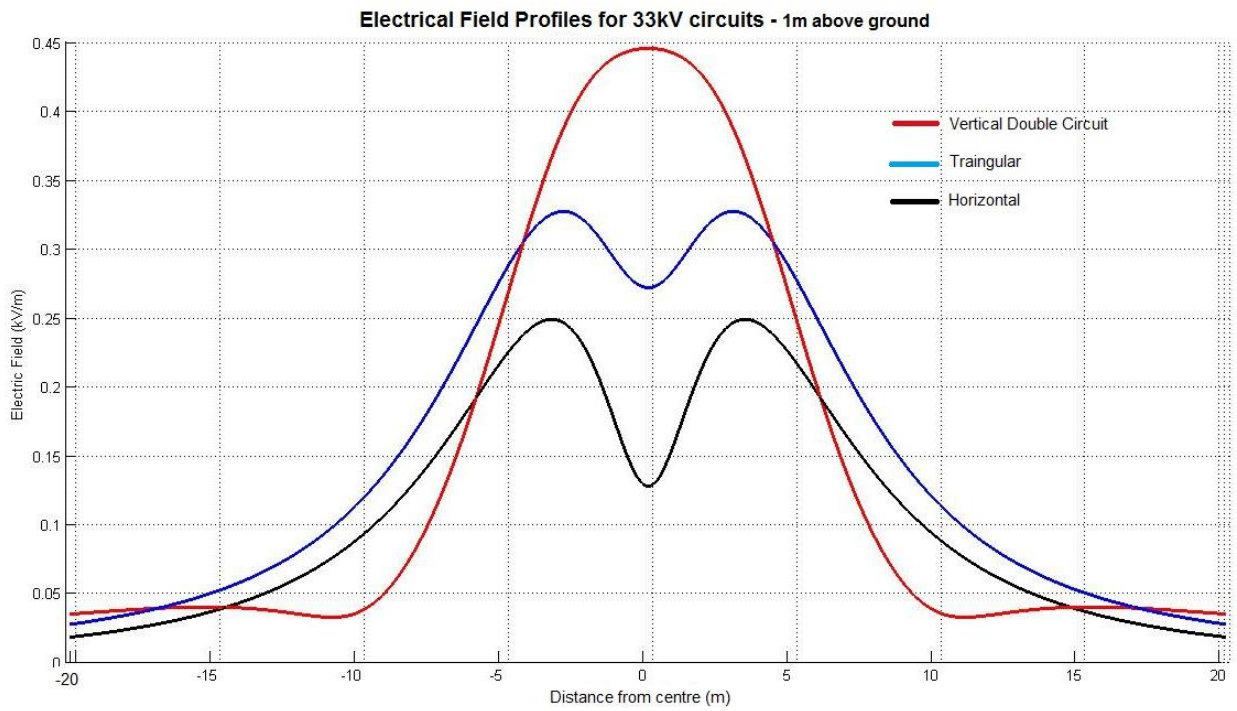


Figure 3.14 Electric field variation for 33kV double circuit, triangular and horizontal configurations, 1m above ground

Similarly, potential variation profile in space could be calculated with the use of above transmission line data.



University of Moratuwa, Sri Lanka.
Electronic Theses & Dissertations
www.lib.mrt.ac.lk

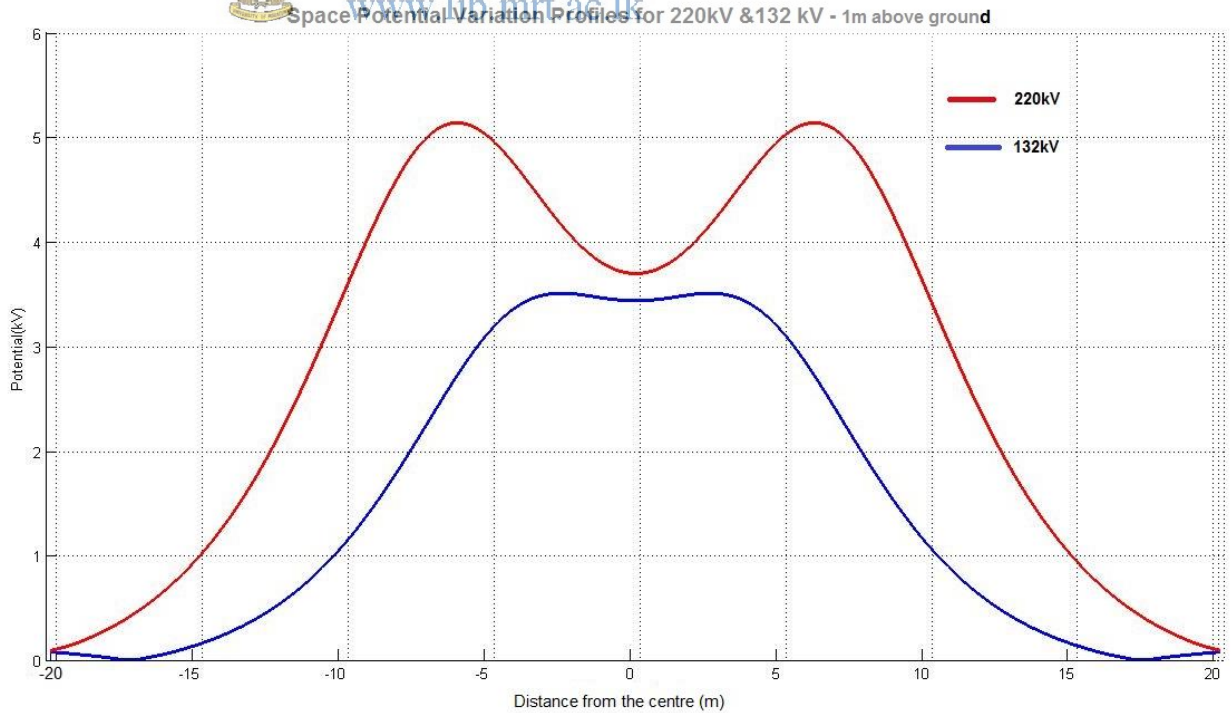


Figure 3.15 Space potential variation for 220kV and 132kV double circuit lines 1m above ground

3.2 Magnetic field modeling

3.2.1 Assumptions;

1. The conductors are infinitely long and straight.
2. The permeability of air is independent of the weather and equal to the permeability of free space.
3. Shielding effects from structures at ground potential are ignored.

By the application of Biot-Savart's law we could derive the magnetic field '**B**' at a point '**P**' distant '**r**' from an infinitely long Straight line conductor carrying a current '**I**' is given by [1]

$$\mathbf{B} = \frac{\mu_0 \mathbf{I}}{2\pi r}$$

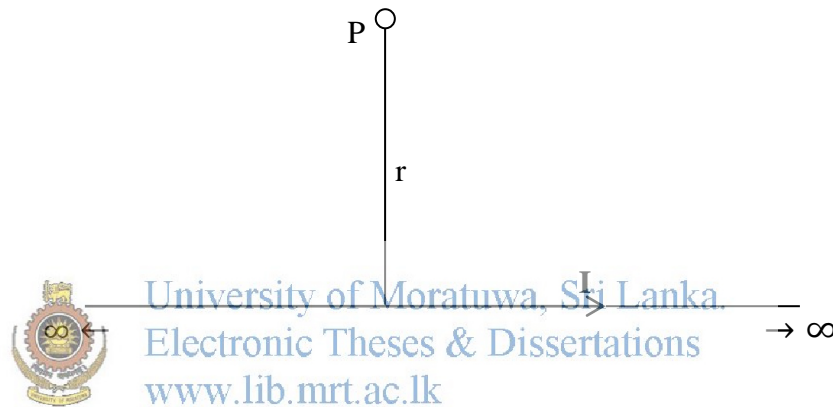


Figure 3.16 An infinitely long conductor carrying current **I**

The direction of **B** is circumferential, i.e. normal to the plane of the paper, and coming out of it, we have

$$\mathbf{B} \times (2\pi r) = \mu_0 \mathbf{I}$$

i.e. the vector **B** multiplied by the length of the contour, is proportional to the current in the wire.

From Ampere's law we define the vector **H**-magnetic field intensity, such that;

$$\mathbf{H} = \frac{\mathbf{B}}{\mu} \quad (= \mathbf{B}/\mu_0 \text{ in free space}) \quad (3.6)$$

Hence in general,

$$\mathbf{H} = \frac{\mathbf{I}}{2\pi r} \quad (3.7)$$

3.2.2 Modeling for 'n' number of conductors

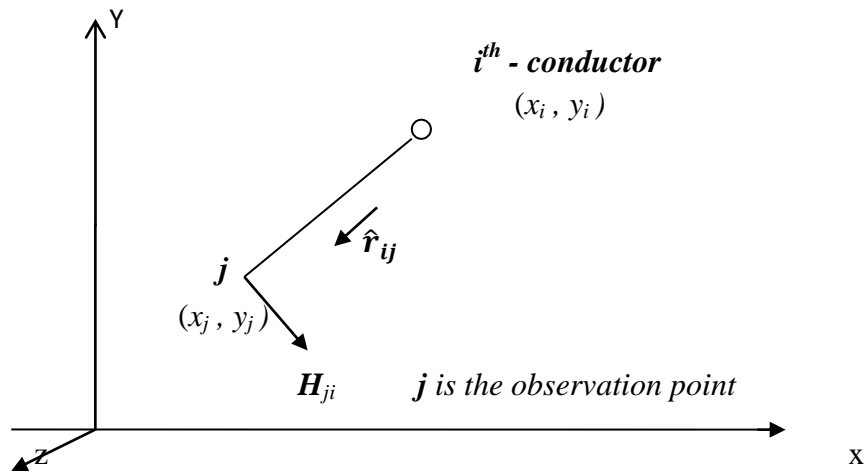



Figure 3.17 Coordinate system for magnetic field calculations

Considering only one conductor, in vectorial notation,

$$\vec{H}_{ji} = \frac{\vec{I}_i \times \hat{r}_{ji}}{2\pi r_{ij}} = \frac{I_i}{2\pi r_{ij}} \hat{\phi}_{ij}$$

$\hat{\phi}_{ij}$ is the unit vector in the direction of the product of the vector current and the vector segment r_{ij} . The unit vector is equal to;

$$\hat{\phi}_{ij} = \frac{y_j \vec{u}_x - x_j \vec{u}_y}{r_{ij}}$$


 University of Moratuwa, Sri Lanka.
 Electronic Theses & Dissertations
www.lib.mrt.ac.lk

\vec{u}_x, \vec{u}_y are the unit vectors in x, y directions.

$$\vec{H}_j = \sum_{i=1}^n \frac{I_i}{2\pi r_{ij}} \hat{\phi}_{ij} \rightarrow \text{Magnetic field intensity}$$

$$\mathbf{B}_j = \mu_{air} \mathbf{H}_j$$

Where $r_{ij} = \sqrt{(x_i - x_j)^2 + (y_i - y_j)^2}$

is the direct distance from i^{th} conductor to the point of interest.

3.2.3 Considering the effects of earth's return currents ;

The magnetic field produced by each conductor and its earth return is expressed by;

$$H_{ij_{earth}} = \sum_{i=1}^n \frac{I_i}{2\pi r'_{ij}} \left(1 + \frac{1}{3} \left(\frac{I_i}{\gamma_{ij}} \right)^4 \right) \hat{\phi}'_{ij}$$

$$\gamma = \sqrt{j \omega \mu (\sigma + j \omega \epsilon)}$$

ω – angular frequency μ – permeability of earth

σ – Earth's Conductivity 0.001 – 0.002 S/m

ϵ – earth's permittivity

$$r'_{ij} = \sqrt{(x_i - x_j)^2 + \left(y_i - y_j + \frac{2}{\gamma} \right)^2}$$



University of Moratuwa, Sri Lanka.
Electronic Theses & Dissertations
www.lib.mrt.ac.lk

$$\hat{\phi}'_{ij} = \left(\frac{x_i - x_j}{r'_{ij}} \hat{u}_x + \left(\frac{y_i - y_j + \frac{2}{\gamma}}{r'_{ij}} \right) \hat{u}_y \right)$$

3.2.4 Resultant effect of magnetic field intensity;

$$H_j = \sum_{i=1}^n \frac{I_i}{2\pi r_{ij}} \hat{\phi}_{ij} - \sum_{i=1}^n \frac{I_i}{2\pi r'_{ij}} \left(1 + \frac{1}{3} \left(\frac{I_i}{\gamma r'_{ij}} \right)^4 \right) \hat{\phi}'_{ij}$$

$$H_j = H_{xj} \hat{u}_x + H_{yj} \hat{u}_y$$

$$H_{xj} = H_{x,r} + j H_{x,im}$$

$$H_{yj} = H_{y,r} + j H_{y,im}$$

$$\vec{H}_r = H_{x,r} \hat{u}_x + H_{y,r} \hat{u}_y \quad (H_r = \sqrt{H_{x,r}^2 + H_{y,r}^2})$$


$$\vec{H}_i = H_{x,im} \hat{u}_x + H_{y,im} \hat{u}_y \quad (H_{im} = \sqrt{H_{x,im}^2 + H_{y,im}^2})$$

$$\text{Absolute value } H_T = \sqrt{H_{x,r}^2 + H_{x,im}^2 + H_{y,r}^2 + H_{y,im}^2}$$

3.2.5 Representation of line currents in phasor form

$$\begin{aligned} \mathbf{I}_i &= \text{phasor representation of phase current} \\ &= I_{ph_{rms}} \cos \phi_i + j I_{ph_{rms}} \sin \phi_i \end{aligned}$$

$$[\mathbf{I}]_n = (\mathbf{I}_i)_{n \times 1} \quad \mathbf{A}$$



University of Moratuwa, Sri Lanka.
Electronic Theses & Dissertations
www.lib.mrt.ac.lk

$$[\mathbf{I}]_n = \begin{bmatrix} I_{a_1} \\ I_{b_1} \\ I_{c_1} \\ \vdots \\ I_{c_n} \end{bmatrix}$$

Further, from the earlier derivation in equation 3.5,

$$\mathbf{H} = \mu \mathbf{B}$$

$$[\mathbf{B}] = \frac{1}{\mu} [\mathbf{H}] \quad (3.7)$$

3.2.6 Flow chart for modeling & simulation of magnetic field around transmission line

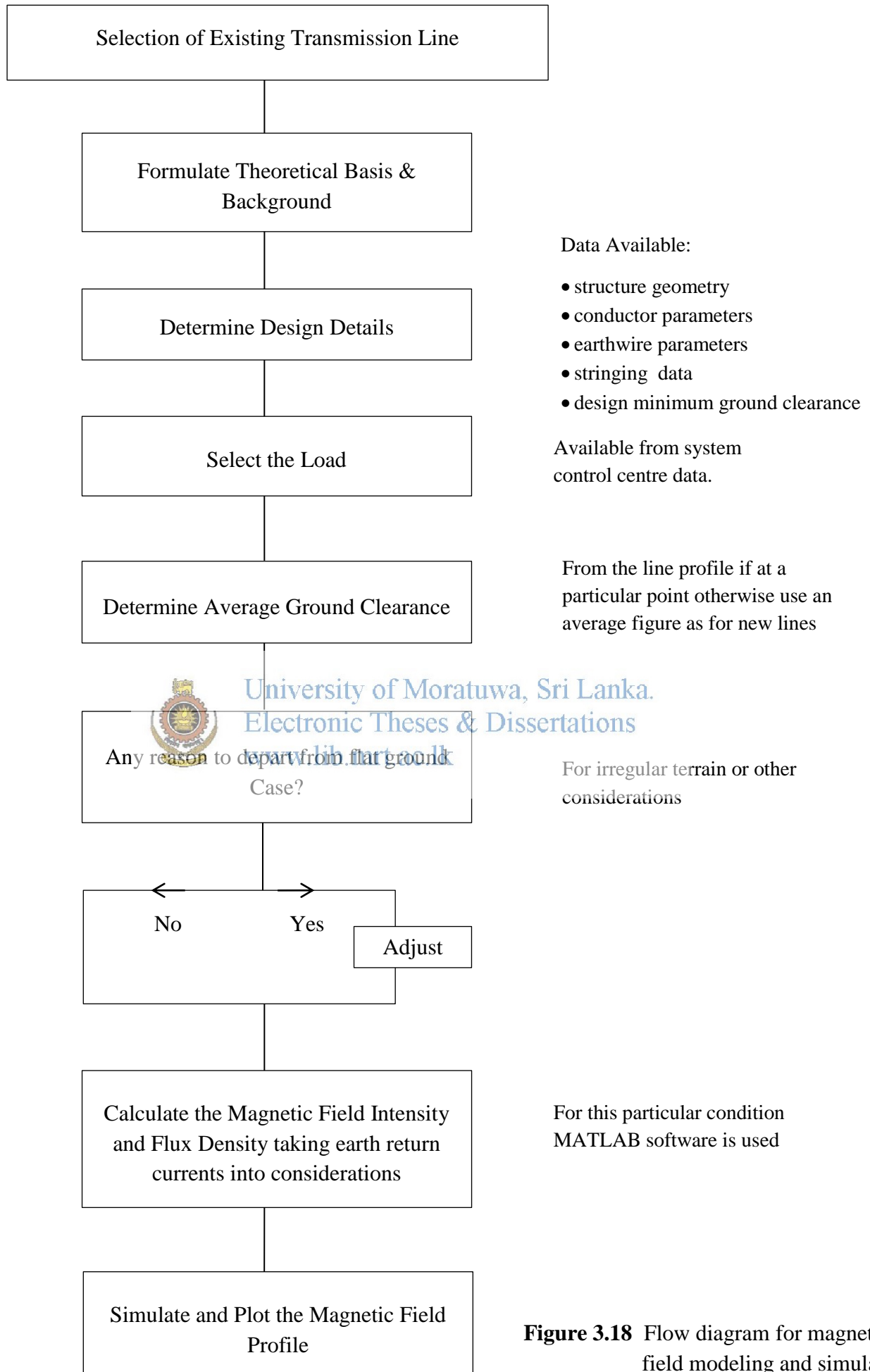


Figure 3.18 Flow diagram for magnetic field modeling and simulation

3.2.7 Simulation of magnetic field profiles using MATLAB

Using the line configuration data used for electric field modeling, magnetic field profiles could be simulated using MATLAB programming. The MATLAB code written for 220kV double circuit twin zebra configuration is attached as **Annex 4**. Some of the profiles drawn are given below. The model develop can accommodate any number of conductors in any configuration and takes the effect of earth conductors also into consideration in calculations. The model also takes the earth return currents into account.

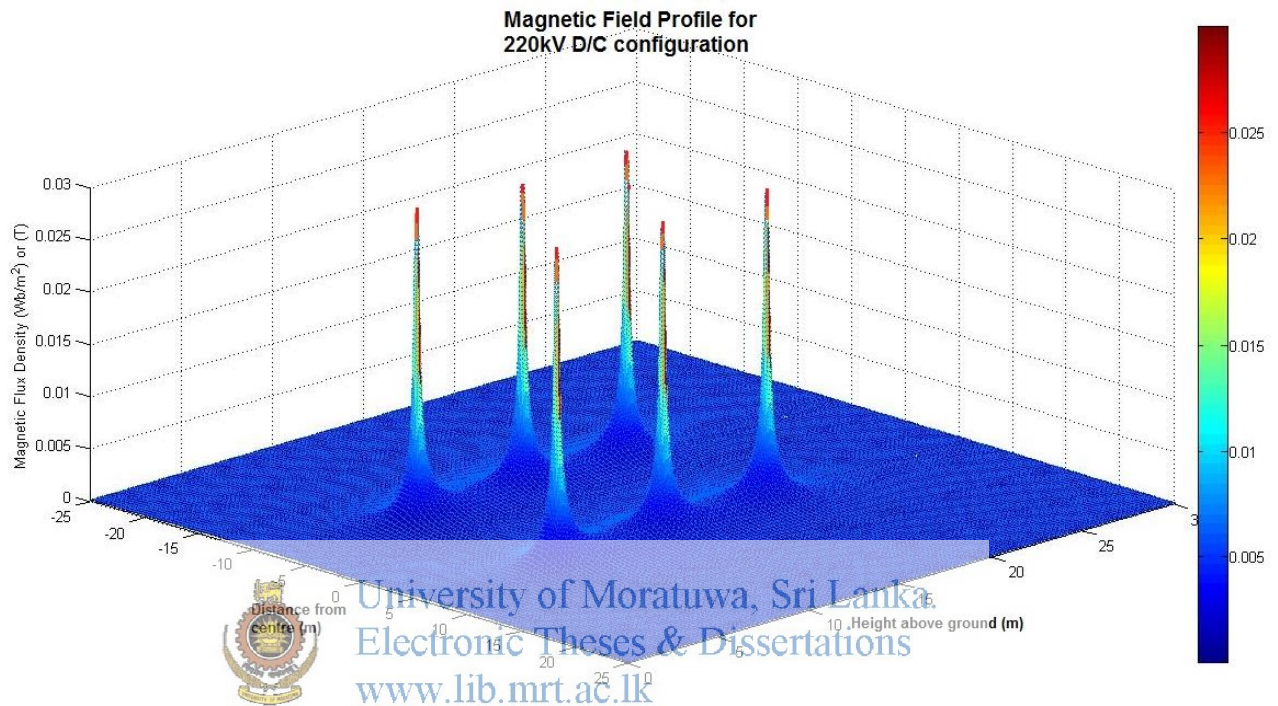


Figure 3.19 Magnetic field variations with respect to height and distance

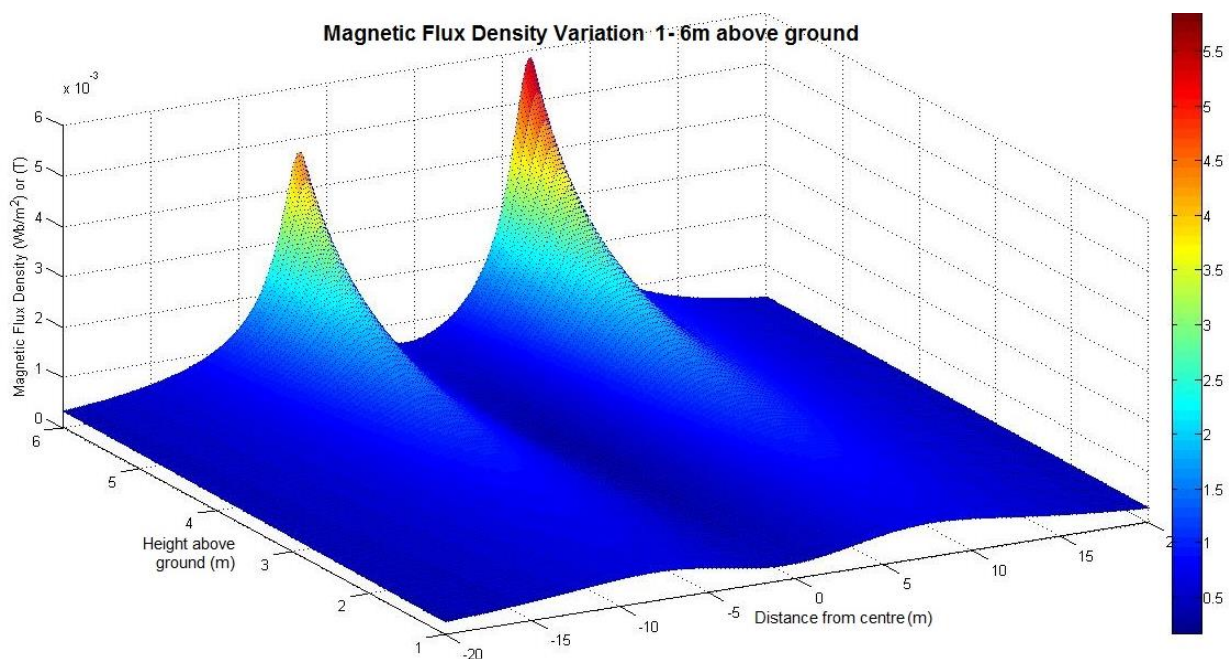


Figure 3.20 3D scheme of magnetic field variations for 220kV D/C configuration

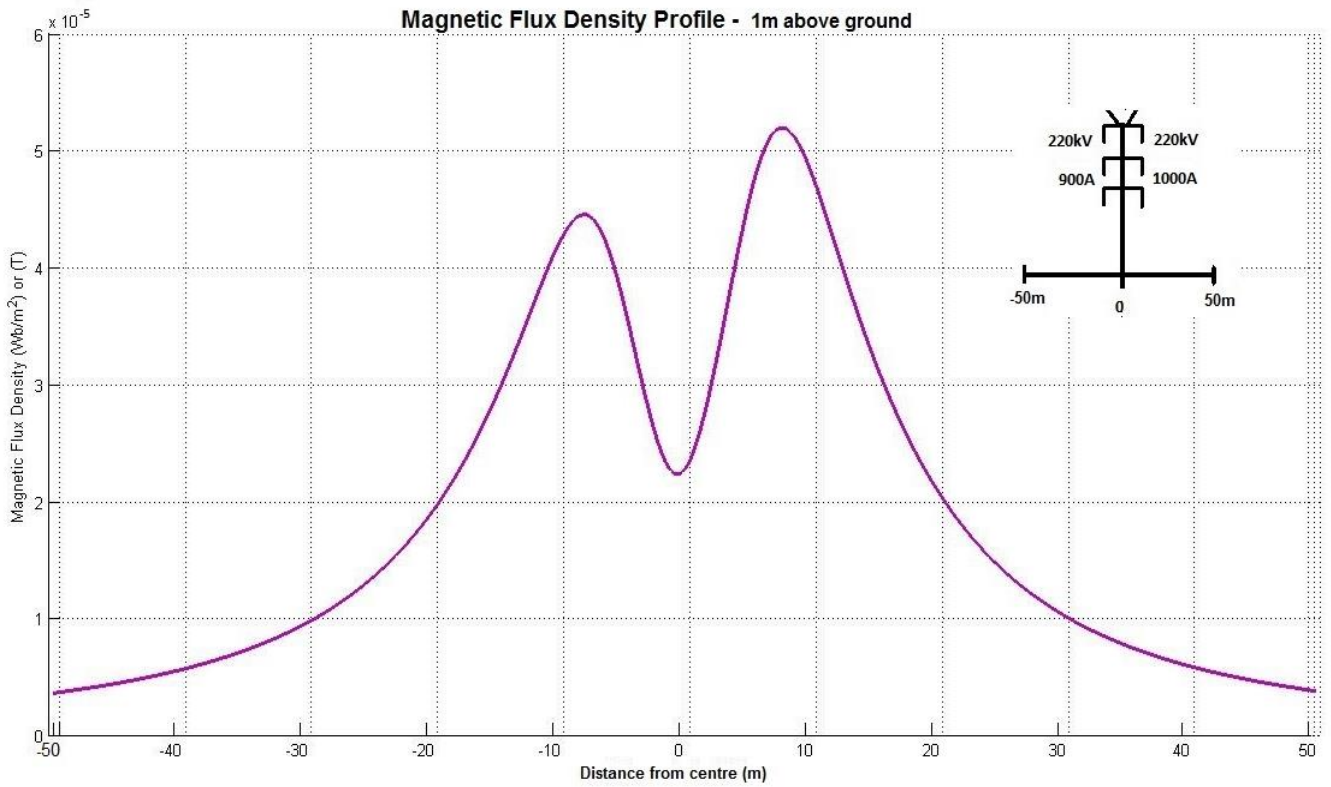


Figure 3.21 Magnetic field variation for 220kV double circuit line 1m above ground

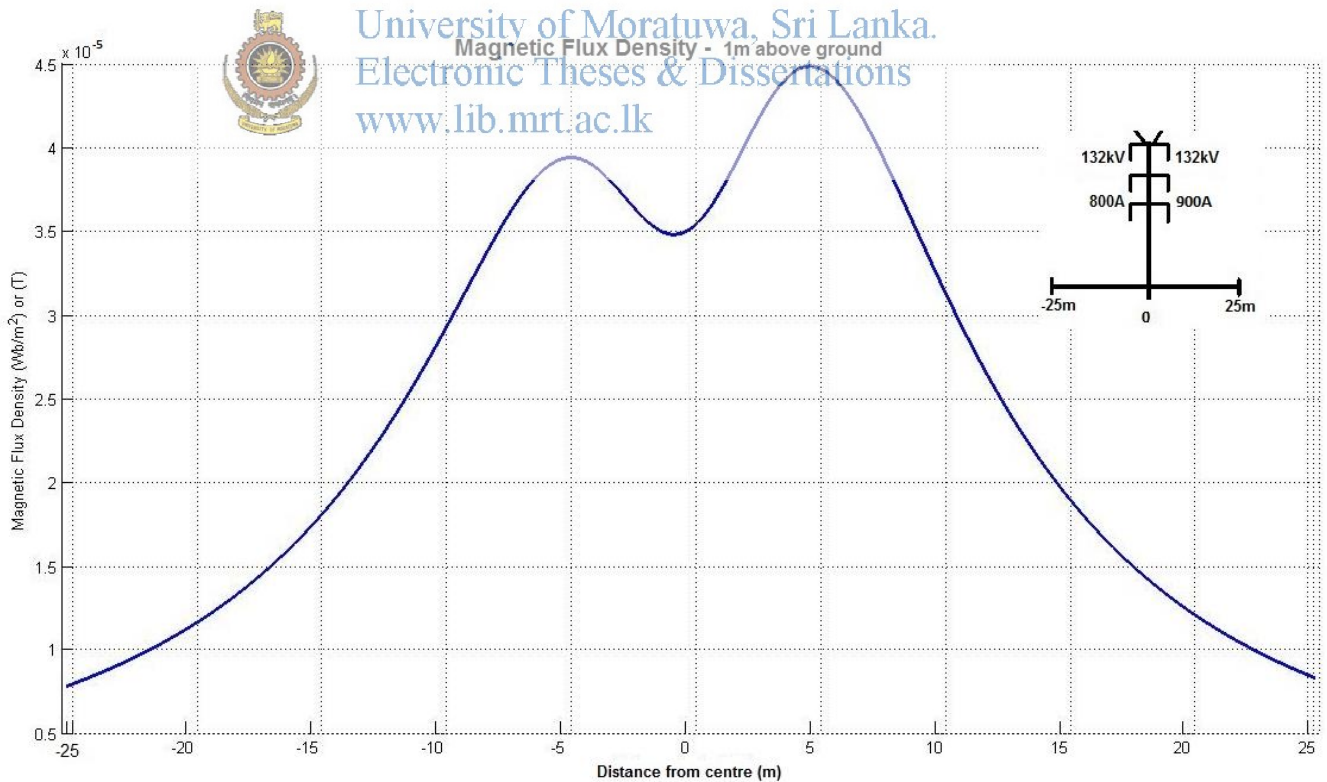


Figure 3.22 Magnetic field variation for 132kV double circuit line 1m above ground

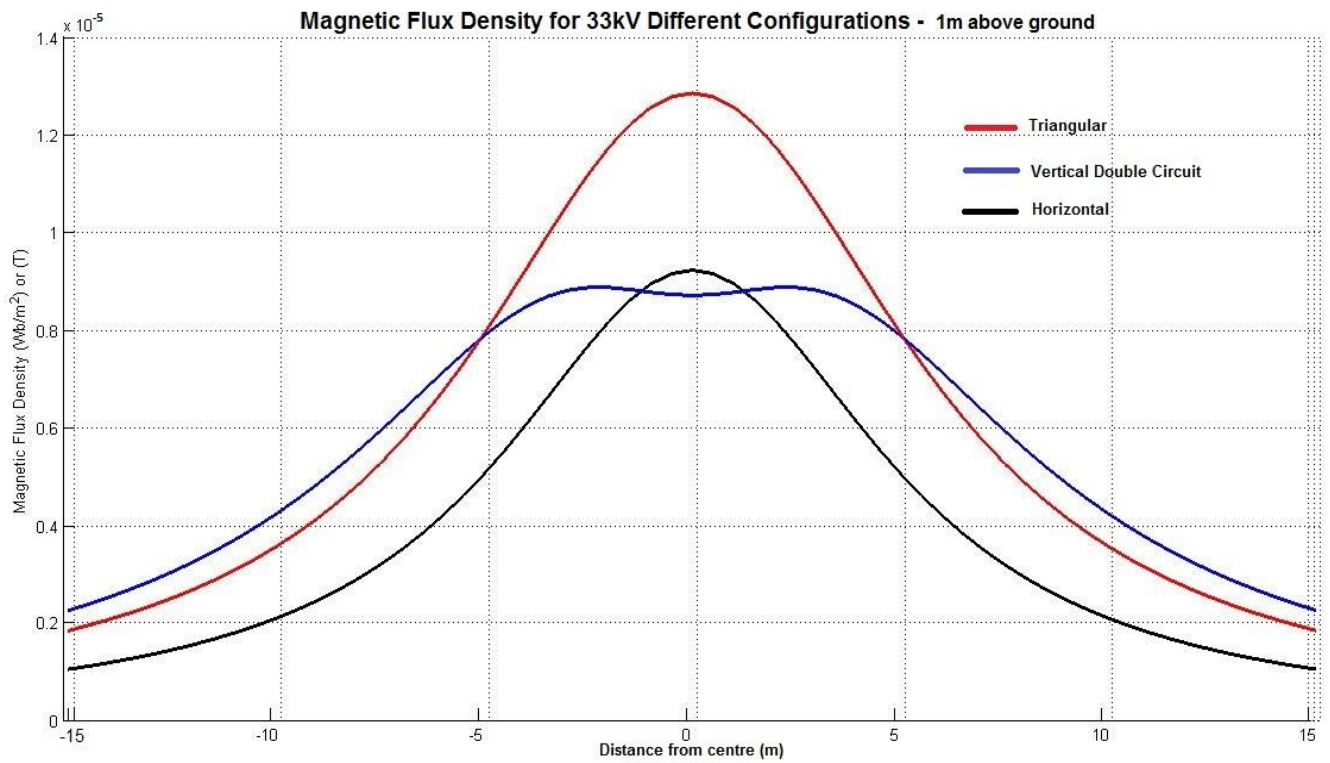


Figure 3.23 Magnetic field variations for 33kV for triangular, vertical double circuit and horizontal configurations 1m above ground



University of Moratuwa, Sri Lanka.
 Electronic Theses & Dissertations
www.lib.mrt.ac.lk

Measuring the field values physically under the transmission lines and shielding of the fields

4.1 Measuring the electric field under the transmission lines

Once the model for the electric field around transmission line was developed, it was required to measure the electric field values physically in the field in order to verify the accuracy of the model. The sites for measuring electric field were selected so to avoid any shielding effects from other structures and bushes at ground potential. Therefore, even terrains like paddy fields and flat grounds were selected avoiding irregular bushy terrains as much as possible.

Locations with nearby transmission lines which could interfere with the measuring fields were also avoided. Clear terrains of at least 200m width were selected for taking measurements. The following figure shows such a location selected for taking measurement for 220kV transmission line.



Figure 4.1 Location selected for taking measurements in 220kV line.

4.1.1 Instruments used for measuring

For measuring the electric fields, AC Electric Field Meter Model ACEF manufactured by Alhpa Lab Inc., USA and the meter measures AC electric field in the vertical direction (same direction as the long axis of the meter). Absolute accuracy of the instrument at 40 Hz – 1 KHz is +/-2% of the reading +/- 1 count (1 count is 1 volt per meter). When taking measurements, the meter was kept at distant as possible from the body in order for measuring the unperturbed electric field as closely as possible.

For measuring the conductor heights, FLUKE 421D Laser Distance Meter was used. The accuracy of the meter is $\pm 1.5\text{mm}$.



Figure 4.2 Taking measurements under the transmission lines keeping the e-field meter as distant as possible, 1m above ground.

4.1.2 Recording the measurements

The electric field measurements taken were recorded along with the values of voltages and currents in the circuits, line configurations, line conductor height etc. The following Table 4.1 gives the recorded measurements for Kotugoda – Veyangoda 220kV double circuit twin zebra transmission line.

TX Line: Kotugoda - Veyangoda				Date : 23.05.2014			
Transmission line Voltage & configuration : 220kV double circuit twin zebra							
Line Currents : 670A, 780A				Line Conductor height (Lowest Phase): 8.6 m			
Distance from centre (m)	Right			Distance from centre (m)	Left		
	Electric field (V/m)	Distance (m)	Electric field (V/m)		Electric field (V/m)	Distance (m)	Electric field (V/m)
0	3502	13.0	1700	0	3502	-13.0	1700
0.5	3472	13.5	1357	-0.5	3580	-13.5	1450
1.0	3650	14.0	1290	-1.0	3550	-14.0	1200
1.5	3750	14.5	1240	-1.5	3700	-14.5	1100
2.0	3850	15.0	1100	-2.0	3900	-15.0	1025
2.5	3980	15.5	1025	-2.5	4000	-15.5	890
3.0	4300	16.0	893	-3.0	4200	-16.0	850
3.5	4450	16.5	685	-3.5	4400	-16.5	690
4.0	4650	17.0	550	-4.0	4600	-17.0	600
4.5	4980	17.5	450	-4.5	4900	-17.5	490
5.0	5200	18.0	395	-5.0	5010	-18.0	400
5.5	5250	18.5	365	-5.5	5200	-18.5	380
6.0	5200	19.0	266	-6.0	5250	-19.0	238
6.5	5275	19.5	208	-6.5	5175	-19.5	202
7.0	5150	20	189	-7.0	5100	-20.0	185
7.5	4896			-7.5	4700		
8.0	4560			-8.0	4650		
8.5	4250			-8.5	4200		
9.0	3940			-9.0	4000		
9.5	3640			-9.5	3800		
10	3210			-10	3450		
10.5	3000			-10.5	3050		
11.0	2800			-11.0	2700		
11.5	2400			-11.5	2450		
12.0	2250			-12.0	2200		
12.5	1980			-12.5	1900		

Table 4.1 Electric field measurements for Kotugoda – Veyangoda 220kV line.

4.1.3 Plotting the profiles of measured electric field values vs modeled values

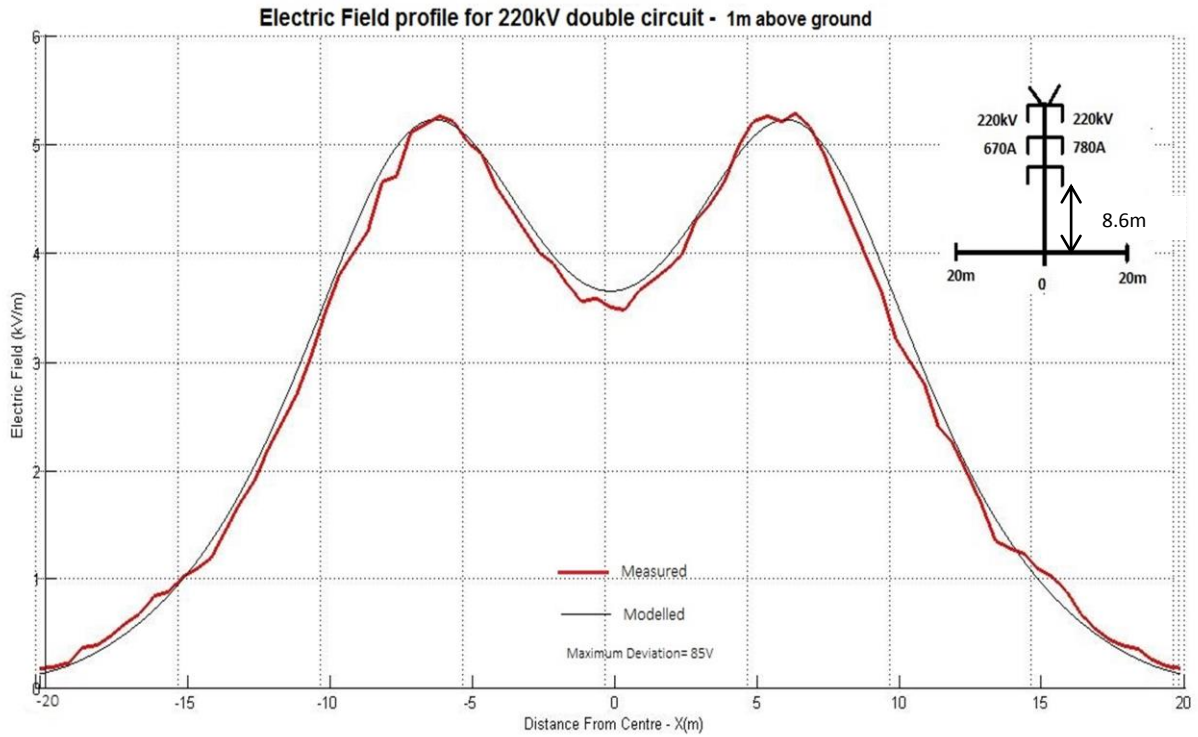


Figure 4.3 Electric field profiles comparing the modeled and measured values for 220kV double circuit configuration

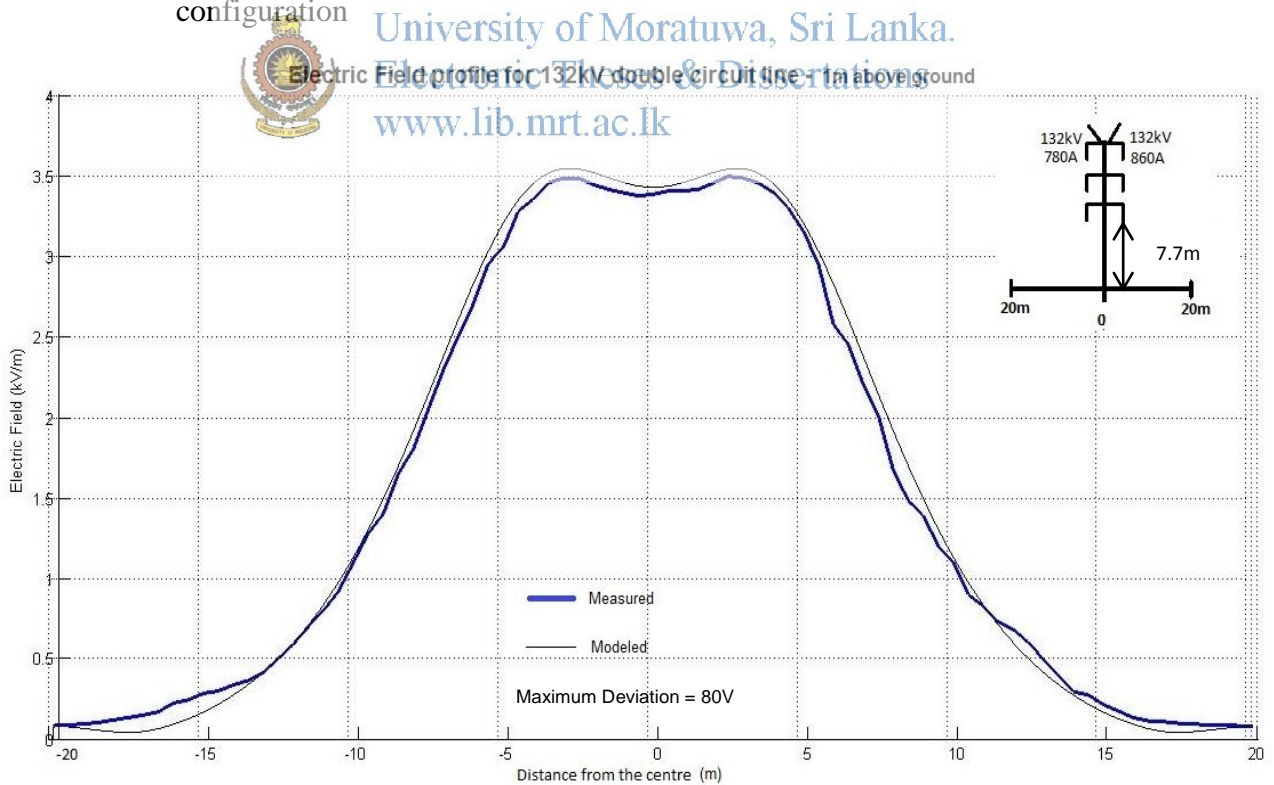


Figure 4.4 Electric field profiles comparing the modeled and measured values for 132kV double circuit configuration

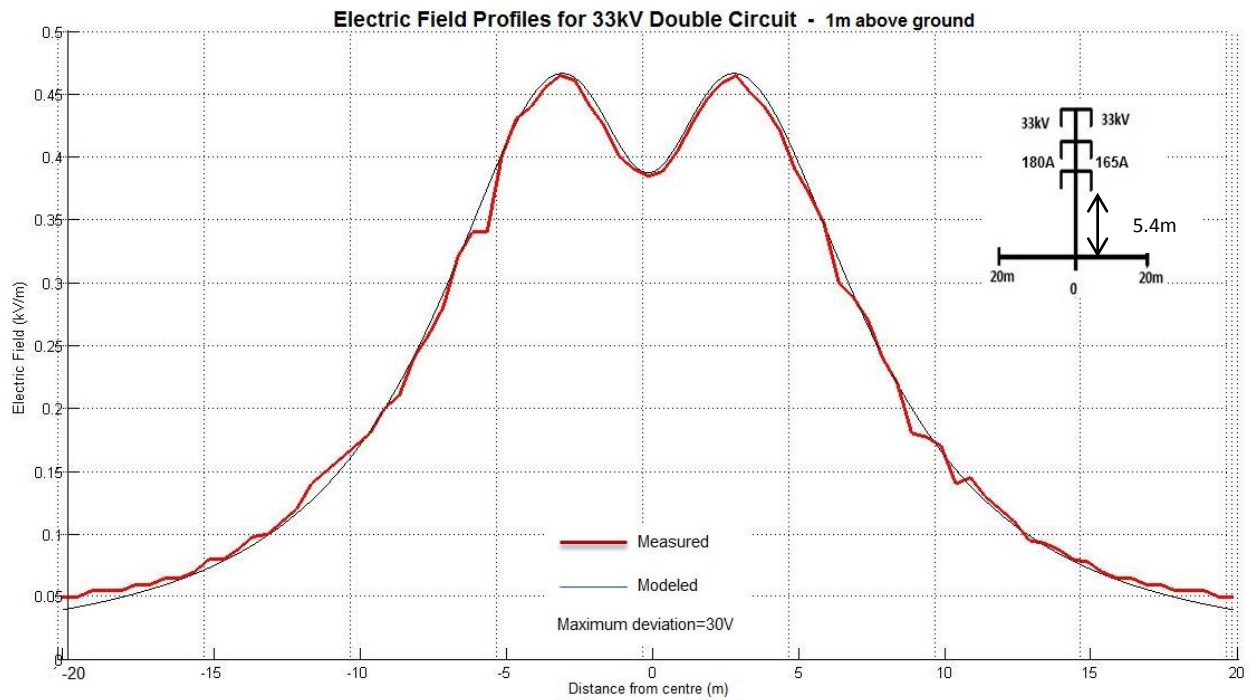


Figure 4.5 Electric field profiles comparing the modeled and measured values for 33kV double circuit configuration

4.1.3 Comparison of the measured values and the modeled values and verification of model



University of Moratuwa, Sri Lanka
Electronic Theses & Dissertations
www.lib.mrt.ac.lk

The field profiles comparing the measured values and the modeled values for electric field are drawn in figures 4.4 and 4.5 for 220kV and 132kV double circuit twin zebra conductor and in figure 4.6 for 33kV double circuit raccoon conductor. The field Measurement data for 132kV Kotugoda - Katunayake and 33kV Bolawatta - Nattandiya double circuit transmission lines are given in **Annex 5** and **Annex 6** respectively.

The deviations between measured and modeled values are primarily due to interference of the person taking measurement with the electric field during the measuring process, changes in the medium of air such as moisture, wind speed etc. During the measuring process the 50Hz electric field which is easily vulnerable for disturbances is disturbed while the modeled electric field represents the unperturbed electric field.

The profiles drawn verify that the measured values are very close to the modeled values and the profile shapes are the same. Since the electric field models developed for 220kV, 132kV and 33kV matches with the measured values, the accuracy of the model developed is amply verified.

4.2 Measuring the magnetic field under the transmission lines

Developing the magnetic field around transmission and the traces of field profiles was discussed in detail in chapter 3. Hence, it was required to measure the magnetic field values physically in the field in order to verify the accuracy of the model. The sites for measuring magnetic field were also selected as per the electric fields, avoiding shielding effects from other structures and bushes at ground potential. Therefore, even terrains like paddy fields and flat grounds were selected avoiding irregular bushy terrains as much as possible.

Clear terrains of at least 200m width were selected for taking measurements. It is also noteworthy that the 50Hz magnetic field is not perturbed easily unlike the electric fields of the same frequency. The following figure shows taking magnetic field measurements for 220kV transmission line.



Figure 4.6 Taking magnetic field measurements under the transmission lines 1m above ground.

4.2.1 Instruments and recording of measurements

For measuring the magnetic fields, Tri-axial ELF Magnetic Field Meter of Model SK-8301 manufactured by Kaise Corporation, Japan and the meter measures AC electric field in the vertical direction (same direction as the long axis of the meter).

TX Line: Kotugoda - Veyangoda				Date : 27 .05.2014			
Transmission line Voltage & configuration : 220kV double circuit twin zebra							
Line Currents : 780A, 860A				Line Conductor height (Lowest Phase): 8.6 m			
Distance from centre (m)	Right			Distance from centre (m)	Left		
	Mag. Field (μ T)	Distance (m)	Mag. Field (μ T)		Mag. Field (μ T)	Distance (m)	Mag. Field (μ T)
0	10.6	13.0	17.6	0	10.6	-13.0	16.67
0.5	10.8	13.5	17.0	-0.5	10.9	-13.5	16.0
1.0	11.5	14.0	16.8	-1.0	10.8	-14.0	15.2
1.5	12.4	14.5	16.0	-1.5	11.4	-14.5	14.6
2.0	13.4	15.0	15.4	-2.0	12.1	-15.0	14.0
2.5	14.5	15.5	14.8	-2.5	13.1	-15.5	13.55
3.0	15.7	16.0	14.0	-3.0	14.2	-16.0	13.0
3.5	17.0	16.5	13.5	-3.5	15.3	-16.5	12.5
4.0	18.5	17.0	13.1	-4.0	16.5	-17.0	12.0
4.5	20.0	17.5	12.5	-4.5	17.45	-17.5	11.8
5.0	21.0	18.0	12.0	-5.0	18.56	-18.0	11.2
5.5	22.0	18.5	11.5	-5.5	19.6	-18.5	10.5
6.0	22.9	19.0	11.1	-6.0	20.6	-19.0	10.3
6.5	23.5	19.5	11.5	-6.5	21.4	-19.5	9.7
7.0	24.0	20	10.5	-7.0	21.8	-20.0	9.5
7.5	24.4	20.5	10.0	-7.5	22.0	-20.5	9.2
8.0	24.5	21.0	9.8	-8.0	22.2	-21.0	8.8
8.5	24.3	21.5	9.5	-8.5	21.95	-21.5	8.5
9.0	24.0	22.0	9.0	-9.0	21.7.	-22.0	8.2
9.5	23.5	22.5	8.8	-9.5	21.3	-22.5	7.9
10	23.0	23.0	8.0	-10	20.73	-23.0	7.6
10.5	22.0	23.5	8.2	-10.5	20.12	-23.5	7.4
11.0	21.5	24.0	7.9	-11.0	19.47	-24.0	7.1
11.5	20.2	24.5	7.9	-11.5	18.7	-24.5	7.0
12.0	19.5	25.0	7.8	-12.0	18.0	-25.0	6.9
12.5	18.84			-12.5	17.27		

Table 4.2 Magnetic field measurements for Kotugoda – Veyangoda 220kV line.

The accuracy of the instrument at 50/60Hz is +/-2% rdg and the resolution is .01 μ T. When taking measurements, the meter was kept as distant as possible from the body in order for measuring the unperturbed magnetic field. For measuring the conductor heights, FLUKE 421D Laser Distance Meter was used. The accuracy of the meter is \pm 1.5mm.

The magnetic field measurements taken were recorded along with the values of currents in the circuits, line configurations, line conductor height etc. The following Table 4.3 gives the recorded measurements for Kotugoda – Veyangoda 220kV double circuit twin zebra transmission line.

4.2.2 Plotting the profiles of measured magnetic field values vs modeled values

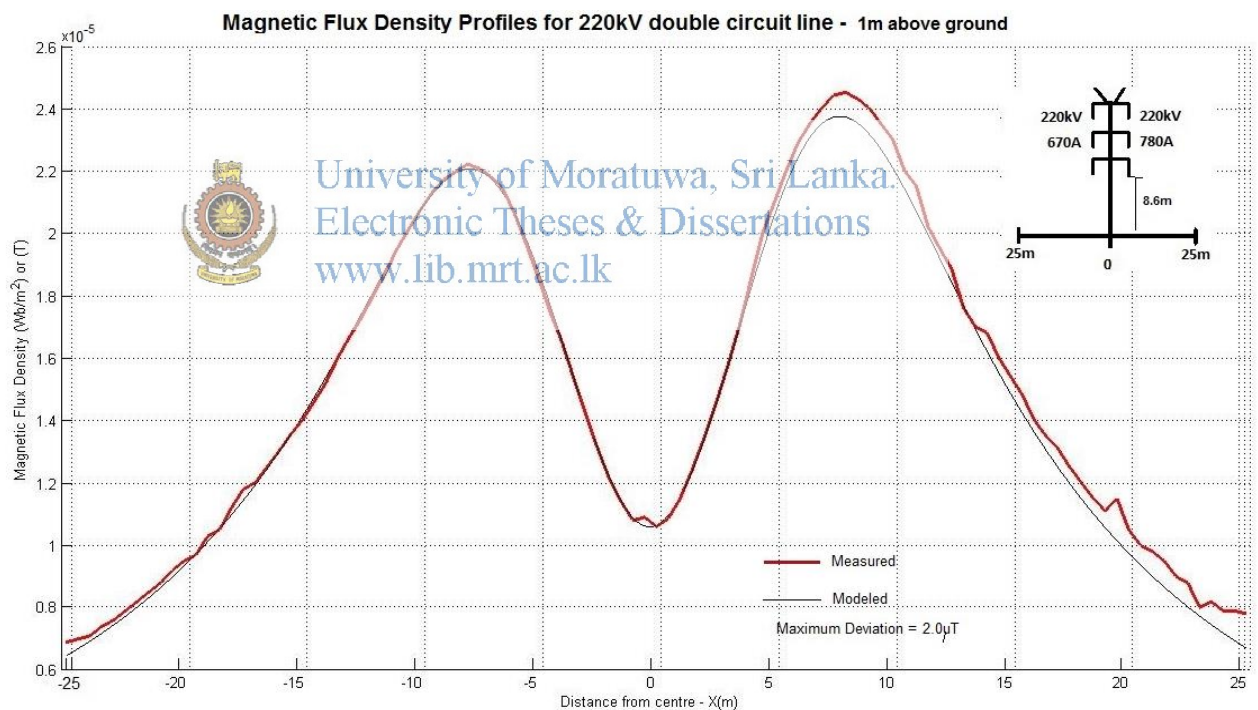


Figure 4.7 Magnetic field profiles comparing the modeled and measured values for 220kV double circuit configuration

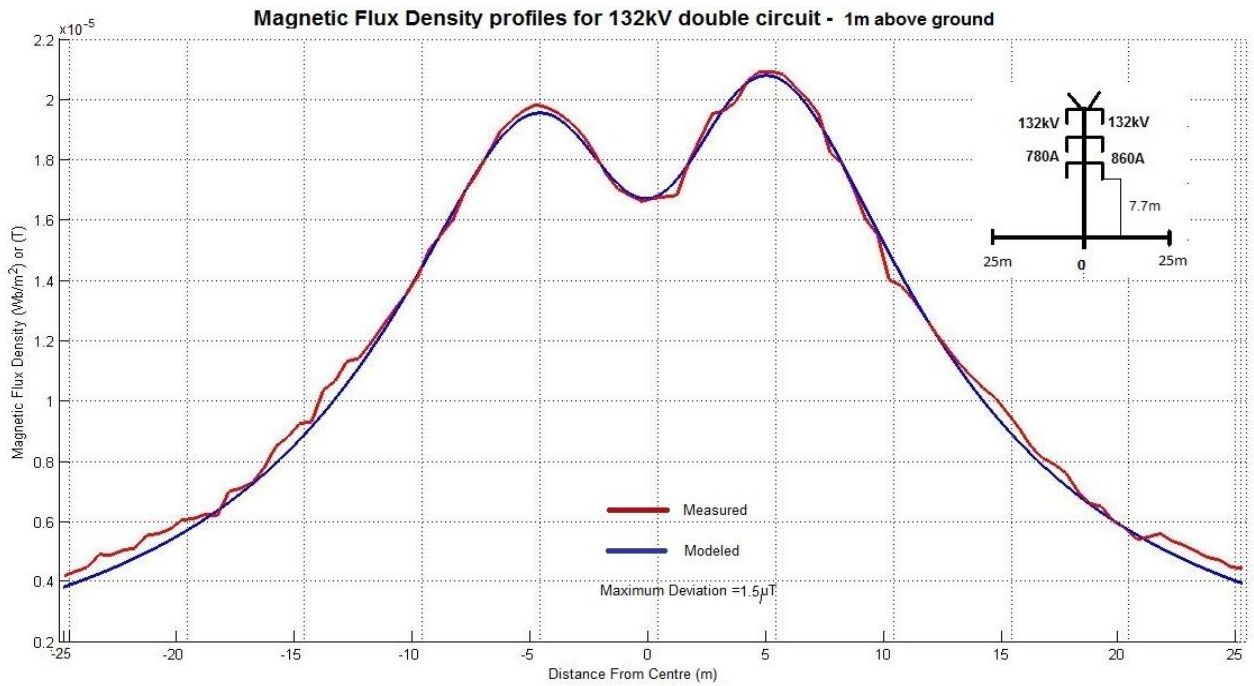


Figure 4.8 Magnetic field profiles comparing the modeled and measured values for 132kV double circuit configuration

Similarly, for 132kV double circuit twin zebra conductor and for 33kV double circuit raccoon conductor transmission lines, the field measurement data are given in **Annex 7** and **Annex 8** respectively. Magnetic field profiles for 132kV and 33kV are given below.



University of Moratuwa, Sri Lanka.
Electronic Theses & Dissertations
www.lib.mrt.ac.lk

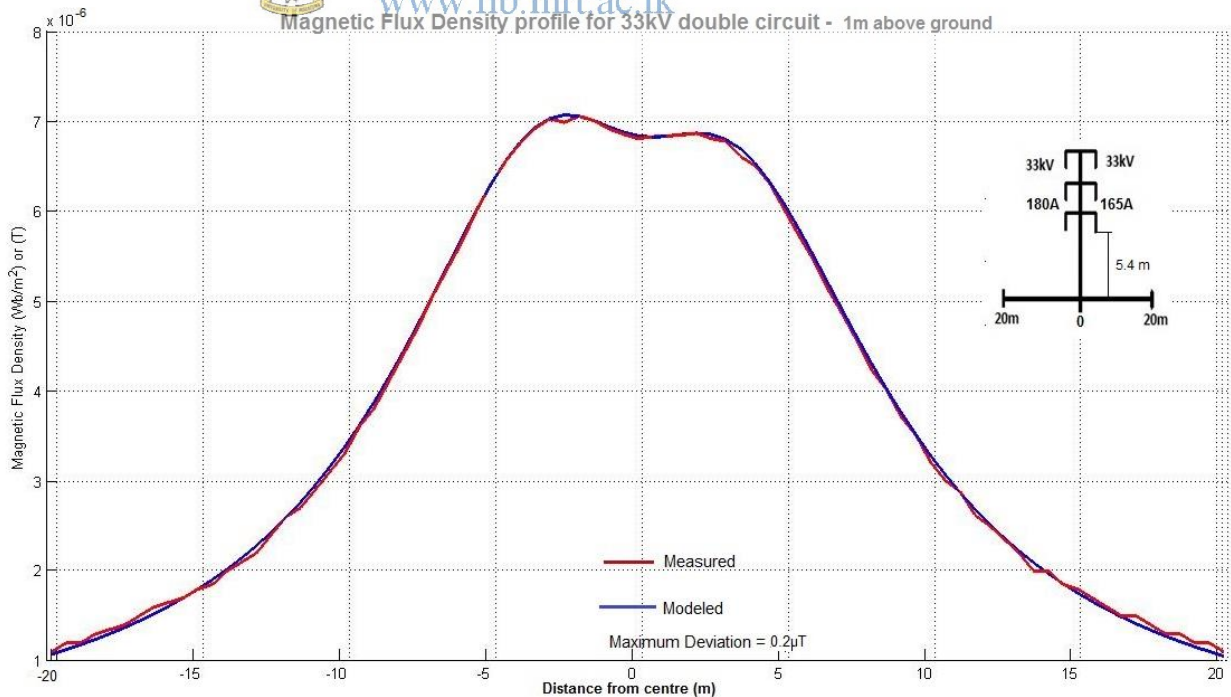


Figure 4.9 Magnetic field profiles comparing the modeled and measured values for 33kV double circuit configuration

4.2.3 Comparison of the measured values and the modeled values and verification of model

The field profiles comparing the measured values and the modeled values for magnetic field are drawn in figures 4.7 and 4.8 for 220kV and 132kV double circuit twin zebra conductors respectively and in figure 4.9 for 33kV double circuit raccoon conductor. The deviations between measured and modeled values are primarily due to changes in the currents during measuring process, changes in the medium of air such as moisture, wind speed etc. The current readings are the average value of the initial and final values measured at the grid substations.

The profiles drawn verify that the measured values are very close to the modeled values and the profile shapes are the same. Since the magnetic field models developed for 220kV, 132kV and 33kV matches with the measured values, the accuracy of the models developed are amply verified.

4.3 Shielding the electromagnetic field under transmission lines

4.3.1 Shielding the electric field

One method to minimize the effects of the electric field is to shield the area of interest from the high-voltage conductors of transmission line. The direct exposure to the transmission line in the close proximity will cause the electric field emitting to have a large influence on the detonator circuits. Shielding reduces the electric field and consequently its effects. Different shielding methods represent alternative means of reaching specific objectives.

The two main methods are shielding by a vertical grid of grounded wires and horizontal grid of grounded wires. Shielding efficiency, SE, may be defined, as shown in Eq. 4.1:

$$SE = \frac{E_u - E_s}{E_u} \quad (4.1)$$

where E_s is the electric field at ground with the shield present and E_u is the unperturbed electric field without the shield [9].

4.3.1.1 Shielding by a vertical grid of grounded wires

Reduction of the ground level electric field off the edge of a transmission-line right-of-way may be achieved with a vertical, fence-like set of parallel Wires.

The geometry of a vertical grid is shown in Figure 4.10. The design parameters considered are the following:

- L_r = distance to the location to be shielded from center line
- L_g = position of electrostatic fence from centerline
- H_{max} = height above ground of the top wire
- H_{min} = height above ground of the bottom wire
- n = number of wires d = diameter of the wires
- S_i = spacing between the wire i and the wire $i + 1$

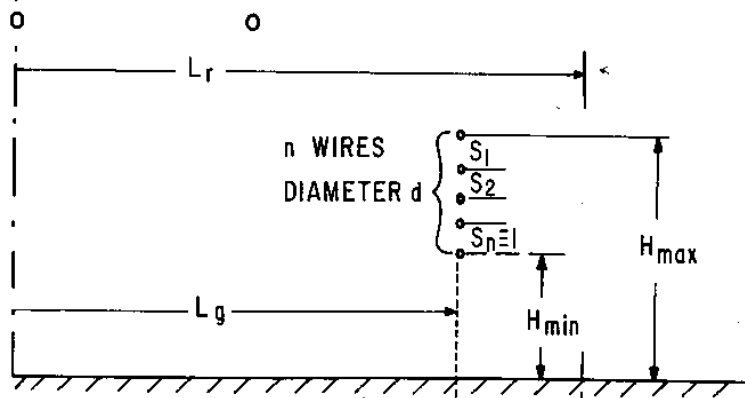


Figure 4.10 Geometry of a vertical grid [9].

A modified concept of shielding efficiency was found of more practical application:

$$SE = \frac{\tilde{E}_u - \tilde{E}_s}{\tilde{E}_u} = \frac{-\tilde{E}_G}{\tilde{E}_u} \quad (4.2)$$

where \tilde{E}_u and \tilde{E}_s are calculated at the point where the shielding efficiency is calculated, \tilde{E}_G is the field induced by the grid charges and \tilde{E}_u is the unperturbed field at the grid location. The functions $E_u(X)$ and $E_s(X)$ depend in a complicated way on the characteristics of the line (flat, delta, vertical, double circuit). Shielding efficiency for vertical grids are determined using design curves which are commonly available in transmission line reference books.

4.3.1.2 Designing a vertical grid of grounded wires

The vertical grid shield design shall be explained in relation to a practical problem that surfaced during the construction of the Outer Circular High-Way at Kaduwela where a rock was found in construction pathway close to the 132kV transmission line.

The Geological and Mines Bureau (GSMB) requested that the electric field to be reduced for the operation of detonators by a designing a vertical shield for safe operations. The main threat for unintentional firing was suspected to be the large electric field present in the close proximity of the 132kV transmission line.



Figure 4.11 The Kaduwela Outer Circular Highway construction site



University of Moratuwa, Sri Lanka.
Electronic Theses & Dissertations
www.lib.mrt.ac.lk

The design procedure is illustrated in the following calculations.

1. As per the measured values and derived values from the model, the unperturbed field in the area 10m away from the Tr. Line center is $E'_r = 1.2 \text{ kV/m}$. This field to be reduced to below 0.2 kV/m . The height of lowest conductor of 132 kV tr.line, $H = 10.5 \text{ m}$.
2. $L_r = 10 \text{ m}$. Design rule suggests that the distance $L_r - L_g$ be one-third of the average height of the grid. The minimum height is to be 6 m for vehicular movements below the grid.

$$L_g = 7 \text{ m for } H_{\max} = 12 \text{ m}$$

$$L_g = 6 \text{ m for } H_{\max} = 18 \text{ m}$$
3. $E_u = 2.5 \text{ kV/m}$ for $L_g = 7 \text{ m}$ ($H_{\max} = 12 \text{ m}$)
 $E_u = 3 \text{ kV/m}$ for $L_g = 6 \text{ m}$ ($H_{\max} = 18 \text{ m}$)
4. Let the desired field be lower than $E_{\max} = 0.2 \text{ kV/m}$. The desired shielding efficiency is

$$SE (3) = \frac{1.2-0.2}{2.5} = 0.4 \quad \text{for } H_{\max} = 12 \text{ m (from 4.2)}$$

$$SE (4) = \frac{1}{3} = 0.33 \quad \text{for } H_{\max} = 18 \text{ m}$$

5. We choose $d = 0.95$ cm (3/8 in.). $H_{\min} = 6$ m

From the shielding efficiency curve (Figure 4.12) for 6m to 12m ($H_{\max} = 12$ m), it is observed that a shielding efficiency of 0.4 can be achieved with three (3) wire vertical grid placed at a distance of 7m away from line center and 3m from the burden. It is also observed that a shielding efficiency of 0.5 can be achieved with five (5) wire vertical grid placed at the same distance. It appears that field present at the location is fully covered. Hence we choose, five wire grid for better shielding. The wires are uniformly spaced.

Hence, $H_{\max} = 12$ m, $d(L_r - L_g) = 3$ m, $SE = 0.40$ for $n = 5$

6. The 5-wire grid from 6 to 12 m is chosen.

It is observed from the shielding efficiency curves that the efficiency for 5 wire mesh grid at a distance of 7m away from the grid is 0.5. This way all the points beyond the shield are kept below the desired electric field of 0.2kV/m.

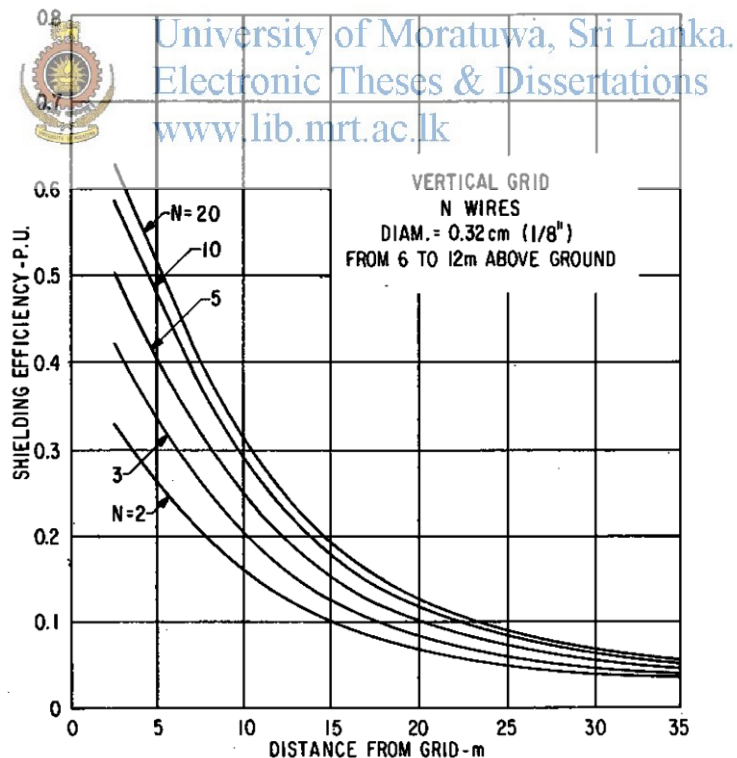


Figure 4.12 Shielding efficiency of vertical grids of Wires[6]

7. Final design of the vertical mesh grid incorporating all the above steps.

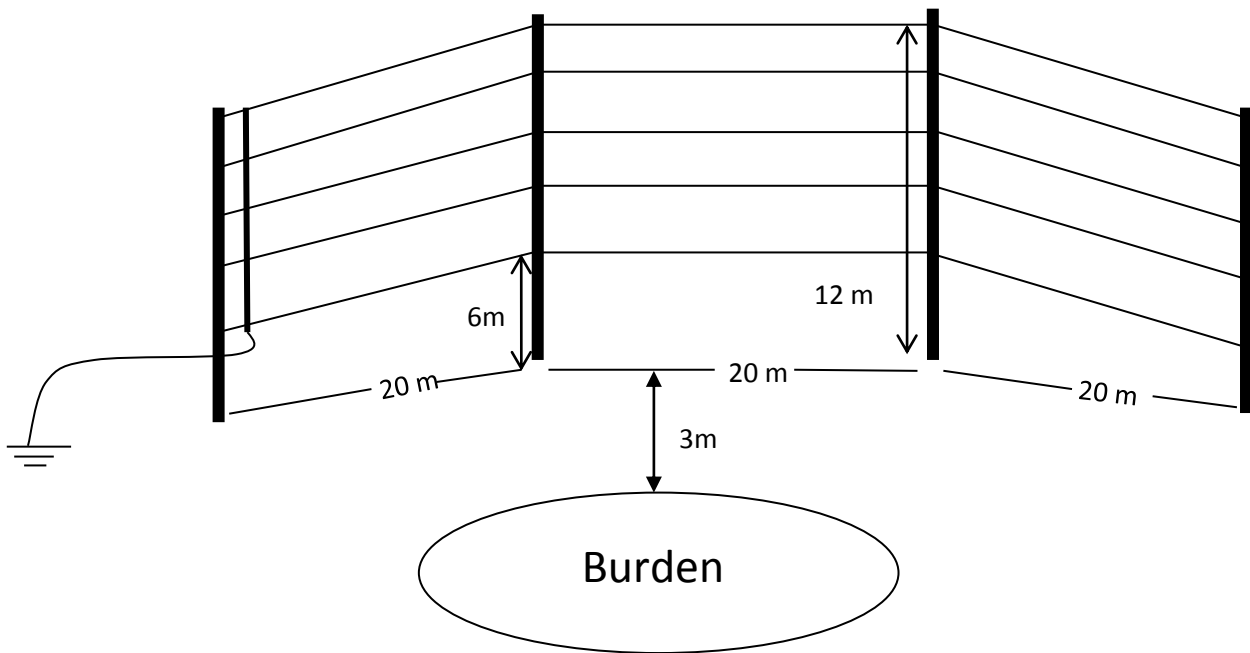


Figure 4.13 Vertical grid shield of equally spaced wires

4.3.1.3 Shielding by a horizontal grid of grounded wires

A horizontal grid of grounded wires can provide effective shielding under it. This type of shielding is effective especially under the transmission lines. Generally these horizontal grid concepts are applied to an infinite grid of parallel wires uniformly spaced at a constant height. It is assumed that the field is induced by high voltage conductors far from the grid and the ground. A perfect shield over a plane would be another plane at zero potential.

The shielding efficiency of an infinite grid, SE_{∞} , is defined as

$$SE_{\infty} = \frac{2\pi H/S}{\ln \frac{2H}{R} + \ln \left[\frac{e^{2\pi H/S} - e^{-2\pi H/S}}{4\pi H/S} \right]}$$

Where, R is the wire size, H is the grid height and S is the spacing of conductors.

The shielding efficiency under a finite grid may be considered as the product of two factors. The first factor is the shielding efficiency of an infinite grid, SE_{∞} . The second factor is the reduction of shielding efficiency because of the edge effects. The dominant independent variable in this case is the ratio of horizontal position to shield grid height.

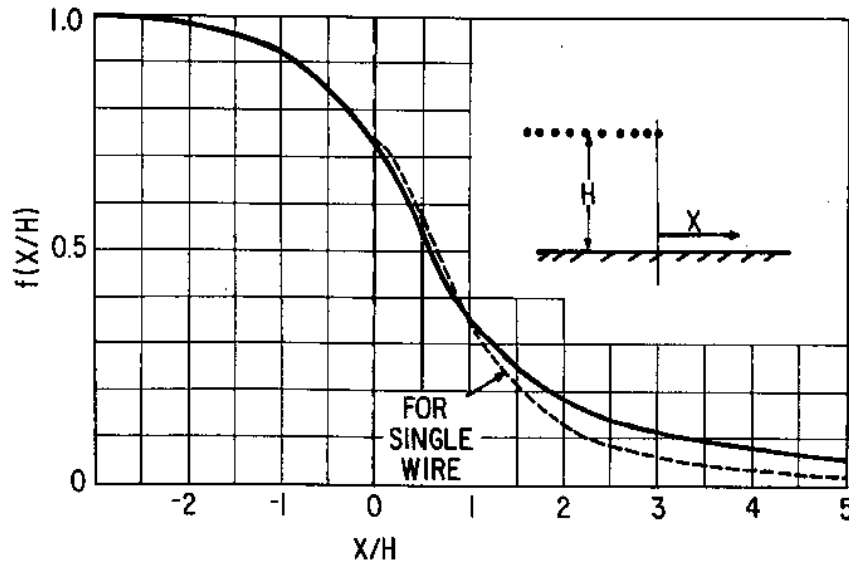



Figure 4.14 Edge factor for horizontal grid of shield wires [6].

$$SE(X) = SE_{\infty} \cdot f\left(\frac{X}{H}\right)$$

The values of $f(X/H)$ were determined from a number of computed and measured solutions and are shown in Figure 4.11. The field under the shield is then

$$E_s(X) = E_u \left[1 - SE_{\infty} \cdot f\left(\frac{X}{H}\right) \right]$$


 University of Moratuwa, Sri Lanka.
 Electronic Theses & Dissertations
www.lib.mrt.ac.lk

4.3.2 Shielding the magnetic field

There are two basic 50Hz magnetic field mitigation (reduction) methods: passive and active. Passive magnetic field mitigation includes rigid magnetic shielding with ferromagnetic and highly conductive materials, and the use of passive shield wires installed near transmission lines that generate opposing cancellation fields from electromagnetic induction. Varying magnetic fields generate eddy currents that act in order to cancel the applied magnetic field. The result is that a part of the magnetic radiation is reflected from the surface of the conductor, a part of the field is absorbed inside, and a part of it penetrates the shield.

Several factors serve to limit the shielding capability of real magnetic shields. One is that, due to the electrical resistance of the conductor, the excited field does not completely cancel the incident field. Also, most conductors exhibit a ferromagnetic response to low-frequency magnetic fields, so that such fields are not fully attenuated by the conductor. Any holes in the shield force current to flow around them, so that fields passing through the holes do not excite opposing electromagnetic fields. These effects reduce the field-reflecting capability of the shield.

For slowly varying, such as 50Hz magnetic fields, shields made of high magnetic permeability metal alloys can be used, such as sheets of Perm alloy and Mu-Metal, or with Nano-crystalline grain structure ferromagnetic metal coatings. These materials do not block the magnetic field, as with electric shielding, but rather draw the field into themselves, providing a path for the magnetic field lines around the shielded volume. The best shape for magnetic shields is thus a closed container surrounding the shielded volume. The effectiveness of this type of shielding depends on the material's permeability, which generally drops off at both very low magnetic field strengths and at high field strengths where the material becomes saturated. So to achieve low residual fields, magnetic shields often consist of several enclosures one inside the other, each of which successively reduces the field inside it.

Because of the above limitations of passive shielding, an alternative used with low-frequency fields is active shielding; using a field created by electromagnets to cancel the ambient field within a volume. Solenoids and Helmholtz coils are types of coils that can be used for this purpose. Active magnetic field mitigation uses electronic feedback to sense a varying 50Hz magnetic field, then generates a proportionally opposing (nulling) cancellation field within a defined area (room or building) surrounded by cancellation coils. Ideally, when the two opposing 180-degree out-of-phase magnetic fields of equal magnitude intersect, the resultant magnetic field is completely cancelled (nullified). This technology has been successfully applied in both residential and commercial environments to mitigate magnetic fields from overhead transmission and distribution lines, and underground residential distribution lines. Additionally, superconducting materials can expel magnetic fields via the Meissner effect[17].



Susceptibility of Detonators to the Electric and Magnetic Fields

5.1 Electric Field Couplings

It was observed in chapter 3, the 50Hz electric fields under the transmission line are significantly large and would be around 5kV/m directly under the conductors of 220kV double circuit twin zebra line. Hence, it was of interest to investigate the behavior of detonators under the influence of electric field.

5.1.1 Testing of detonators placed inside electric fields

In the initial testing, a parallel metal sheet arrangement with 0.5m x 0.5m plates was used for providing a uniform field for the detonators. Initially, this was setup at the high voltage laboratory of the University but did not apply the electric field across the detonator, since the size of the explosion was unpredictable.

Then, it was tested in a blasting site of W.A.Perera & Company at Panagoda under the supervision of license holders in blasting industry. The detonator was placed between the metal parallel plates with its leads projecting towards the plates but not touching the plates. With this arrangement, voltages of 2200V and 1450V were applied across the detonator using hand driven portable exploder or shot blaster and the capacitor charge build-up type exploder respectively. But no explosion was observed. Further, 660V/m electric field (with the 230V only supply available at the site) was also applied across the detonator but no firing was observed. When, 230V mains supply was applied to the detonator, firing occurred. The size of the explosion observed was significantly large that even the parallel metal plates were pierced. Hence, it was concluded that under normal laboratory conditions, this kind of an explosion cannot be handled.

It was decided to measure the induced currents in a conductor placed inside the electric field instead of placing the detonator itself directly. By this way, it is possible to determine the induced currents in the bridge wire of the detonator placed inside electric fields. 230V ac supply was applied across the parallel plates with a separation of 350mm and the conductor was placed between plates. But no appreciable current i.e. at least in the range of milli-ampere was observed.



Figure 5.1: Investigating the behavior of detonator placed in an electric field in open air

Later, with the milli-ampere meter connected, the voltage was raised up to 5kV across the parallel plates with a separation of 350mm but no induced current in the conductor was observed. A galvanometer was also connected across the conductor (figure 5.1) to see any sign of inducements due the electric field applied and no movement was observed in the galvanometer. Since any induced current could not be observed in the milli-ampere range, a digital oscilloscope was connected across a 0.5Ω shunt resistor to observe induced currents in the region of micro-amperes.

But, no induced currents in the conductor placed in a electric field over 12000V/m could be observed even in the range of micro-amperes. Hence, it was concluded that no significant current is induced in a bridge wire of an electro explosive device (EED) placed in a 50Hz electric field emanating under a transmission line so as to initiate an inadvertent firing.

The effect of transient electric fields, in free space, shows that the minimum energy threshold for ignition of commercial EEDs is not met for pulsed electric fields of 100kV/cm transient electrical fields in free space are unlikely to cause ignition of commercial EEDs without the occurrence of a secondary effect such as electrical breakdown between leads due to surface flashover or other mechanisms [3].

Z



Figure 5.2: Investigating the induced currents in a conductor placed in an electric field

5.1.2 Testing of detonators placed inside electric fields

The Institute of Makers of Explosives (IME) Safety Library Publication 20, July, 2001, provides recommended tables of distance between electric field emitters and electric detonators of a nominal one ohm bridgewire resistance. This information has been useful to the blasting community for many years and undoubtedly has assisted in preventing inadvertent initiation of electro-explosive devices by strong electric fields [15]. The following log-log plot shows the acceptable electric field strength, (E Field in volts/meter), as a function of frequency in megahertz, (MHz), that normal electric detonators can be exposed to while minimizing the risk of inadvertent initiation due to electric fields under different frequencies.

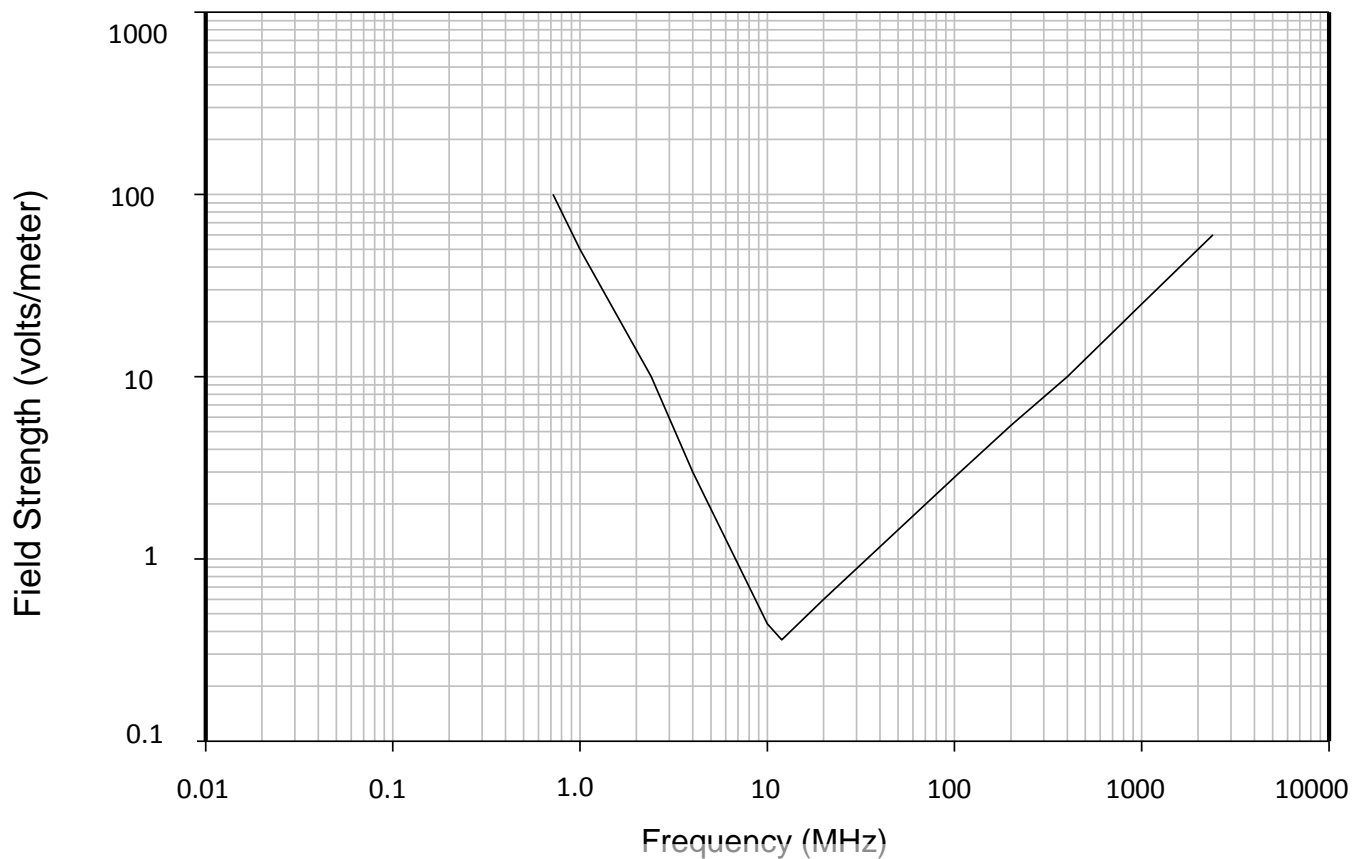


Figure 5.3 Acceptable electrical field strength for a commercially available electrical detonator



University of Moratuwa, Sri Lanka.
 Electronic Theses & Dissertations
www.lib.mrt.ac.lk

The above chart is a plot of acceptable RF field strengths as a function of frequency, in volts per meter, from sources of radiating electromagnetic energy in a location where any part of the electric detonator is expected to be present with respect to the sources of electric field emission. It has to be understood that the above plot applies to far field conditions only, that is, circumstances where the electric detonator and its lead-wires is separated from the source by a distance of at least a few wavelengths.

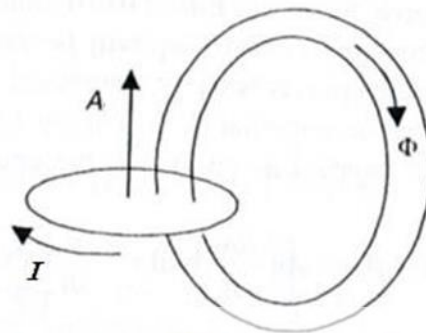
It is also observable from the plot that there is no possibility of 50Hz electric field of any strength to have an impact on the detonator and electric fields of more than 0.7 MHz (700,000 Hz) only will have impacts on commercially available detonators.

5.2 Magnetic field couplings

5.2.1 Relationship between induced emf (E) and magnetic flux (B)

Lenz's law states that "The direction of the induced electromagnetic force (emf) is such that any current which it produces, tends to oppose the change of flux"[1].

When the circuit is a simple, single-turn one, then the 'flux-linkage' is the amount of the flux Φ which is passing through the single-turn coil. Then notation Φ is used to denote the flux-linkage with a coil as well as through a loop. We explain the significance of the Lenz's law with reference to Figure 5.1.



University of Moratuwa, Sri Lanka.

Electronics Theses & Dissertations

www.lib.mrt.ac.lk

In this Figure, if the resultant flux through the circuit has the direction A and is increasing, induced current in the circuit will tend to set up a flux in the direction opposite to A. Hence the direction of the current must be as shown by the arrow A.

The Faraday's law of induction can be formally stated giving the emf induced in a wire loop C (Figure 5.2) as follows:

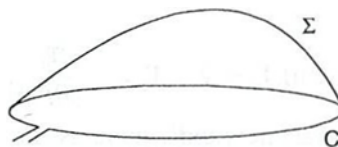


Figure 5.5 Induced emf in the wire loop.

$$E = - \frac{d\Phi}{dt} \quad (5.1)$$

Where Φ is the surface integral of \mathbf{B} evaluated over any surface Σ with its edge on C.

Thus, in words, the Faraday's law is:

The emf in the circuit is proportional to the rate of change of the flux linked by it, and the sense of the current flowing in the circuit is such that it (i.e. the current) opposes the change of the flux Φ [2].

Now, the emf of a battery is the energy supplied per unit charge delivered; and an electric force \mathbf{E} is set up within a wire connecting the terminals, and hence (Figure 5.6):

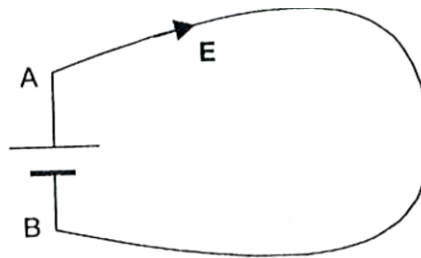


Figure 5.6 Battery loop.

The energy supplied per unit charge, $E = \int_A^B E_1 dl$
 i.e. the line integral of E along the wire, $= V_A - V_B$



University of Moratuwa, Sri Lanka.
 Electronic Theses & Dissertations
www.lib.mrt.ac.lk

Hence the generalization of Eq. (5.1), for any loop whether of wire or otherwise is

$$\oint E_1 dl = - \frac{d\Phi}{dt} \quad (5.2)$$

If we consider an element δl contour δC , enclosing an area δA , then

$$\Phi = B \cdot \delta A$$

\therefore Equation (5.2) becomes

$$\oint E_1 dl = - \delta A \cdot \frac{\partial B}{\partial t}$$

$$E = - \delta A \cdot \frac{\partial B}{\partial t} \quad (5.3)$$

Where, E is the induced emf, δA is the loop area and $\frac{\partial B}{\partial t}$ is the rate of change of flux density with respect to time. This verifies the Neumann's law which states that "When the flux

linked with a coil (or circuit) is changed in any manner, then an emf is set up in the circuit such that it (the emf) is proportional to the rate of change of the flux-linkage with the circuit”.

5.2.1.1 The time taken for detonator for firing

Normal current required for firing = 1A

The Joule heating required, for the detonator to fire ≥ 5 mJ (from Specification.)

$$\therefore \text{Energy} = I^2 \cdot r \cdot t = 5 \text{ mJ} \quad r = 2 \text{ ohm}$$

$$\text{Time taken;} \quad t = 2.5 \text{ ms}$$

Minimum Current Requirement for

detonator to fire = 50 mA (from Specification.)

$$\text{Time taken;} \quad t = 1 \text{ s}$$

The time taken for detonator to fire would be $2.5 \text{ ms} \leq t \leq 1 \text{ s}$ depending on the current provided for the detonator.

5.2.2 Minimum flux density requirement for firing



University of Moratuwa, Sri Lanka.
Electronic Theses & Dissertations
www.lib.mrt.ac.lk
 $B(t) = \sqrt{2} \cdot B_{rms} \sin \omega t$

$$\text{Energy} = I^2 \cdot R \cdot t$$

Considering a loop area of 1 m^2 with one detonator

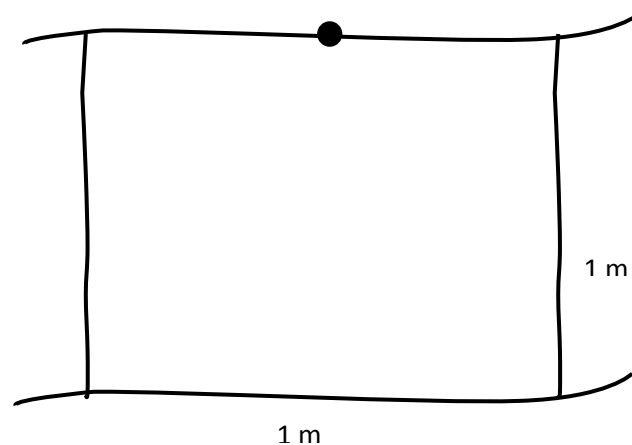


Figure 5.7 1 m^2 detonator circuit loop.

Resistance of the lead wire = 0.1 Ω / m and detonator resistance = 2 Ω

$$\begin{aligned} \text{From equation 5.2 and 5.3; } E &= \frac{-d\phi}{dt} = -\delta A \frac{dB}{dt} \\ &= -A \cdot \omega \cdot B_{rms} = -1 \cdot (2\pi f) B_{rms} \end{aligned}$$

For a loop resistance of 3 ohm ,

$$I = \frac{V}{R} = \frac{\omega \cdot B_{rms}}{3} \geq 50\text{mA}$$

$$B_{rms} \geq 47.75 \times 10^{-5} \text{ T}$$

When the flux density, **B** exceeds 47.75x10⁻⁵ T, there is a possibility of detonator firing.

$$\begin{aligned} \text{Energy supplied} &= I^2 r t = \left(\frac{\omega \cdot 47.75 \times 10^{-5}}{3}\right)^2 \times 2 \times 1 > 5 \text{ mJ} \quad r = 2 \Omega, t = 1\text{s} \\ &> 5 \text{ mJ} \end{aligned}$$

This implies that when a flux density of value exceeds 47.75x10⁻⁵ T, the detonator would initiate firing and the distance at which this occurs could be determined from the magnetic flux density variation profile simulated for 0.5m above the ground. (figure 5.5).

It is observed from the magnetic field profiles for rated loading, infrequent high loading and emergency short time loading, the safe distance for 220kV transmission line is 32m away from the center of the line.

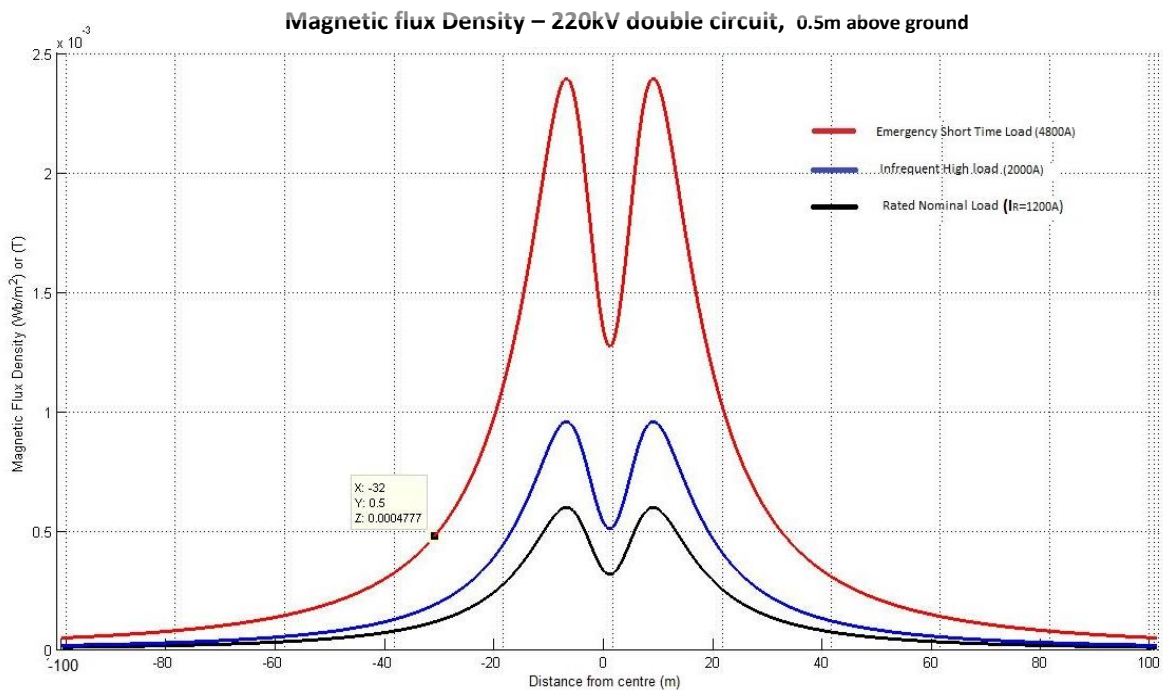


Figure 5.8 Flux density variations 0.5m above ground for different loadings for 220kV double circuit twin conductor configuration.

Similarly, for 132kV twin zebra conductor double circuit configuration, the flux density profiles 0.5m above ground can be plotted as follows.

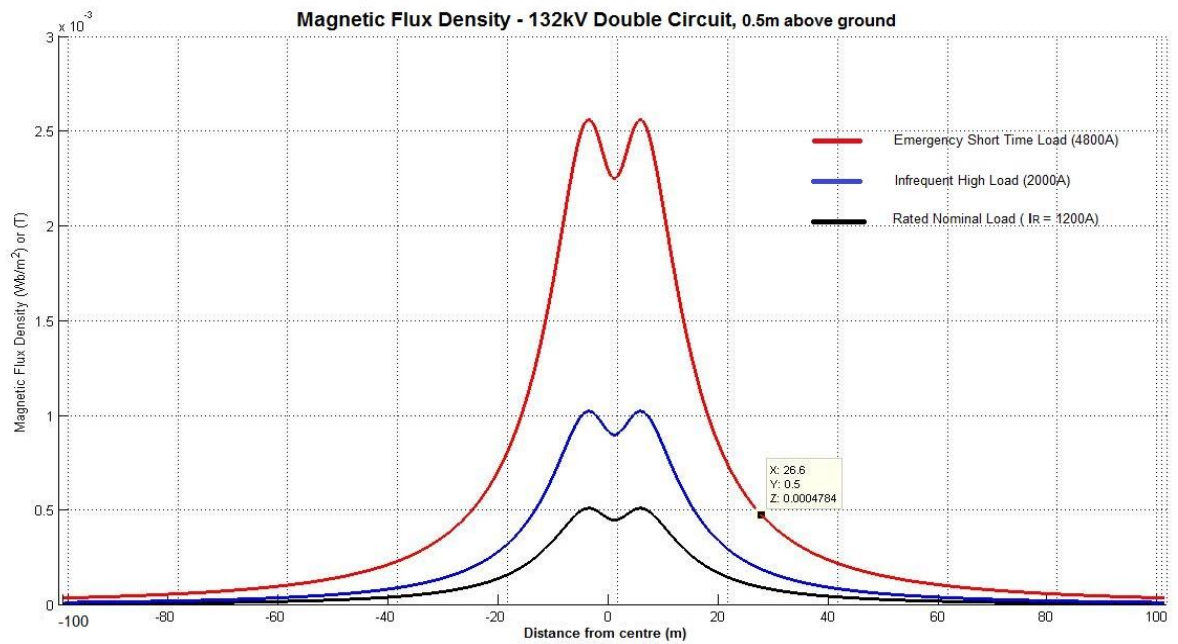


Figure 5.9 Flux density variations 0.5m above ground for different loadings for 132kV double circuit twin conductor configuration.

It is observed, considering only the magnetic field variations for rated loading, infrequent high loading and emergency short time loading, the safe distance for 132kV transmission line is 26.6m from the center of the line.

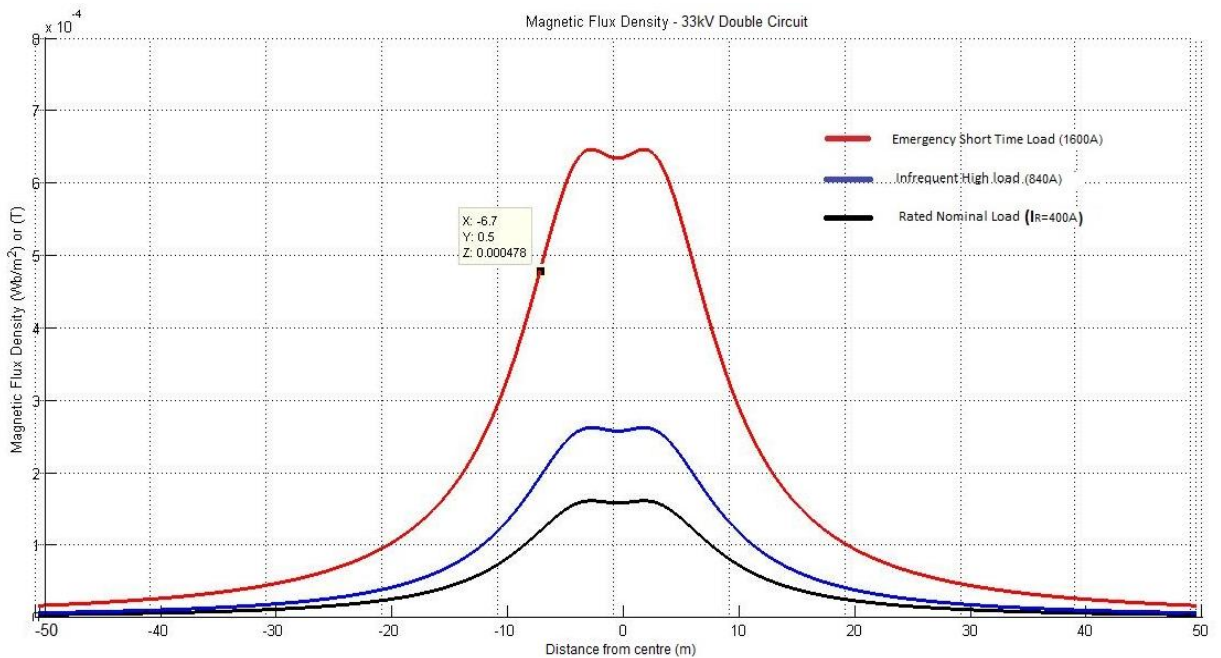


Figure 5.10 Flux density variations 0.5m above ground for different loadings for 33kV double circuit Lynx conductor configuration.

Similarly, for 132kV twin zebra conductor double circuit configuration, the flux density profiles 0.5m above ground can be plotted as above.

It is observed considering only the magnetic field variations for rated loading, infrequent high loading and emergency short time loading, the safe distance for 33kV transmission line is 6.7m from the center of the line.

5.2.3 Inducements of current in the detonator circuits caused by surges occurring in the transmission lines.

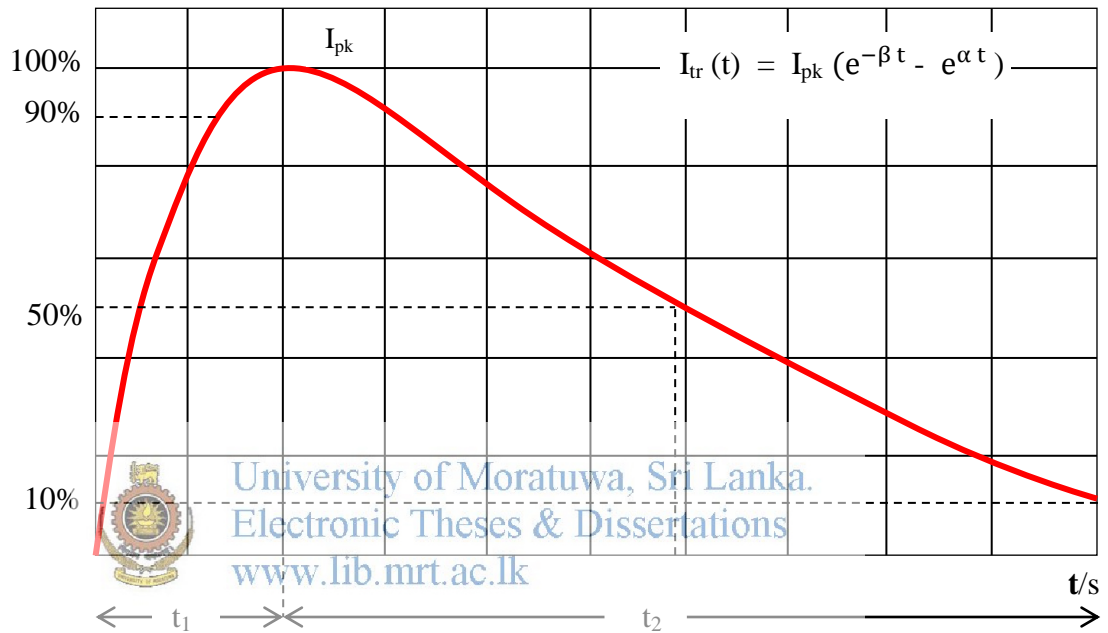


Figure 5.11 A typical current surge that occurs in a transmission line.

From Eqn (5.2), Emf induced $E = -\delta A \cdot \frac{dB}{dt}$

$$= -A \cdot \frac{\Delta B}{\Delta t} \quad \Delta B = B_D$$

For t_1 of Surge

$$E = \frac{-B_D}{t_1} \rightarrow I_1 = \frac{B_D}{Rt_1}$$

For t_2 of Surge

$$E = \frac{B_D}{t_2} \rightarrow I_2 = \frac{B_D}{Rt_2}$$

For both inducements to cause the detonator initiation;

$$\begin{aligned}
 5 \text{ mJ} &\leq I_1^2 r t_1 + I_2^2 r t_2 \\
 &\leq \frac{B_D^2}{R^2 t_1^2} \cdot r \cdot t_1 + \frac{B_D^2}{R^2 t_2^2} \cdot r \cdot t_2 \\
 &\leq \frac{r B_D^2}{R^2} \left(\frac{1}{t_1} + \frac{1}{t_2} \right) \\
 B_D &\geq \sqrt{\frac{5 \times 10^{-3} \times R^2}{r \left(\frac{1}{t_1} + \frac{1}{t_2} \right)}} \quad (5.4)
 \end{aligned}$$

This gives the minimum requirement of flux linkage in order for detonation to take place [1].

5.2.4 Inducements caused by transmission line faults

Transmission line fault currents will depend on the type of fault, the fault level, line impedance etc. Three phase line-to-line fault will cause the most severe currents due to the low impedance compared to other types of faults. Depending on the fault level, the fault currents in 220kV system could be as high as 40kA but on the average, a fault current of 25kA is considered for 220kV system and fault currents of 20kA and 15kA are considered for 132kV and 33kV systems respectively.

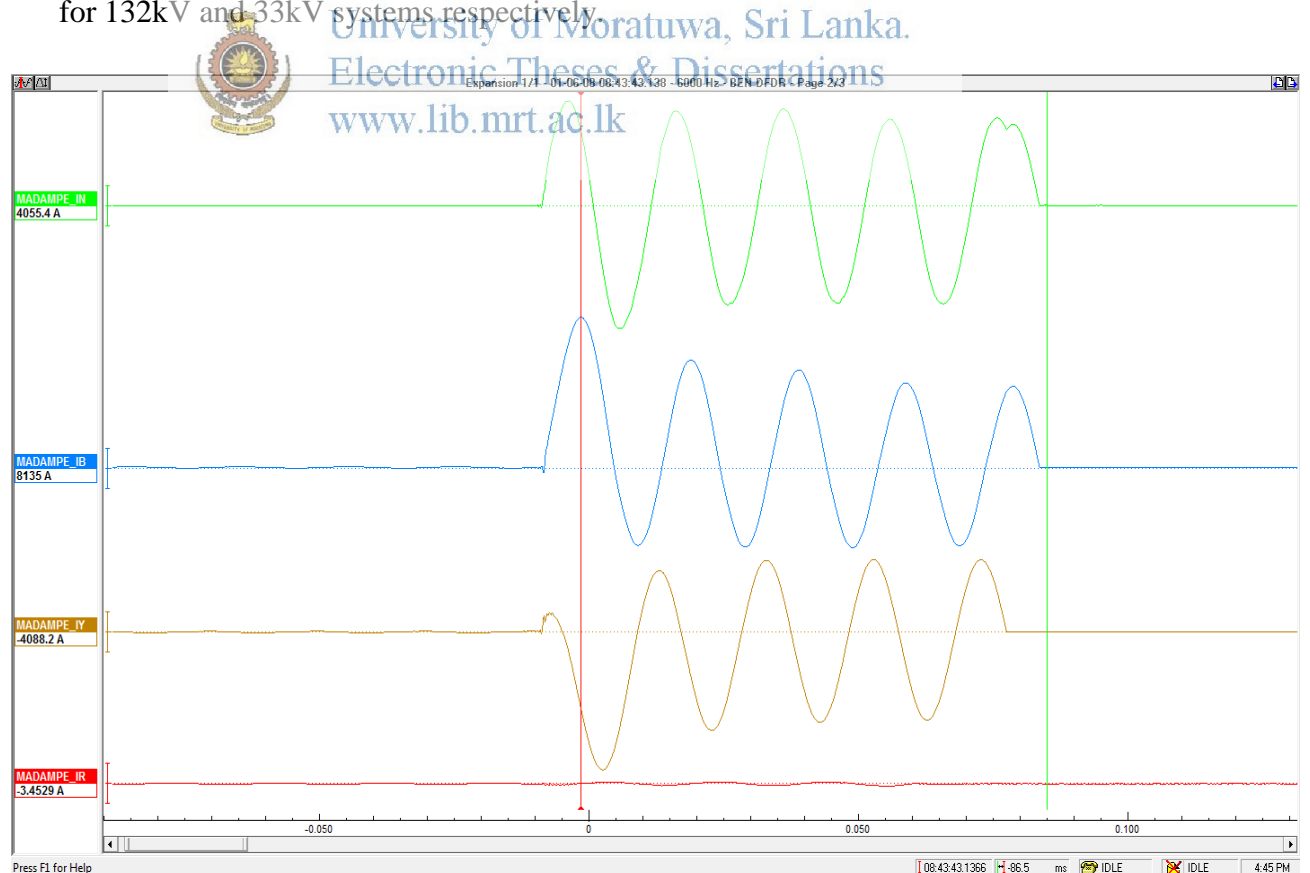


Figure 5.12 A phase to phase to earth fault that occurred in Kotugoda - Madampe 132kV transmission line.

It is evident from most of the transmission line faults that the fault rise time is around half a cycle while the average fault persistent time is about four cycles (Cycle time is 20ms for a 50Hz system). Taking these facts into account we can find a minimum flux linkage requirement for detonator initiation and the minimum safe distance.

$$\text{From equation 5.2 and 5.3; } E = \frac{-d\phi}{dt} = -\delta A \frac{dB}{dt}$$

$$\text{For the fault rise time } E = -1. \frac{\Delta B}{t_1}$$

$$\text{For the fault persistent time } E = -\delta A. \omega. \Delta B$$

$$\delta A = 1m^2, t_1 = 10ms, t_2 = 80ms, \omega = 2\pi f, r = 2 \Omega, R = 3 \Omega$$

$$I = \frac{E}{R}, \text{ Therefore, } \text{Energy}_1 = \left(\frac{\Delta B}{Rt_1}\right)^2 \times 2 \times t_1$$

$$\text{Energy}_2 = \left(\frac{100\pi.\Delta B}{R}\right)^2 \times 2 \times t_2$$

$$\text{Energy}_1 + \text{Energy}_2 \geq 5mJ$$

$$\frac{B^2}{4^2 \times 10 \times 10^{-3}} \times 2 + \frac{(100\pi.B)^2}{4^2} \times 2 \times 80 \times 10^{-3} \geq 5 \text{ mJ}$$

 www.lib.mrt.ac.lk

$$B \geq 167.75 \times 10^{-5} \text{ T}$$

This implies that when the flux density exceeds the value $167.75 \times 10^{-5} \text{ T}$, the detonator would initiate firing and the distance at which this occurs could be determined from the magnetic flux density variation profile simulated for 0.5m above the ground (figure 5.10).

It is observed from this magnetic field profile for a fault current of 20kA, the safe distance for 220kV transmission line is 31.4m from the center of the line.

In the similar manner, fault currents of 15kA and 10kA are considered for 132kV and 33kV circuits to find safe distances under fault conditions. It can be observed that the safe distances under these fault conditions for 132kV and 33kV double circuit configurations are 10.2m and 9.1m respectively.

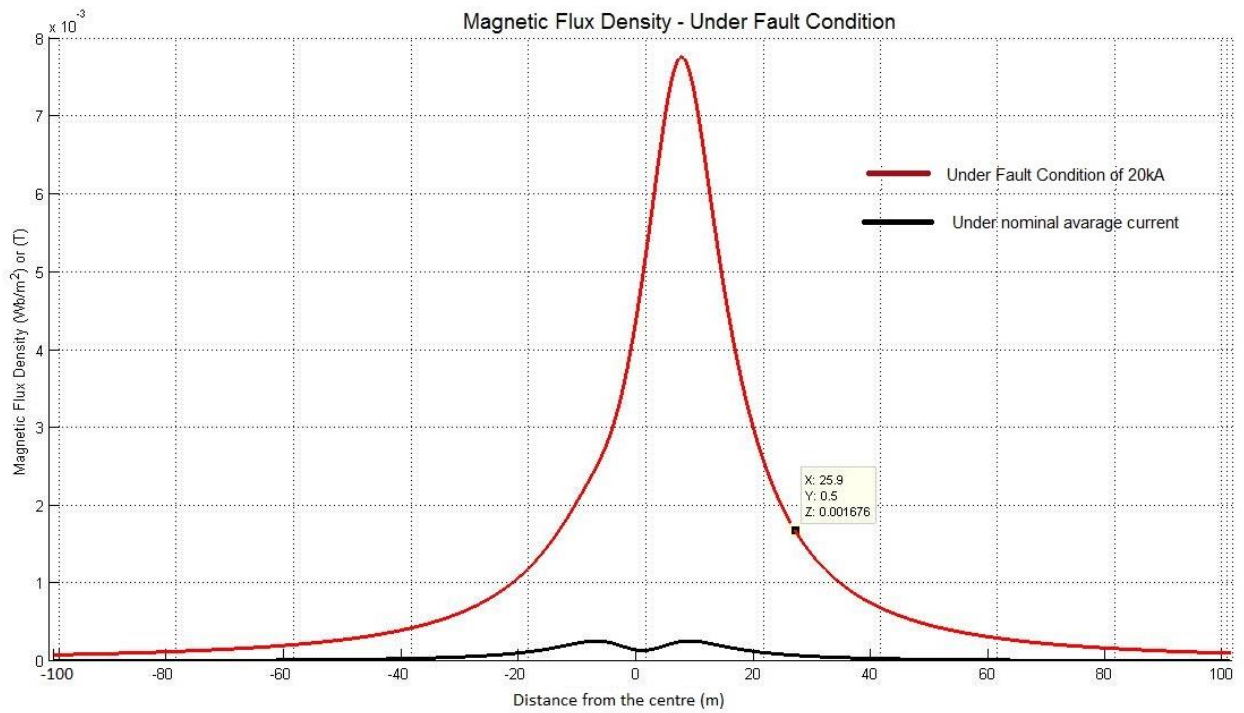


Figure 5.13 Flux density variations 0.5m above ground due to a line fault of 20kA for 220kV double circuit twin conductor configuration.

5.2.5 Inducements caused by travelling lightning waves in transmission lines

Lightening is always a major threat encountered in the blasting industry and in Chapter 2 also it was mentioned that all explosive activities to be suspended at the sign of thunder storms approaching or if there is any possibility of occurrence lightening. There may not be any sign of lightening or raining in the vicinity, but there is a possibility that from lightening travels several miles as travelling waves along the power transmission lines and inducing currents in detonator circuits in close proximity sufficient enough to cause unanticipated firing. The travelling waves could cause currents of several kA at the discharge but we consider 20kA discharge current in the 220kV transmission line due to a direct stroke.

Here, we consider a travelling wave with a lesser steepness assuming it has travelled more than 25km.

From Eqn (5.3), for $t_1 = 100\mu s$ and $t_2 = 800\mu s$, $R = 3\Omega$, $r = 2\Omega$

The requirement in flux density for inducing 5mJ in detonator circuit is given by

$$B_D \geq \sqrt{\frac{5 \times 10^{-3} \times R^2}{r \left(\frac{1}{t_1} + \frac{1}{t_2} \right)}} = 141.4 \times 10^{-5} T$$

This implies that when the flux density exceeds the value 141.4×10^{-5} T, the detonator would initiate firing and the distance at which this occurs could be determined from the magnetic flux density variation profile simulated for 0.5m above the ground (figure 5.5.) for the lightning surge.

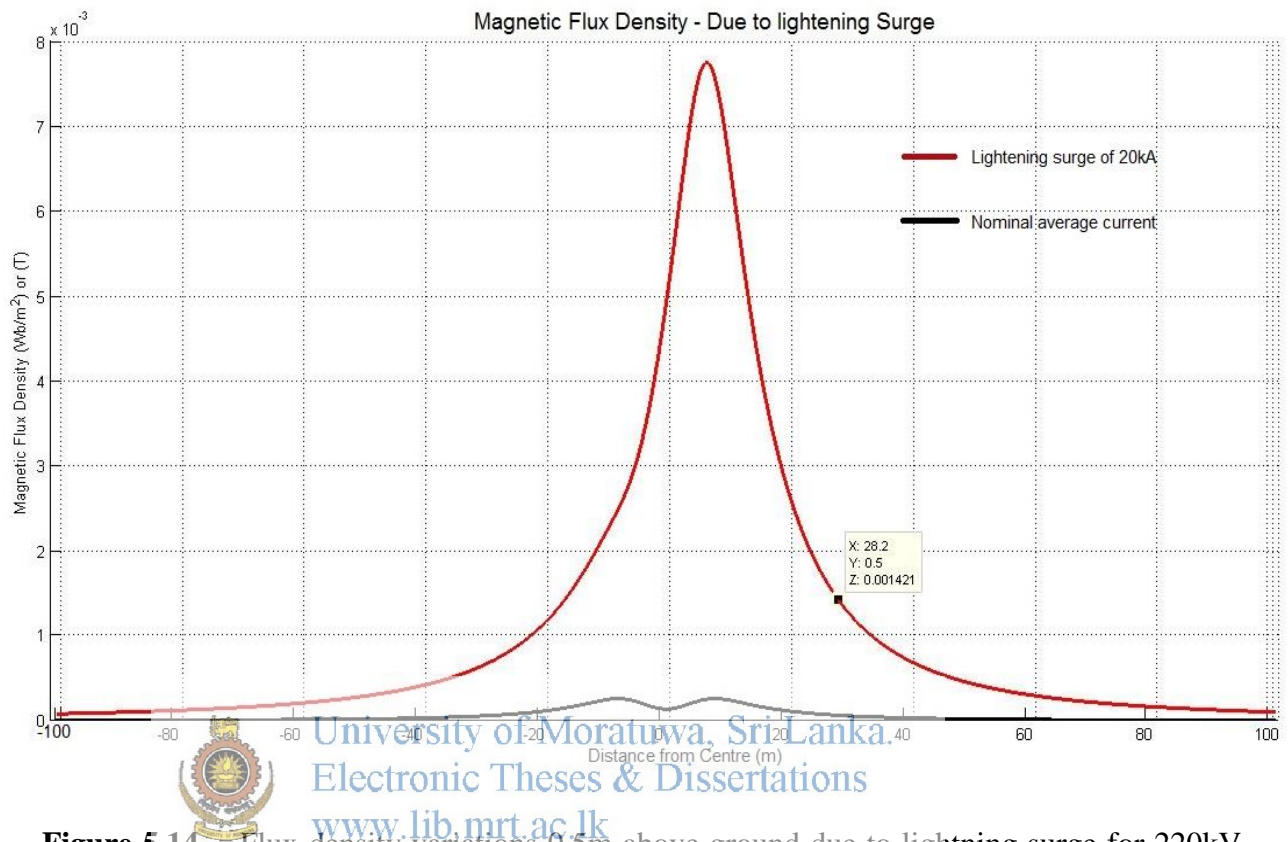


Figure 5.14 Flux density variations 0.5m above ground due to lightning surge for 220kV double circuit twin conductor configuration.

It is observed from the magnetic field profile for a lightning surge of 20kA, the safe distance for 220kV transmission line is 29.5m from the center of the line.

Similarly, lightning discharge currents of 15kA and 10kA with the same impulse shape with $t_1 = 200\mu\text{s}$ and $t_2 = 1000\mu\text{s}$ are considered for 132kV and 33kV circuits to find safe distances under lightning waves travelling conditions. It can be observed that the safe distances under these conditions for 132kV and 33kV double circuit configurations are 16.6m and 8.3m respectively.

5.2.6 Inducements caused by switching surges in transmission lines

As with lightning surges, the reason switching surges are a concern is that they can produce significantly large current surges when flashover or discharges occur. The switching surge comes in many different forms, and has many different sources and generally they occur in clusters. Switching surge could possess sharp steep fronted waveforms and the magnitudes

could rise up to 3pu due to reflections [16], [14]. For a switching surge having parameters of $t_1 = 20\mu s$ and $t_2 = 80\mu s$, from Eqn (5.3),

$$B_D \geq \sqrt{\frac{5 \times 10^{-3} \times R^2}{r \left(\frac{1}{t_1} + \frac{1}{t_2} \right)}} = 60 \times 10^{-5} \text{ T}$$

This implies that when the flux density exceeds the value $60 \times 10^{-5} \text{ T}$, the detonator would initiate firing and the distance at which this occurs could be determined from the magnetic flux density variation profile simulated for 0.5m above the ground (figure 5.12) for switching surge.

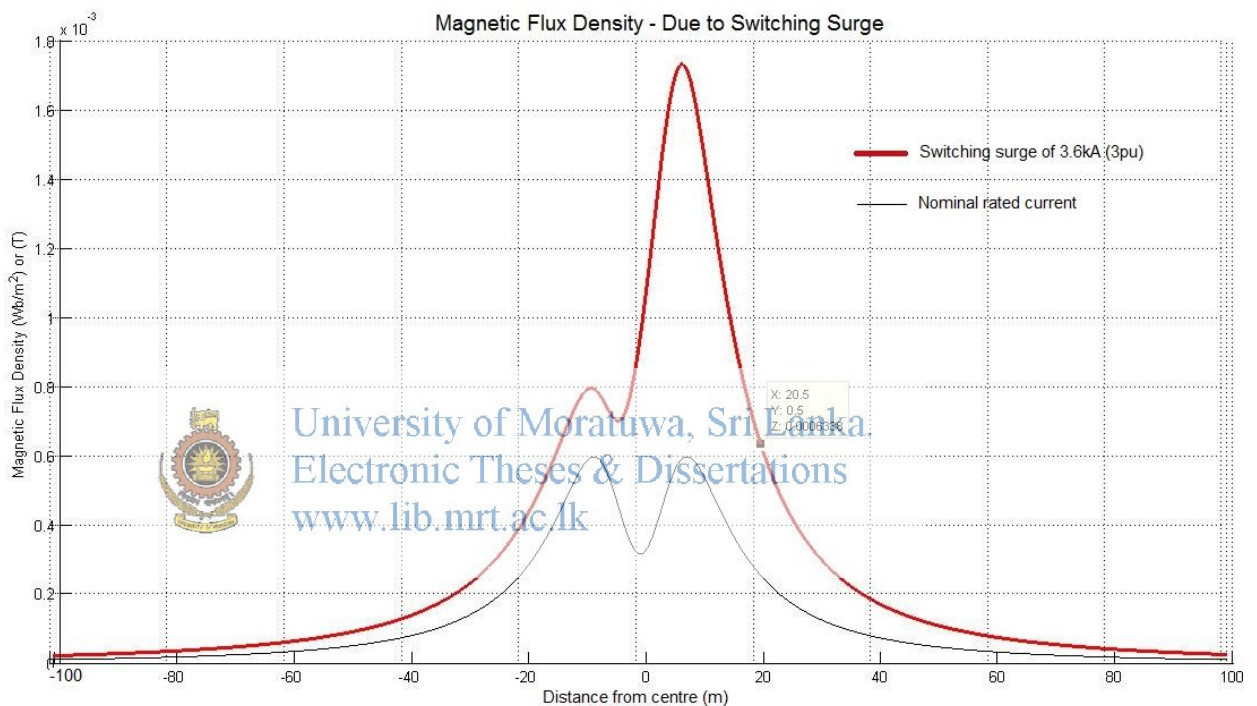


Figure 5.15 Flux density variations 0.5m above ground due to switching surge for 220kV double circuit twin conductor configuration.

It is observed from the magnetic field profiles for a switching surge with a peak of 3.6kA, the safe distance for 220kV transmission line is 17.7m from the center of the line.

Similarly, switching surge currents of 3.6kA and 1.2kA with the same impulse shape with $t_1 = 20\mu s$ and $t_2 = 80\mu s$ are considered for 132kV and 33kV circuits to find safe distances under switching impulse conditions. It can be observed that the safe distances under these conditions for 132kV and 33kV double circuit configurations are 11.5m and 5.2m respectively. The safe distances for 33kV horizontal and triangular configurations were also considered with switching currents of 600A for each and the safe distances are 3.1m and 4.0m are respectively.

The summary of different scenarios considered, relevant magnetic flux densities and the corresponding are currents given in Table 5.1.

Voltage	Circuit Configuration	Loading currents ($B_{\min} = 47.75 \times 10^{-5} \text{ T}$)			3 \emptyset Fault current ($B_{\min} = 167.75 \times 10^{-5} \text{ T}$) kA	Lighting Surges ($B_{\min} = 141.4 \times 10^{-5} \text{ T}$) kA	Switching Surges ($B_{\min} = 60 \times 10^{-5} \text{ T}$) kA
		Nominal Rated Load (kA)	Infrequent High Load (kA)	Emergency Short Time Loads (kA)			
220 kV	Double Circuit	1.40	2.0	4.8	20	20	3.6
132 kV	Double Circuit	1.407	2.0	4.8	15	15	3.6
33 kV	Double Circuit	0.4	0.64	1.6	10	10	1.2
33 kV	Horizontal	0.2	0.32	0.8	10	10	0.6
33 kV	Triangular	0.2	0.32	0.8	10	10	0.6

Table 5.1 The currents corresponding to different loading conditions, faults, lightening and switching conditions

5.3 Safe Distances



University of Moratuwa, Sri Lanka.
Electronic Theses & Dissertations
www.lib.mrt.ac.lk

The safe distances for the different scenarios considered with a safety margin of 20% are given in Table 5.2.

Voltage	Circuit Configuration	Safe Distance (m)						Rounded off Safe Distance with a Tolerance of 20% (m)
		Nominal Rated Loads	Infrequent High Load	Emergency Short Time Loads	3 \emptyset Faults	Lighting Surges	Switching Surges	
220 kV	Double Circuit	14	18	32	25.9	28.2	20.5	40
132 kV	Double Circuit	7.0	14.9	26.6	19.7	19.5	7.1	35
33 kV	Double Circuit	--	--	6.7	10.7	10	5.2	15
33 kV	Horizontal	--	--	4.0	6	6.1	3.1	10
33 kV	Triangular	--	--	7.0	6.9	10.6	4	15

Table 5.2 The safe distances corresponding to different loading conditions, faults, lightening and switching conditions

5.4 Discussion on results

The statement of safe distance table could be used as means to assist the mine and quarry operators and commercial blasters. The tables include all of the common types of transmission lines that would be encountered around mines, quarries and other blasting operations in Sri Lanka.

The table was derived from analytical calculations for “worst case scenarios”. They are based on less than 50mA no-fire level and 5mJ minimum joule heating of commercial supreme short-delay detonators (the only type of detonators used in Sri Lanka). Since, the electric detonator is considered to be in the category of weapons, they are imported only by the Defense Ministry and issued to license holders in blasting industry through Geological Survey and Mines Bureau (GSMB). Field tests have shown the results in the table to be conservative although detonators were not used directly in the investigations. When deciding the burden and the area to be involved in the blasting, the proximity of the transmission lines are to be considered in the first place along with other possible hazards like lightening, radio frequency transmitters, electrostatic charges and other sources of extraneous electricity. If the burden comes close to the unsafe distances proposed in this research, precautionary measures are to be adopted. If there is a compulsory requirement of rock blasting within the unsafe distances from transmission lines, use of normal detonators could be employed as an alternative. Switching off the transmission line is also an alternative but one has to keep in mind that the risk of travelling lightening waves is still a threat.

As far as the author of this thesis is concerned, no guideline or published research paper was found on safe distances for operation of detonators from transmission lines to make comparisons with. But, the results derived for safe distance levels from transmission lines are quite reasonable and amply justified when comparing with guidelines drafted for Tables of Distances—RF Sources and Electric Detonators [15].

5.4.1 RF Sources Presenting Hazards to Blasting Operations

Commercial AM broadcast transmitters (0.535 to 1.605 MHz) are potentially the most hazardous. This is because they combine high power and low enough frequency so that there is little loss of RF energy in the lead wires of electrical detonators. Frequency- modulated FM and TV transmitters are also likely to create hazardous situations. Although their power is extremely high and antennas are horizontally polarized, the high-frequency currents are rapidly attenuated in detonators or lead wires. These RF sources usually employ antennas on top of high towers.

Mobile radio, as well as other wireless products, must be rated as potentially hazard because, although their power is low, they can be brought directly into a blasting area.

Transmitter Power Delivered to Antenna (kW)	Minimum Distance (m)
Up to 4.0	219
5.0	244
10.0	344
25.0	546
50.0	762
100.0	1097
500.0	2438

Table 5.3 Recommended Distances for Commercial AM Broadcast Transmitters (0.535 to 1.605 MHz)

MINIMUM DISTANCE (m)					
Transmitter Power delivered to Antenna (kW)	MF 1.7 to 3.4 MHz Fixed Mobile, Maritime	HF 28 to 29.7 MHz Amateur	VHF 35 to 36 MHz Public Use 42 to 44 MHz Public Use 50 to 54 MHz Amateur	VHF 144-148 MHz 150-161.6 MHz Public Use	UHF 450 to 470 MHz Public Use Cellular Telephones Above 800 MHz
0.5	98	318	250	82	53
0.6	107	349	273	90	58
1.0	138	450	352	115	75
1.5	169	552	432	141	92
10.0	438	1,425	1,115	365	236

Table 5.4 Recommended Safe distances from FM, VHF/UHF TV and Cellular transmitters [15]

In comparison with the safe distances for radio frequency radiations, the safe distance values suggested for transmission lines are reasonable and justifiable. When deciding the safe distances for transmission lines, it is very important to identify the line configurations, parameters and line voltages. Identification of the maximum currents that could occur in the transmission line is also a critical factor to be considered since it is the magnetic field emanating the currents that causes inducements in the detonator circuits.

Conclusions and Recommendations

6.1 Conclusions

6.1.1 The simulated results of the models developed for the electric fields and the magnetic fields are verified by the field measured data as the field measuring values very closely follow the simulated values of the model. Therefore, the models can be used reliably for the purposes of further investigations and analysis. Further, the developed model is a comprehensive tool for calculating electric and magnetic fields around the transmission lines in any earth and line profile as it has taken the real parameters into account and capable of accommodating any line configurations with any number of conductors.

6.1.2 No significant induced current (not at least in the range of mA) is observed on the conductors in the presence of electric fields. Hence, it could be concluded that the minimum energy threshold for ignition of commercial electro explosive devices in Sri Lanka is not met in the electric fields in free space under transmission lines.

6.1.3 The magnetic fields developing around transmission lines due to nominal rated loads, infrequent high loads, emergency short term loads, fault currents, switching currents and currents due to travelling lightening surges could be significant enough to induce currents in the circuits those meet the minimum energy threshold for ignition of EEDs. Therefore, detonators should not be used in explosive blasting within unsafe regions under transmission lines.

6.1.4 The following safe distance levels are proposed for safe operations of electro explosive devices.

Voltage	Circuit Configuration	Safe Distance from the line centre (m)
220 kV	Double Circuit (twin conductor)	40
132 kV	Double Circuit (twin conductor)	35
33 kV	Double Circuit	15
33 kV	Horizontal	10
33 kV	Triangular	15

Table 6.1 Statement of safe distances for the operation of detonators

6.2 Recommendations

- 6.2.1** Commercial EEDs should be tightly packed and shorted to reduce loop area and prevent unanticipated detonation. The individual loop areas of the detonator circuits are also recommended to be kept as small as possible so as to prevent inducement of current due to magnetic flux linking them. The trolleys and containers used for transportation of EEDs should be of metal construction.
- 6.2.2** If EEDs and explosives are to be stored close to the transmission lines, the distance of safe margins recommended are to be followed. Buildings and rooms in which EEDs are stored should have conductive grade flooring and metal mats.
- 6.2.3** The model and results of this study could be used for Developing Specifications for safe exposure levels related to health hazards for Sri Lankan context adopting international standards like **IRPA**, **WHO**, **ICNIRP** (International Commission on Non Ionizing Radiation Protection).
- 6.2.4** The models can also be used as a tool for field calculations in planning and designing of future transmission lines for achieving safe values stipulated in the regulations.
- 6.2.5** Most of the defense related weapons are equipped with EEDs and this model could be used for safe handling, storage and transportation of these after identifying the EED specifications.
- 6.2.6** Active or passive shielding of 50Hz frequency magnetic fields to be used during the circuit connection procedure if detonator circuits are to be used inside the unsafe regions.
- 6.2.7** If there is a mandatory requirement of rock blasting within the unsafe distances from transmission lines, use of normal detonators could be employed as an alternative. Switching off the transmission line is also an alternative but one has to keep in mind that the risk of travelling lightening waves is still a threat.
- 6.2.8** The work presented in this study may be used for further future investigation of electromagnetic compatibility of EEDs.

References

- [1] A. Pramanik, "Electromagnetism, Theory and Applications," Prentice Hall Publishers, India, 2004.
- [2] William H. Hayt, Jr., "Engineering Electromagnetics," Third Edition, , Mc Grow Hill Publishers, 2001.
- [3] D. V. Reale, J. Mankowski, and J. Dickens, "Susceptibility of Electro-Explosive Devices to High Pulsed Electric Fields," *IEEE Transactions on electro Magnetic Compatibility*, pp. 211-214, 2012.
- [4] K.R.Lee, J.E.Bennett, W.H. Pinkston and J.E. Bryant, "New method of assessing EED susceptibility to electromagnetic radiation." *IEEE Transactions on Electromagnetic Compatibility*, vol.33 no.4, pp. 328-333, 1991.
- [5] J. Parson, J. Dickens, J. Walter, and A. A. Neuber, "Pulsed magnetic field excitation sensitivity of match-type electric blasting caps," *Rev.Sci.Instrum.*, . *IEEE Transactions on Electromagnetic Compatibility*, vol.81, 105115, 2010.
- [6] "Transmission line Reference Book," Electrical Power Research Institute (EPRI) Publishers, 2005 & 1992.
- [7] M.S.H. Salameh and M.A.S. Hossouna, "Arranging overhead power transmission line conductors using Swarm Intelligence technique to minimize electromagnetic fields," *Progress in Electromagnetics Research B*, Vol.26, 213-236, 2010
- [8] H. Verakis and D. Nicholas, "Electric Blasting systems- Requirements for shunting and circuit testing," *Mine Safty and Health Administration, United States Department of Labour*, November, 2006.
- [9] J. F. Rodrigues, R. C. Creppe, L. G. C. Porto, "To Estimate the Elecric Field Near Electric Energy Transmission Systems by Use Simple Software," *Departamento de Engenharia Electrica, Faculdade de Engenharia, Bauru/UNESP*, 2007.
- [10] P. C Sligmann, "The design of circuits for electrical softfiring," *Journal of the South African Institue of Mining and metallurgy*, October 1978.
- [11] I.M.Nejdawi, O.A. Alani and M.S.H. Al Salameh, "Using Non-Linear Particle Optimisation (PSO) Algorithm to reduce the magnetic fields from overhead high voltage transmission lines." *IJRRAS 4(1)*. July 2010.

- [12] S.Tupsie, A. Isaramongkolrak, P. Oao-la-or, "Analysis of Electromagnetic Field Effects Using FEM for Transmission Line Transposition," *World Economy of Science, Engineering and Technology* 29 2009.
- [13] "Predicted EMF Levels for 132kV (9C6) & 330kV (9C5) Transmission Lines," *Tomago – Brandy Hill & Brandy Hill – Stroud*, TransGrid, Australia, 2011.
- [14] R. D. Begamure, "Extra High Voltage AC Transmission Engineering." Second Edition, Wiley Eastern Limited, 1990.
- [15] "Safety Guide for the Prevention of Radio Frequency Hazards in the Use of Commercial Electric Detonators," *Addendum to IME Safety Library Publication 20 (SLP-20)*, Institute of Manufacturers of Explosives, July, 2001.
- [16] R. F. Kerendian, S. Pazouki, A. Rajabloo, "Evaluation Methods of Limiting Switching Overvoltage during Line Energization," *International Journal of Science and Engineering Investigations*, vol. 2, issue 16, May 2013.
- [17] S. Celozzi, R. Araneo, G. Lovat, "Electromagnetic Shielding," *Appendix B*, Copyright © John Wiley & Sons, Inc. 2008.
- [18] C. Berry, "A Guide to Radio Frequency Hazards with Electric Detonators," *Occupational Safety and Health Program, IME Safety Library Publication NO. 20*, N.C. Department of Labour Raleigh, September, 2009.
- [19] H. Yildirim and O. Kalenderli, "Computation of electric field induced currents on biological bodies near High Voltage transmission lines." *XIIIth International Symposium on High Voltage Engineering*, Netherlands, Smit(ed) © 2003 Millpress, Rotterdam, 2003.



භූ විද්‍යා සමීක්ෂණ හා පතල් කායකිංශය

புவிச்சரிதவியல் அளவை, சுரங்கங்கள் பணியகம்

GEOLOGICAL SURVEY & MINES BUREAU

නො: 569, එපිටමුල්ල පාර,

පිටකෝට්ටේ, ශ්‍රී ලංකා.

இல.: 569, எப்பிட்டமுல்ல வீதி,

பிடகோட்டே, இலங்கை.

No.: 569, EPITAMULLA ROAD,
PITAKOTTE, SRI LANKA.

2013-03-12

My Ref. DDM/11/03/13-01

Eng.W.D. Anura S. Wijayapala,
Senior Lecturer,
University Of Moratuwa,
Moratuwa.

Reg. Post

Dear Sir,

Request for a study on effects of electromagnetic field due to high voltage transmission lines on sensitive detonator firing circuits

The mission of the Geological Survey and Mines Bureau (GSMB) is to provide Geo-Scientific Information, advice and services to the policy makers and the community and to promote and manage the mineral resources of the country for economic development while ensuring environmental sustainability. It regulates exploration, extraction, value addition, transportation and trading of minerals.

The GSMB also conducts awareness programmes to public officers of Divisional Secretariats, Grama Niladhari, Police Officer etc., and licence holders on the regulations gazetted under the Mines and Mineral Act and on environmental protection activities that should be followed with mining activities.

Also awareness programmes are conducted considering the importance of making the public, specially the school children and students of higher educational institutes aware on our mineral resources and geo-hazards.

One such hazard observed recently is the premature blasting of explosives by licence holders probably due to unintentional and unknown causes. Many such incidents have been recorded in mines in recent times and such incidents needs to be prevented to ensure safety of human lives and property while ensuring efficient mining activities such as explosive blasting.

One such common cause for occurrence of unintentional blasting is lightening which could be avoided if proper precautions are taken in advance. The other suspected cause that initiates premature firing of explosive is believed to be the extraneous electricity interfering from high voltage transmission lines with the detonator firing circuits.

A detail study needs to be carried out for finding the effects of induced voltages on the electric detonator firing circuits from the high voltage transmission lines that runs in the vicinity of the mines carrying out explosions. I would be grateful if you could arrange a research level study to investigate into the impacts of extraneous electricity caused by nearby transmission lines and to develop a statement of safe distances of operation for sensitive detonator firing circuits to avoid inappropriate triggering. This would ensure safety of persons working in and around the mines and quarries avoid unexpected damages to property.

Further, the safety distances are different in different countries due to national restrictions and if such safe distances could be predicted accurately, we could educate the public, the licence holders and related officials to take appropriate measures accordingly and ensure safe explosive firing in the mines and quarries.

Your kind attention, in this regards, is much appreciated.

Thank You,



Eng. D. Sajjana de Silva.
Deputy Director (Mines)



University of Moratuwa, Sri Lanka.
Electronic Theses & Dissertations
www.lib.mrt.ac.lk

Specification for Supreme Short Delay Detonators

Description	CEFAP Specifications
Construction	Aluminium shell filled with ASA and PETN as primary and secondary charge. These detonators should have delay numbers ranging from 0 to 9, with a nominal time interval of 25 milliseconds for 7 and 8 and 75 milliseconds for 9
shell	Aluminium with a conical depression at the bottom, length varying for different delay numbers.
Strength	No.6 or 8
Leg(Lead) Wire colour	Should specify
Shell Diameter	6.5 ± 0.05 mm
Leg (Lead) Wire Diameter	24 SWG iron wire
Lead Wire Resistance	0.1 - 0.3ohms/m
Leg(Lead)wire length	4 and 9 m
Fuse Head resistance	1.6 to 2.0 ohms
Firing Energy	2.5 to 3.0 mJ/ohm
Firing Current per series	1 to 1.2 Amps
No firing (No Initiation) Current	50 mAmps
Year of manufacture	Current
Shelf Life	Min. of 05 Years
Packing	Each case should contain detonators of the same delay number only. Five detonators are held in bunch and five such bunches are banded to make a bundle of 25 detonators. Two bundles of 25 detonators each are wrapped in kraft paper and make into a packet, and suitable labelled. 20 to 50 such packets are placed in a wooden case, inside of which is lined with water proof paper. The case is fastened with plastic straps or wires. Entire consignment is desired in 20 foot containers.

MATLAB Script for electric field around 220kV TX Line

```

=====
=====
% 220kV Configuration
=====
=====
clc
clear all
close all

e_r=1; %relative permitivity of air
S=[200 200 200 200 200 200 200 200]; %sub conductor spacing - diameter in mm
N=[ 2 2 2 1 2 2 2 1]; %number of sub conductors per line
d=[ 28.6 28.6 28.6 18 28.6 28.6 28.6 18]; %sub conductor diameter in mm
h=[ 7 12.8 18.5 27 7 12.8 18.5 27]; %Height above ground in m
x=[ -6.5 -6.5 -6.5 -6 6.5 6.5 6.5 6];
Vp_p =[220 220 220 0 220 220 220 0]; %Phase to Phase value of conductor
voltage
phase =[ 0 120 240 0 0 120 240 0]; %Phase angle of the conductor voltages

e_0= 8.8541878176e-12;
e_m=e_r*e_0;
D=S./sin(pi./N);
d_eq=(N.*d.*(D).^ (N-1)).^(1./N); %equivalent diameter in bundle conductor

n=size(S,2); %number of lines
P=zeros(n,n); %Maxwell potential matrix

for j=1:n
    for i=1:n
        if(i==j)
            P(i,j)=(1/(2*pi*e_m))*log(4*h(1,i)*1000/d_eq(1,i));
        else
            den=(x(1,i)-x(1,j))^2+(h(1,i)-h(1,j))^2;
            num=(x(1,i)-x(1,j))^2+(h(1,i)+h(1,j))^2;
            num=4*h(1,i)*h(1,j)+den;
            P(i,j)=(1/(2*pi*e_m))*log(sqrt(num/den));
        end
    end
end
end
end

```



University of Moratuwa, Sri Lanka.

Electronic Theses & Dissertations

www.lib.mrt.ac.lk

```

P_inv=inv(P);
V_r=Vp_p.*cosd(phase)/sqrt(3);%
V_i=Vp_p.*sind(phase)/sqrt(3);%
Q_r=V_r*P_inv;%
Q_i=V_i*P_inv;%

x_N=[-20:0.1:20];
% y_N=[20:0.1:20];
y_N=1*ones(1,100);

x_points=size(x_N,2);
y_points=size(y_N,2);
Ex=zeros(x_points,y_points);
Ey=zeros(x_points,y_points);
V=zeros(x_points,y_points);

j_com=sqrt(-1);
for j=1:size(y_N,2)
    for i=1:size(x_N,2)
        for k=1:n
            C0=(x_N(1,i)-x(1,k))/((x(1,k)-x_N(1,i))^2+(h(1,k)-y_N(1,j))^2);
            C1=(x_N(1,i)-x(1,k))/((x(1,k)-x_N(1,i))^2+(h(1,k)+y_N(1,j))^2);
            C2=C0-C1;
            C3=C2/(2*pi*e_m);
            C4=(Q_r(1,k)+j_com*Q_i(1,k));
            Ex(i,j)=Ex(i,j)+C4*C3;

            end
        end
    end

for j=1:size(y_N,2)
    for i=1:size(x_N,2)
        for k=1:n
            C0=(y_N(1,j)-h(1,k))/((x(1,k)-x_N(1,i))^2+(h(1,k)-y_N(1,j))^2);

```



```

C1=(y_N(1,j)+h(1,k))/((x(1,k)-x_N(1,i))^2+(h(1,k)+y_N(1,j))^2);
C2=C0-C1;
C3=C2/(2*pi*e_m);
C4=(Q_r(1,k)+j_com*Q_i(1,k));
Ey(i,j)=Ey(i,j)+C4*C3;
    end
end
end

E_real_2=real(Ex).^2+real(Ey).^2;
E_imag_2=imag(Ex).^2+imag(Ey).^2;

E=sqrt(E_real_2+E_imag_2); % Intensity in kV/m

% ----- 3D plot for Electric Field-----
[plot_X plot_Y]=meshgrid(x_N,y_N);
surf(plot_X,plot_Y,E)
title('Electric Field (1m above ground)');
xlabel('Horizontal axis- X');
ylabel('Vertical axis- Y');
zlabel('Electric Field (kV/m)');
%-----

for j=1:size(y_N,2)
    for i=1:size(x_N,2)
        for k=1:n
            C0=sqrt(((x(1,k)-x_N(1,i))^2+(h(1,k)-y_N(1,j))^2));
            C1=log(C0/h(1,k));
            C2=sqrt(((x(1,k)-x_N(1,i))^2+(h(1,k)+y_N(1,j))^2));
            C3=log(C2/h(1,k));
            C4=(C1-C3)/(2*pi*e_m);
            V(i,j)=V(i,j)+(Q_r(1,k)+j_com*Q_i(1,k))*C4;
        end
    end
end
end

```



```
V_abs=sqrt(real(V).^2+imag(V).^2); %Potential in kV
```

```
%-----  
figure  
%-----
```

```
%----- 3D plot for Potential-----  
[plot_X plot_Y]=meshgrid(x_N,y_N);  
surf(plot_X,plot_Y,V_abs')  
title('Potential for 245kV Double CCT Line');  
xlabel('Horizontal axis- X');  
ylabel('Vertical axis- Y');  
zlabel('Potential(kV)');  
-----
```



MATLAB Script for Magnetic Field around 220kV TX Line

```

=====
% 220kV Double Circuit Configuration
=====

clc
clear all
close all

u_r_air =1; %Relative permeability of air
u_r_soil=1; %Relative permeability of soil
e_r_soil=1; %Relative permittivity of earth
sigma =0.001; %Conductivity of earth
f =50; %Frequency in Hz
h= [ 7 12.8 18.5 27 7 12.8 18.5 27 ]; %Height above ground in m
x= [ -6.5 -6.5 -6.5 -6 6.5 6.5 6.5 6 ]; %Horizontal placement in m
I_amp= [1200 1200 1200 0 1470 1470 1470 0 ]; %Amplitude of Conductor phase
current in A
I_phase=[ 0 120 240 0 0 120 240 0 ]; %Current phase angle in degrees
University of Moratuwa, Sri Lanka
Electronic Theses & Dissertations
www.lib.mrt.ac.lk
n=size(h,2); %number of lines
u_air =u_r_air*4*pi*10e-7;
u_soil =u_r_soil*4*pi*10e-7;
e_soil =e_r_soil*8.8541878176e-12;
j_comp =sqrt(-1);
I_phasor=I_amp.*(cosd(I_phase)+j_comp*sind(I_phase));

x_N=[-20:0.1:20];% [0 70 100 700 1000 -1000];;
% y_N=.01*ones(1,100);
y_N=[1:0.1:6.0]; %[0];
x_points=size(x_N,2);
y_points=size(y_N,2);

%-----Effect of Conductor Current -----
H_line_x=zeros(x_points,y_points);
H_line_y=zeros(x_points,y_points);

```

```

%Conductor effect - x axis
for j=1:y_points
    for i=1:x_points
        for k=1:n
            r=sqrt((x_N(1,i)-x(1,k))^2+(y_N(1,j)-h(1,k))^2);
            H_line_x(i,j)=H_line_x(i,j)+(I_phasor(1,k)./(2*pi*r))*(h(1,k)-
y_N(1,j))/r;
        end
    end
end

```

```

%Conductor effect - y axis
for j=1:y_points
    for i=1:x_points
        for k=1:n
            r=sqrt((x_N(1,i)-x(1,k))^2+(y_N(1,j)-h(1,k))^2);
            H_line_y(i,j)=H_line_y(i,j)-(I_phasor(1,k)./(2*pi*r))*(x(1,k)-
x_N(1,i))/r;
        end
    end
end

```



University of Moratuwa, Sri Lanka.
Electronic Theses & Dissertations
www.lib.mrt.ac.lk

```

H_real_2=real(H_line_x).^2+real(H_line_y).^2;
H_imag_2=imag(H_line_x).^2+imag(H_line_y).^2;

```

```

H=5.3*sqrt(H_real_2+H_imag_2);

```

```

%-----Effect of Earth's Current-----

```

```

H_e_line_x=zeros(x_points,y_points);
H_e_line_y=zeros(x_points,y_points);

```

```

% Earth's effect -x axis
for j=1:y_points
    for i=1:x_points
        for k=1:n

```



```

Y=sqrt(j_comp*2*pi*f*u_soil*(sigma+j_comp*2*pi*f*e_soil));
r=sqrt((x_N(1,i)-x(1,k))^2+(y_N(1,j)+h(1,k)+ 2/Y)^2);
phi_x=-((h(1,k)+y_N(1,j)+2/Y)/r);
H_e_line_x(i,j)=H_e_line_x(i,j)-
(I_phasor(1,k)/(2*pi*r))*(1+(1/3)*(2/(Y*r))^4)*phi_x;
    end
end
end

```

```
%Earth's effect -y axis
```

```

for j=1:y_points
    for i=1:x_points
        for k=1:n
            Y=sqrt(j_comp*2*pi*f*u_soil*(sigma+j_comp*2*pi*f*e_soil));
            r=sqrt((x_N(1,i)-x(1,k))^2+(y_N(1,j)+h(1,k)+ 2/Y)^2);
            phi_y=(x_N(1,i)-x(1,k))/r;
            H_e_line_y(i,j)=H_e_line_y(i,j)-
(I_phasor(1,k)/(2*pi*r))*(1+(1/3)*(2/(Y*r))^4)*phi_y;
        end
    end
end

```



University of Moratuwa, Sri Lanka.
Electronic Theses & Dissertations
www.lib.mrt.ac.lk

```

H_e_real_2=real(H_e_line_x).^2+real(H_e_line_y).^2;
H_e_imag_2=imag(H_e_line_x).^2+imag(H_e_line_y).^2;

```

```
H_e=sqrt(H_e_real_2+H_e_imag_2);
```

```
%----- Total Magnetic Field-----
```

```
H_total=sqrt(H_real_2+H_imag_2+H_e_real_2+H_e_imag_2); %Total magnetic field in A/m
```

```
%----- Total Magnetic Flux Density -----
```

```
B_total=u_air*H+u_soil*H_e; %Total magnetic flux density in Wb/m2
```

```
[plot_X plot_Y]=meshgrid(x_N,y_N);
```

```
=====
```

```
%      Plot Component of H due to conductor current alone
```

```
=====
```

```
surf(plot_X,plot_Y,H')
```

```
title('Magnetic Field -Component of H due to conductor current alone ');
```

```
xlabel('Horizontal axis- X (m)');
```

```
ylabel('Vertical axis- Y');
```

```
zlabel('Magnetic Field (A/m)');
```

```
figure
```

```
=====
```

```
%      Plot Component of H due to earth current
```

```
=====
```

```
surf(plot_X,plot_Y,H_e')
```

```
title('Magnetic Field -Component of H due to earth current');
```

```
xlabel('Horizontal axis- X(m) ');
```

```
ylabel('Vertical axis- Y');
```

```
zlabel('Magnetic Field (A/m)');
```

```
figure
```

```
=====
```

```
%      Plot Resultant H due to conductor and earth current
```

```
=====
```

```
surf(plot_X,plot_Y,H_total')
```

```
title('Magnetic Field -Total');
```

```
xlabel('Horizontal axis- X(m)');
```

```
ylabel('Vertical axis- Y');
```

```
zlabel('Magnetic Field (A/m)');
```

```
figure
```

```
%=====
%      Plot Resultant B due to conductor and earth current
%=====

surf(plot_X,plot_Y,B_total')
title('Magnetic Flux Density -Total');
xlabel('Horizontal axis- X(m)');
ylabel('Vertical axis- Y');
zlabel('Magnetic Flux Density (Wb/m^2) or (T)');
```



University of Moratuwa, Sri Lanka.
Electronic Theses & Dissertations
www.lib.mrt.ac.lk

TX Line: Kotugoda - Katunayaka				Date : 23.05.2014			
Transmission line Voltage & configuration : 132kV double circuit twin zebra							
Line Currents : 780A, 860A				Line Conductor height (Lowest Phase): 7.7m			
Distance from centre (m)	Right			Distance from centre (m)	Left		
	Electric field (V/m)	Distance (m)	Electric field (V/m)		Electric field (V/m)	Distance (m)	Electric field (V/m)
0	3380	13.0	501	0	3380	-13.0	420
0.5	3400	13.5	401	-0.5	3370	-13.5	370
1.0	3400	14.0	301	-1.0	3390	-14.0	342
1.5	3410	14.5	280	-1.5	3410	-14.5	305
2.0	3450	15.0	220	-2.0	3440	-15.0	290
2.5	3490	15.5	180	-2.5	3480	-15.5	250
3.0	3480	16.0	140	-3.0	3480	-16.0	230
3.5	3450	16.5	120	-3.5	3450	-16.5	175
4.0	3390	17.0	115	-4.0	3350	-17.0	155
4.5	3295	17.5	105	-4.5	3275	-17.5	140
5.0	3150	18.0	100	-5.0	3050	-18.0	125
5.5	2950	18.5	95	-5.5	2950	-18.5	110
6.0	2575	19.0	95	-6.0	2701	-19.0	100
6.5	2450	19.5	90	-6.5	2501	-19.5	95
7.0	2200	20	85	-7.0	2291	-20.0	90
7.5	2010			-7.5	2050		
8.0	1670			-8.0	1800		
8.5	1482			-8.5	1650		
9.0	1390			-9.0	1401		
9.5	1200			-9.5	1280		
10	1100			-10	1100		
10.5	900			-10.5	920		
11.0	830			-11.0	801		
11.5	732			-11.5	702		
12.0	685			-12.0	594		
12.5	605			-12.5	505		

TX Line: Bolawatta - Nattandiya				Date : 23.05.2014			
Transmission line Voltage & configuration : 33kV double circuit single racoon							
Line Currents : 180A, 165A				Line Conductor height (Lowest Phase): 5.4m			
Distance from centre (m)	Right			Distance from centre (m)	Left		
	Electric field (V/m)	Distance (m)	Electric field (V/m)		Electric field (V/m)	Distance (m)	Electric field (V/m)
0	384	13.0	95	0	384	-13.0	100
0.5	388	13.5	93	-0.5	390	-13.5	98
1.0	404	14.0	88	-1.0	400	-14.0	88
1.5	426	14.5	80	-1.5	424	-14.5	80
2.0	445	15.0	78	-2.0	440	-15.0	80
2.5	458	15.5	70	-2.5	460	-15.5	70
3.0	464	16.0	65	-3.0	464	-16.0	65
3.5	450	16.5	65	-3.5	455	-16.5	65
4.0	438	17.0	60	-4.0	439	-17.0	60
4.5	420	17.5	60	-4.5	430	-17.5	60
5.0	390	18.0	55	-5.0	400	-18.0	55
5.5	370	18.5	55	-5.5	340	-18.5	55
6.0	347	19.0	55	-6.0	340	-19.0	55
6.5	300	19.5	50	-6.5	320	-19.5	50
7.0	288	20	50	-7.0	280	-20.0	50
7.5	270			-7.5	258		
8.0	240			-8.0	240		
8.5	220			-8.5	210		
9.0	180			-9.0	200		
9.5	177			-9.5	180		
10	170			-10	170		
10.5	140			-10.5	160		
11.0	145			-11.0	150		
11.5	130			-11.5	140		
12.0	120			-12.0	120		
12.5	110			-12.5	110		

TX Line: Kotugoda - Katunayaka				Date : 23.05.2014			
Transmission line Voltage & configuration : 132kV double circuit twin zebra							
Line Currents : 780A, 860A				Line Conductor height (Lowest Phase): 7.7m			
Distance from centre (m)	Right			Distance from centre (m)	Left		
	Mag. Field (μ T)	Distance (m)	Mag. Field (μ T)		Mag. Field (μ T)	Distance (m)	Mag. Field (μ T)
0	16.0	13.0	11.2	0	16.0	-13.0	11.3
0.5	16.5	13.5	10.8	-0.5	16.5	-13.5	11.1
1.0	16.8	14.0	10.4	-1.0	16.8	-14.0	10.5
1.5	17.9	14.5	10.1	-1.5	17.0	-14.5	10.0
2.0	18.7	15.0	9.6	-2.0	17.5	-15.0	9.5
2.5	19.5	15.5	9.1	-2.5	18.2	-15.5	9.1
3.0	19.6	16.0	8.5	-3.0	18.8	-16.0	8.5
3.5	19.9	16.5	8.1	-3.5	19.2	-16.5	7.8
4.0	20.6	17.0	7.9	-4.0	19.5	-17.0	7.29
4.5	20.9	17.5	7.6	-4.5	19.7	-17.5	7.1
5.0	20.9	18.0	7.0	-5.0	19.8	-18.0	7.0
5.5	20.8	18.5	6.6	-5.5	19.6	-18.5	6.9
6.0	20.4	19.0	6.5	-6.0	19.3	-19.0	6.8
6.5	20.0	19.5	6.01	-6.5	18.9	-19.5	6.5
7.0	19.5	20	5.8	-7.0	18.2	-20.0	6.5
7.5	18.2	20.5	5.4	-7.5	17.5	-20.5	6.3
8.0	17.86	21.0	5.8	-8.0	16.93	-21.0	5.99
8.5	17.0	21.5	5.6	-8.5	16.0	-21.5	5.85
9.0	16.0	22.0	5.42	-9.0	15.5	-22.0	5.76
9.5	15.5	22.5	5.22	-9.5	15.0	-22.5	5.56
10	14.0	23.0	5.02	-10	14.1	-23.0	5.23
10.5	13.8	23.5	4.82	-10.5	13.5	-23.5	5.12
11.0	13.37	24.0	4.73	-11.0	13.0	-24.0	4.99
11.5	12.8	24.5	4.5	-11.5	12.45	-24.5	4.8
12.0	12.2	25.0	4.45	-12.0	11.9	-25.0	4.5
12.5	11.7			-12.5	11.4		

TX Line: Bolawatta - Nattandiya				Date : 25.05.2014			
Transmission line Voltage & configuration : 33kV double circuit single raccoon							
Line Currents : 180A, 165A				Line Conductor height (Lowest Phase): 5.4m			
Distance from centre (m)	Right			Distance from centre (m)	Left		
	Mag. Field (μ T)	Distance (m)	Mag. Field (μ T)		Mag. Field (μ T)	Distance (m)	Mag. Field (μ T)
0	6.8	13.0	2.2	0	6.8	-13.0	2.2
0.5	6.82	13.5	2.0	-0.5	6.85	-14.0	2.1
1.0	6.83	14.0	2.0	-1.0	6.91	-13.5	2.0
1.5	6.84	14.5	1.85	-1.5	7.0	-14.0	1.85
2.0	6.86	15.0	1.8	-2.0	7.05	-15.0	1.8
2.5	6.8	15.5	1.7	-2.5	6.98	-15.5	1.7
3.0	6.77	16.0	1.6	-3.0	7.02	-16.0	1.65
3.5	6.6	16.5	1.5	-3.5	6.91	-16.5	1.6
4.0	6.5	17.0	1.5	-4.0	6.75	-17.0	1.5
4.5	6.3	17.5	1.4	-4.5	6.55	-17.5	1.4
5.0	6.01	18.0	1.3	-5.0	6.3	-18.0	1.35
5.5	5.72	18.5	1.3	-5.5	6.0	-18.5	1.3
6.0	5.45	19.0	1.2	-6.0	5.65	-19.0	1.2
6.5	5.12	19.5	1.2	-6.5	5.35	-19.5	1.2
7.0	48.4	20.0	1.1	-7.0	5.05	-20.0	1.1
7.5	4.54	20.5		-7.5	4.7	-20.5	
8.0	4.22	21.0		-8.0	4.4	-21.0	
8.5	4.0	21.5		-8.5	4.1	-21.5	
9.0	3.7	22.0		-9.0	3.8	-22.0	
9.5	3.5	22.5		-9.5	3.6	-22.5	
10	3.2	23.0		-10	3.3	-23.0	
10.5	3.0	23.5		-10.5	3.1	-23.5	
11.0	2.88	24.0		-11.0	2.9	-24.0	
11.5	2.62	24.5		-11.5	2.7	-24.5	
12.0	2.5	25.0		-12.0	2.6	-25.0	
12.5	2.35			-12.5	2.4		